NGU Rapport 2001.061

# Geochemistry of recent sediments and assessment of metal contamination in depositional areas of the Mid-Norwegian shelf and Vøringplatået

Norges geologiske undersøkelse
7491 TRONDHEIM
Tlf. 73 90 40 00
Telefaks 73 92 16 20

# RAPPORT

Rapport nr.: 2001.061 | ISSN 0800-3416 | Gradering: Open

Tittel:
Geochemistry of recent sediments and assessment of metal contamination in depositional areas of the Mid-Norwegian shelf and Vøringplatået

Forfatter:
Aivo Lepland

Oppdragsgiver:
NGU

Fylke:

Kommune:

Kartblad (M=1:250.000)

Kartbladnr. og -navn (M=1:50.000)

Forekomstens navn og koordinater:

Sidetall: 103 Pris: 125,-
Kartbilag: 0

Feltarbeid utført: 1999
Rapportdato: June 30, 2001
Prosjektnr.: 2948.00
Ansvarlig:

Sammendrag:

This report presents data on major and trace element abundances in short (< 0.5m) sediment cores that were collected from Holocene and glaciomarine sequences at 31 localities in the Mid-Norwegian shelf and Vøringplatået. The primary objectives of this investigation were the characterisation of the sediment types and sea bottom conditions, and the environmental assessment of the seabed.

Most of major and trace elements were analysed by ICP-AES except for Hg, Cd, Pb, As, Se and Sn, which were measured by atomic absorption. Leco SC analyser was used for the C and S determinations.

A reliable estimation of the contaminant levels in the sediments requires control upon the natural background. The geographical changes in elemental abundances are therefore evaluated in context of textural and mineralogical variability. The contents and mineral composition of the clay fraction appear to be the most crucial variables influencing the geographical distribution of trace elements in the investigated area.

The concentration versus depth profiles of metal contaminants such as Hg, Cd and As do not bear obvious signs of increased contaminant loads in the recent sediments. The consistent upward increase of Pb profiles and the highest enrichments either in surface or sub-surface (2-6 cm) intervals are, on the other hand, interpreted to reflect pollution history of gasoline related Pb emissions during the second half of the last century. The elevated Ba concentrations within top 6 cm of sediments at some stations, particularly in the Norskerenna, reflect recent barite discharge from oil exploration sites. The importance of diagenetic processes upon the post-depositional redistribution and/or concentration of metal contaminants is generally limited, except on the Vøringplatået where authigenic Fe-oxides locally scavenge As and some other metals.



| Emneord: Marine geology | Geochemistry | Sedimentology |
|---|---|---|
| Seabed sediments | Trace element | Contamination |

**CONTENTS**

**TABLES**



**FIGURES**

## 1. INTRODUCTION

This geochemical and sedimentological study of recent sediments from off-shore central Norway was undertaken with the aim to characterise the geographical variability of sediment types and sea bottom conditions, and to evaluate the environmental state of the seabed. The extent of recent environmental change has been characterised by comparing the abundances of metal contaminants such as As, Cd, Hg, Pb in the surface samples with deeper, pre-industrial sediment intervals. A reliable estimation of contaminant levels in stratigraphical and, particularly, geographical contexts depends heavily on the correct understanding of natural variability of the sediment matrix - increased levels of metals in one sample compared to another do not necessarily imply the higher contamination levels, but may be related to differences in the matrix mineralogy. The geographical changes of geochemical parameters are therefore evaluated in the context of textural and mineralogical variability. Besides the primary depositional controls influencing the geochemical signatures of sediments, secondary processes including diagenetic re-cycling are also considered.

The textural and geotechnical characteristics of these sediment cores from off-shore central Norway have been treated in earlier NGU report by Rise (2000). These data and interpretations combined with XRD mineralogy have provided a sedimentological framework for the geochemical interpretations presented in this report.

## 2. MATERIALS

The sediment cores reported here were collected from 31 locations off-shore central Norway (Fig. 1; Table 1). The sampling cruise with M/S Michael Sars was organised by the Institute of Marine Research and the Geological Survey of Norway in April 1999 (Bjerkli et al., 1999). Most of the cores were obtained from the sedimentary basins and depressions on the continental shelf, including Trænadjupet, Sklinnadjupet, Suladjupet, Kråkenesdjupet, Svinøydjupet and the northern end of the Norskerenna (Fig. 1). Besides these basins, sediment cores were also taken form the shelf slope NW of the Trænadjupet and from the Vøringplatået.

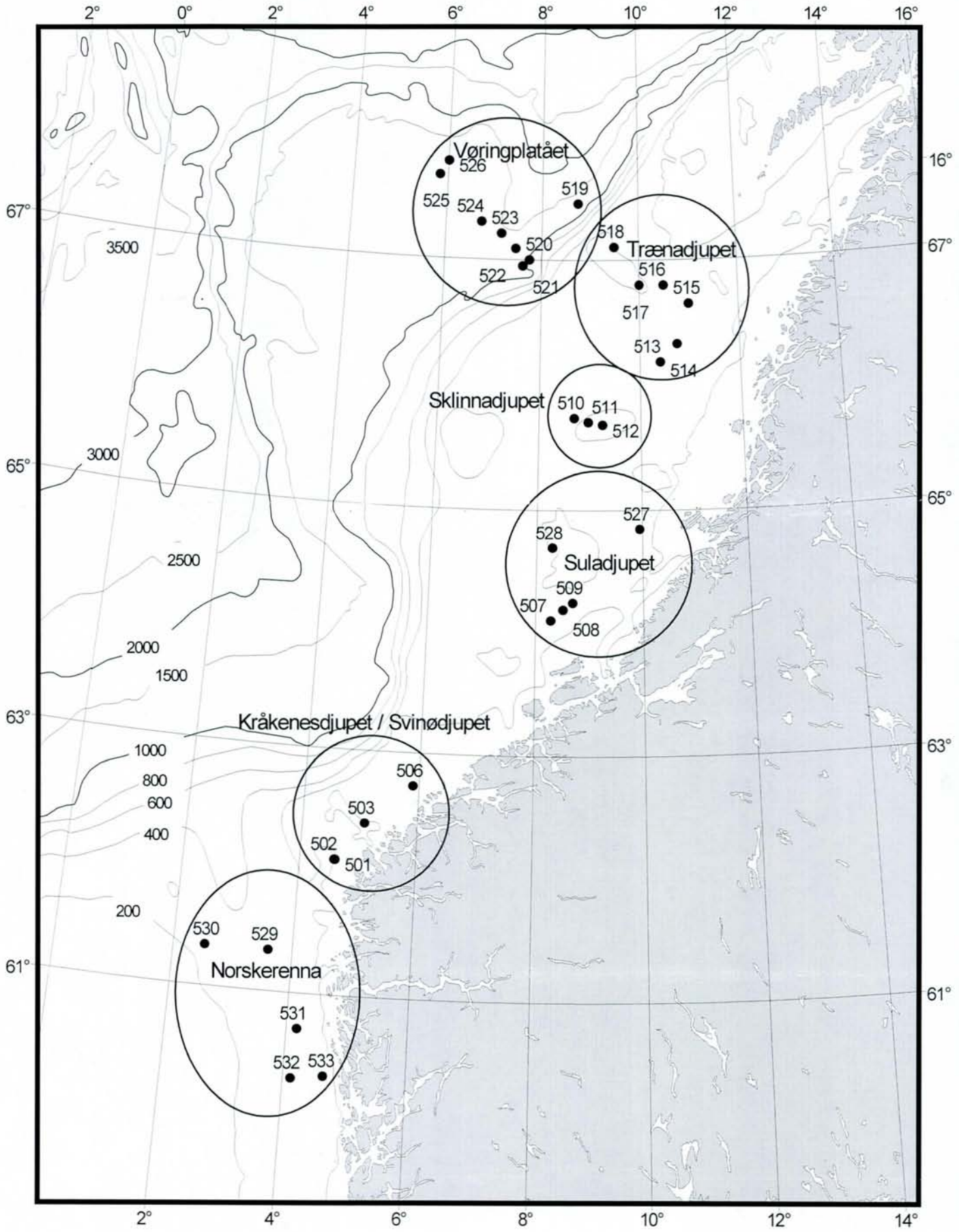


*Fig. 1. Sample stations and geographical names of depositional areas in the Mid-Norwegian shelf and Vøringplatået. Note that the Vøringplatået area includes some shelf-slope stations.*

The distribution of Holocene sediments on the continental shelf off-shore central Norway is patchy and the accumulation areas alter with erosional bottoms where glaciomarine sediments are exposed. The sections with Holocene sediments were the primary targets of sampling, but cores were also obtained from the glaciomarine sequences. The sediment type in individual stations, either Holocene mud or sand, or glaciomarine silty clay, is specified in Table 1. The chemical composition of both Holocene and glaciomarine sediments is reported, but the discussion about factors influencing sediment chemistry is primarily focused on the Holocene sediments.

**Table 1. Geographical coordinates and type of surface sediment of sampled stations.**

| Station | Latitude | Longitude | Sediment type |
|---|---|---|---|
| 501 | 62,10167 | 4,613333 | Holocene sand |
| 502 | 62,10167 | 4,598333 | Holocene sand |
| 503 | 62,41 | 5,081666 | Holocene sand |
| 506 | 62,73333 | 5,896667 | Holocene sand |
| 507 | 64,10167 | 8,283334 | Holocene mud |
| 508 | 64,18833 | 8,505 | Holocene mud |
| 509 | 64,24667 | 8,688334 | Holocene mud |
| 510 | 65,735 | 8,695 | Holocene mud |
| 511 | 65,70167 | 8,97 | Holocene mud |
| 512 | 65,68 | 9,246667 | Holocene mud |
| 513 | 66,18667 | 10,40833 | Glaciomarine silty clay |
| 514 | 66,33 | 10,75 | Glaciomarine silty clay |
| 515 | 66,64833 | 10,99833 | Holocene mud |
| 516 | 66,79833 | 10,49833 | Holocene mud |
| 517 | 66,8 | 10,00167 | Holocene mud |
| 518 | 67,10167 | 9,493333 | Holocene mud |
| 519 | 67,45 | 8,751667 | Holocene mud |
| 520 | 66,99834 | 7,75 | Holocene mud |
| 521 | 66,95 | 7,616667 | Holocene mud |
| 522 | 67,08667 | 7,465 | Glaciomarine silty clay |
| 523 | 67,205 | 7,163333 | Holocene mud |
| 524 | 67,29667 | 6,745 | Glaciomarine silty clay |
| 525 | 67,66333 | 5,83 | Glaciomarine silty clay |
| 526 | 67,77834 | 6,01 | Holocene mud |
| 527 | 64,84666 | 9,95 | Holocene mud |
| 528 | 64,69167 | 8,3 | Holocene mud |
| 529 | 61,33167 | 3,598333 | Holocene mud |
| 530 | 61,32833 | 2,53 | Holocene silty sand |
| 531 | 60,71 | 4,176667 | Holocene mud |
| 532 | 60,31333 | 4,131667 | Holocene mud |
| 533 | 60,345 | 4,655 | Holocene mud |

A multicorer (Barnett et al., 1984) was used as a sampling device, providing means for simultaneous recovery of up to 6 short cores with an undisturbed sediment-water interface. Two types of plastic tubes with inside diameters of 59mm and 96mm were used. The length of recovered sediment column ranged typically between 20 and 40 cm (Bjerkli et al., 1999). The on-board subsampling for geochemical analyses was done from 96 mm tubes at 1 cm intervals from the sediment surface down 10 cm and then, depending on the core length at 15-16, 25-26, 35-36 and 45-46 cm. All geochemical samples were immediately frozen.

## 3. METHODS

The applied analytical methods and the detection limits of individual elements are shown in Table 2. Most of the reported major and trace elements were analysed using Thermo Jarrell Ash ICP-AES 61. For these analyses acidified aqueous sample solutions were obtained by dissolving 1 g of freeze-dried sediment in 7N $HNO_3$ in an autoclave at 120 °C for 1 hour (Norsk Standard NS 4770).

Hg concentrations were measured using the CETAC M-6000A atomic absorption cold vapor Hg Analyser. Perkin Elmer graphite furnace atomic adsorption (GFAA) system SIMAA 6000 was used for Cd, Pb, As, Se and Sn determinations. Sample preparation for atomic absorption analyses included digestion of 100 mg sample in mixed acid including 1 ml aqua regia and 3 ml HF. Free HF in aqueous sample solution was complexed by adding 3 ml boric acid ($H_3B0_3$). Analysis volume of 100 ml was obtained by adding water to the sample solution.

The contents of total carbon ($C_{tot}$), organic carbon ($C_{org}$) and total sulphur were determined on the Leco SC-444 analyser using 100-350 mg of sample. Carbonate was removed by 10% HCl prior organic carbon measurements. The abundance of carbonate carbon ($C_{carb}$) has been calculated as difference between $C_{tot}$ and $C_{org}$.

**Table 2. Applied analytical methods and detection limits of individual elements.**

| Element | Method | Detection limit |
|---|---|---|
| Si | ICP-AES | 1000 ppm |
| Al | ICP-AES | 200 ppm |
| Fe | ICP-AES | 50 ppm |
| Ti | ICP-AES | 10 ppm |
| Mg | ICP-AES | 1000 ppm |
| Ca | ICP-AES | 2000 ppm |
| Na | ICP-AES | 2000 ppm |
| K | ICP-AES | 1000 ppm |
| Mn | ICP-AES | 2 ppm |
| P | ICP-AES | 100 ppm |
| Cu | ICP-AES | 10 ppm |
| Zn | ICP-AES | 20 ppm |
| Ni | ICP-AES | 20 ppm |
| Co | ICP-AES | 10 ppm |
| V | ICP-AES | 10 ppm |
| Mo | ICP-AES | 10 ppm |
| Cd | ICP-AES | 10 ppm |
| Cr | ICP-AES | 10 ppm |
| Ba | ICP-AES | 10 ppm |
| Sr | ICP-AES | 20 ppm |
| Zr | ICP-AES | 10 ppm |
| Ag | ICP-AES | 10 ppm |
| Be | ICP-AES | 2 ppm |
| Li | ICP-AES | 10 ppm |
| Sc | ICP-AES | 2 ppm |
| Ce | ICP-AES | 100 ppm |
| La | ICP-AES | 10 ppm |
| Y | ICP-AES | 2 ppm |
| Hg | AA/HMS-1 | 0.01 ppm |
| Cd | AA | 0.02 ppm |
| Pb | AA | 0.4 ppm |
| As | AA | 3 ppm |
| Se | AA | 1 ppm |
| Sn | AA | 3 ppm |
| Total C | Leco | 0.07% |
| Total organic C | Leco | 0.1% |
| Total S | Leco | 0.01% |

## 4. RESULTS

### 4.1. Texture

The spatial variations of textural characteristics including median diameter, sand content and clay content are shown on Figs. 2-4. Additional data on sediment grain-size and geotechnical parameters can be found in an earlier NGU report (Rise, 2000)

### 4.2. Mineralogy

Qualitative analyses of the mineral composition in clay fraction (< 2 μm) by X-ray diffraction have indicated the occurrence of smectite, illite, chlorite, quartz and calcite in all samples. Most samples contain traces of mixed-layer illite-smectite, kaolinite, amphibole, plagioclase and K-feldspar (NGU Analyserapport 1999.0117). Ratios of background-corrected peak heights at 14Å, 10Å and 7Å (diffraction patterns of untreated, air-dried samples) have been used to estimate the relative abundances of smectite, illite and chlorite, respectively. The 14 Å reflection may be a composite of smectite, chlorite and vermiculite in case of untreated samples. Yet, smectite, as a main contributor to the 14 Å peak is indicated by a distinct reduction of this peak after ethylene glycol saturation and after 500 °C heat treatment. The reflection at 7Å does not belong entirely to chlorite as kaolinite has its main peak also at that position. However, the positions of other peaks and peak modifications after 500 °C heat treatment suggest that kaolinate is a relatively minor component in these sediments, and the 7Å peak results primarily from chlorite. The behaviour of the 14 Å peak upon ethylene glycol and 500 °C heat treatments suggests that chlorite in these samples is represented by a Fe-rich variety. Geographical variations for the ratios smectite/illite and chlorite/illite are shown in Figs. 5-6.

### 4.3. Geochemistry

Geographical variations of elements that in all analysed surface samples had concentrations above instrumental detection limits are graphically illustrated in Figs. 7-37. The concentration ranges of individual elements in those figures are divided into five classes using the

ArcView© "natural breaks" classification method. The complete set of tabulated geochemical data for the sediment cores can be found in the NGU Analyserapport 1999.0118.

Shallow stratigraphical, concentration vs. depth profiles, covering between 2 to 8 depth intervals were obtained from 19 stations. Two sets of stratigraphical profiles ("a" and "b") are given for each station. In order to facilitate the straightforward comparison between stations, the individual parameters have constant x-axes on the "a" sets (Figs. 38a-56a); x-axes of the "a" set range from 0 to the highest value of particular parameter in the entire dataset. The "b" set focuses on relative stratigraphical changes and the x-axes are variable (Figs. 38b-56b), scaled after lowest and highest concentration values of individual parameters at each station. The concentrations of elements such as Cu, Ni, Hg, Se, Ni, Li and Ce were in some depth intervals below instrumental detection limits, and in those cases data-points are not shown in the concentration versus depth profiles. The discussion on the stratigraphical variations focuses primarily on 12 stations with analytical data for 3 or more depth intervals.

## 5. DISCUSSION

### 5.1. Geographical relationships

A relatively scattered sampling net and large distances between individual stations do not allow traditional geographical trend analyses such as source-transport-sink interpretations. The geochemical trend interpretations are furthermore complicated by significant variations in sediment texture and mineralogy.

For spatial characterisation of elemental abundances, the entire study area is divided into 6 geographically confined sub-areas with similar textural, mineral and chemical composition (Fig. 1). Note that the Vøringplatået area includes three shelf-slope stations. The average grain-size and elemental abundances have been calculated for the Holocene sediments within each sub-area, excluding stations with glaciomarine sediments and some atypical Holocene stations (Table 3). The bar diagrams in Fig. 57 illustrate the textural and geochemical differences between sub-areas. The x-axes of the bar diagrams are relative, scaled after highest and lowest values for each individual parameter. The bar heights of parameters vary between 100% (highest value) and 10% (lowest value).

**Table 3. Average contents of clay, silt and sand, and elemental abundances in 6 areas. Number of stations that were used calculating averages for each area are indicated in parenthesis. Fig. 57 is the graphical representation of this table.**

| Area | Clay (%) | Silt (%) | Sand (%) | S (%) | TOC (%) | $C_{carb}$ (%) | Al (%) | Fe (%) | Ti (%) | Mg (%) | Ca (%) |
|---|---|---|---|---|---|---|---|---|---|---|---|
| Kråkenesdjupet / Svinøydjupet (4) | 2,40 | 21,43 | 75,90 | 0,13 | 0,45 | 1,00 | 5,86 | 1,82 | 0,27 | 0,65 | 4,20 |
| Suladjupet (3) | 7,00 | 77,83 | 15,17 | 0,32 | 0,83 | 1,79 | 6,70 | 2,89 | 0,35 | 1,30 | 6,01 |
| Sklinnadjupet (3) | 9,60 | 89,23 | 1,17 | 0,42 | 0,91 | 2,43 | 7,09 | 3,48 | 0,37 | 1,61 | 7,65 |
| Trænadjupet (3) | 8,73 | 86,53 | 4,73 | 0,35 | 0,80 | 2,65 | 6,41 | 3,15 | 0,35 | 1,46 | 8,12 |
| Vøringplatået (4) | 10,98 | 83,70 | 5,33 | 0,50 | 1,57 | 3,37 | 5,16 | 3,00 | 0,35 | 1,33 | 9,91 |
| Norskerenna (3) | 11,88 | 75,95 | 12,18 | 0,34 | 1,35 | 2,25 | 5,81 | 3,01 | 0,31 | 1,28 | 6,48 |

| Area | Na (%) | K (%) | Mn (ppm) | P (ppm) | Zn (ppm) | Co (ppm) | V (ppm) | Cr (ppm) | Ba (ppm) | Sr (ppm) | Zr (ppm) |
|---|---|---|---|---|---|---|---|---|---|---|---|
| Kråkenesdjupet / Svinøydjupet (4) | 2,51 | 1,68 | 532,00 | 649,00 | 61,88 | 17,75 | 51,28 | 46,78 | 552,00 | 368,75 | 136,00 |
| Suladjupet (3) | 3,00 | 1,94 | 631,33 | 661,67 | 90,77 | 21,57 | 95,10 | 71,10 | 442,33 | 370,67 | 151,67 |
| Sklinnadjupet (3) | 3,61 | 2,16 | 1190,00 | 599,00 | 108,67 | 24,03 | 110,67 | 84,93 | 441,33 | 420,33 | 156,00 |
| Trænadjupet (3) | 3,20 | 1,98 | 1192,00 | 573,67 | 103,83 | 23,23 | 98,73 | 76,43 | 377,33 | 428,33 | 146,33 |
| Vøringplatået (4) | 4,10 | 1,56 | 2512,50 | 667,75 | 92,50 | 25,33 | 107,00 | 59,55 | 476,50 | 555,75 | 169,25 |
| Norskerenna (3) | 2,96 | 2,00 | 1856,00 | 613,50 | 102,50 | 23,60 | 105,75 | 77,43 | 428,75 | 301,50 | 190,75 |

| Area | Be (ppm) | Li (ppm) | Sc (ppm) | La (ppm) | Y (ppm) | Hg (ppm) | As (ppm) | Cd (ppm) | Pb (ppm) | Se (ppm) |
|---|---|---|---|---|---|---|---|---|---|---|
| Kråkenesdjupet / Svinøydjupet (4) | 5,46 | 14,75 | 6,78 | 21,43 | 19,38 | 0,02 | 5,79 | 0,29 | 26,87 | 2,60 |
| Suladjupet (3) | 8,02 | 32,60 | 10,97 | 24,70 | 21,03 | 0,02 | 8,40 | 0,12 | 33,91 | 2,96 |
| Sklinnadjupet (3) | 9,60 | 45,40 | 12,10 | 29,87 | 21,33 | 0,03 | 9,78 | 0,12 | 32,71 | 1,42 |
| Trænadjupet (3) | 8,76 | 39,13 | 10,97 | 27,17 | 20,63 | 0,03 | 9,60 | 0,13 | 29,85 | 1,97 |
| Vøringplatået (4) | 8,06 | 33,65 | 9,55 | 17,68 | 18,23 | 0,02 | 16,61 | 0,20 | 33,25 | 2,02 |
| Norskerenna (3) | 8,31 | 45,25 | 9,26 | 25,10 | 18,25 | 0,02 | 21,49 | 0,11 | 46,39 | 2,74 |

### 5.1.1. Major elements

The relative proportions of the sediment-forming minerals largely determine the major element composition of marine sediments. These principal minerals include (i) clay minerals, (ii) carbonates, (iii) biogenic opal and (iv) detrital quartz and feldspars. The mutual proportions of relatively Al-rich clay minerals and Si-rich quartz and feldspars (with exception of anorthite) are generally controlled by sediment texture, and fine-grained sediments, as expected, are typically rich in Al. The major element contents of fine-grained sediments are also dependent upon the phases of clay minerals. Chlorite and particularly smectite can be considered as relatively poor in Al but rich in Fe and Mg, whereas the reverse generally applies for in illite and kaolinite.

*5.1.1.1. Silicon*

The sandy sediments from Kråkenesdjupet/Svinødjupet and glaciomarine stations of Vøringplatået and Trænadjupet have the highest Si contents (Fig. 7), reflecting elevated quartz contents in the coarse-grained sediments. Fine texture and significant carbonate dilution control relatively low Si contents in sediments from Vøringplatået (Fig. 7).

*5.1.1.2. Aluminium, Potassium*

The distribution of Al in study area (Fig. 8) reveals an unusual relationship in which the fine sediments from Norskerenna and Vøringplatået (Figs. 2-4) are relatively Al-poor compared to slightly coarser sediments from Suladjupet, Skinnadjpet and Trænadjupet. The low Al content on the Vøringplatået is likely due to (i) high dilution factor by carbonate minerals (Figs. 17-18; Table 4) reducing the relative abundance of Al and (ii) higher abundance of Al-poor smectite (Fig. 5) in this area. The average grain-size of smectite tends to be extremely fine (Gibbs, 1977), consistent with highest smectite abundances in the finest sediments on the Vøringplatået. Relatively high chlorite and smectite abundances in the Norskerenna may also explain lower Al contents in this area compared to illite and Al-rich Suladjupet, Skinnadjpet and Trænadjupet. Similar Al contents in clayey Norskerenna and neighbouring sandy Kråkenesdjupet/Svinødjupet suggest the presence of significant proportion of coarse-grained aluminosilicates (feldspars) in the latter area.

The pattern of K variations (Fig. 9) generally coincides with that of Al (Fig. 8). Illite dominated sediments in Suladjupet, Skinnadjpet and Trænadjupet have highest K concentrations while carbonate and smectite rich sediments of the Vøringplatået are lowest in K (Fig. 9).

*5.1.1.3. Magnesium, Iron, Titanium*

The spatial variations of Mg, Fe and Ti are generally in phase with each other (Figs. 10-12). This indicates the common carrier phases of these elements, most likely smectite and/or

chlorite, over the entire study area. The distribution of Fe can also be influenced by diagenetic mobilisation and/or re-precipitation. However, the good correspondence between Fe on one hand and Ti and Mg on the other hand suggest that the fraction of Fe participating in diagenetic processes is relatively minor and most of Fe in the surface sediments is locked up in detrital phases.

High Mg/Al and Fe/Al ratios in sediments from the Vøringplatået (Figs. 13-14) are consistent with elevated smectite content in this area (Fig. 5). Due to extensive carbonate dilution, Mg and Fe concentration are intermediate at the Vøringplatået and do not properly reflect relatively high smectite abundance in these sediments.

Distinct Mg and Fe depletions and low Mg/Al and Fe/Al ratios in sediments from Kråkenesdjupet/Svinødjupet (Figs. 10-14) are consistent with limited chlorite and/or smectite content (Figs. 5-6) and low overall clay abundance in this area (Fig. 4). These low values of Mg, Fe, Mg/Al and Fe/Al suggest that minerals poor in Fe and Mg, such as feldspars, are the principal Al bearing phases in Kråkenesdjupet/Svinødjupet.

*5.1.1.4. Organic Carbon, Manganese*

Highest $C_{org}$ contents are found in sediments of Norskerenna and Vøringplatået while sediments in Kråkenesdjupet/Svinødjupet are most $C_{org}$ depleted (Fig. 15). Good correlation of these variations with clay abundance (Fig. 4) indicates winnowing of organic matter from relatively high-energy environments with coarse-grained sediments, and transport towards the calmest basins in the area.

Authigenic oxyhydroxide species are the principal carrier phases of Mn (represented as $MnO_x$ where $x = \sim 2$) in surficial marine sediments. The build-up of elevated concentrations of $MnO_x$ in surface layers is driven by sediment burial and reductive dissolution of Mn(IV) and Mn(III) in sub-oxic diagenetic environment (Berner, 1980). Since the precipitation of reduced Mn(II) phases requires very unusual geochemical environment, seldom found in marine sediments (Roy, 1992), dissolved Mn(II) is transported back to the oxygenated zone by upward diffusion, where it oxidises and precipitates as $MnO_x$. Reducing conditions are typically achieved within 1-2 cm sediment depth in fine-grained, organic rich marine

sediments and in those cases $MnO_x$ enrichment typically occurs in surface sediments. Subsurface $MnO_x$ enrichment at oxic-sub-oxic interface may form if oxic conditions persist several centimetres into the sediment column (c.f. Thomson et al., 2001).

The geographical pattern of Mn contents, showing highest abundances in organic-rich, clayey sediments of Norskerenna and Vøringplatået (Fig. 16) may reflect fine grain-size of $MnO_x$ particles, and hydraulic sorting and transport of those particles towards the calmest basins in the area. Relatively shallow oxic zone and concentration of $MnO_x$ in thin surface layer may be an alternative explanation for high Mn concentrations in Norskerenna and Vøringplatået, but this is not supported by the stratigraphical relationships discussed below.

#### *5.1.1.5. Calcium, Carbonate Carbon*

Spatial variations of Ca and $C_{carb}$ are well in phase (Figs. 17-18), consistent with calcite as their principal carrier phase. Under the condition that $C_{carb}$ is entirely locked up in calcite, the content of calcite would range from 7.2% in the Kråkenesdjupet to 31.4% in the Vøringplatået (Table 4).

### 5.1.2. Trace elements

#### *5.1.2.1. Barium*

The geographical trends of Ba in surface sediments of the neighbouring Skagerrak have allowed tracking of sediment transport from the off-shore hydrocarbon exploration sites where barite has been used as a component of drilling mud (Lepland et al., 2000). It was also expected to see such "drilling barite" influence in samples discussed here since several exploration sites occur within the limits of the study area (Fig. 19). The occurrences of highest Ba concentrations (> 600 ppm) in close vicinity to exploration sites suggest the contribution of the "drilling barite" to the overall Ba budget of those stations. Relatively high Ba contents in the sediments of the Vøringplatået compared to Suladjupet, Skinnadjpet and Trænadjupet may indicate elevated Ba content in the smectite-rich matrix sediments.

**Table 4. Calculated calcite contents in the surface sediments.**

| Station | Carbonate-C (%) | Calcite (%) |
|---|---|---|
| 501 | 0,87 | 7,22 |
| 502 | 1,06 | 8,86 |
| 503 | 1,00 | 8,30 |
| 506 | 1,09 | 9,09 |
| 507 | 1,67 | 13,91 |
| 508 | 1,89 | 15,74 |
| 509 | 1,81 | 15,04 |
| 510 | 2,38 | 19,80 |
| 511 | 2,43 | 20,22 |
| 512 | 2,47 | 20,61 |
| 513 | 1,47 | 12,28 |
| 514 | 1,73 | 14,38 |
| 515 | 2,66 | 22,20 |
| 516 | 2,61 | 21,73 |
| 517 | 2,67 | 22,23 |
| 518 | 2,52 | 21,03 |
| 519 | 3,02 | 25,18 |
| 520 | 2,58 | 21,47 |
| 521 | 2,88 | 23,98 |
| 522 | 1,91 | 15,88 |
| 523 | 3,76 | 31,31 |
| 524 | 3,74 | 31,13 |
| 525 | 3,77 | 31,43 |
| 526 | 3,81 | 31,78 |
| 527 | 1,31 | 10,92 |
| 528 | 1,91 | 15,90 |
| 529 | 2,17 | 18,08 |
| 530 | 2,89 | 24,11 |
| 531 | 2,71 | 22,55 |
| 532 | 2,15 | 17,92 |
| 533 | 1,99 | 16,60 |

*5.1.2.2. Phosphorous*

Areal distribution of P does not correlate with any other parameter considered in this study (Fig. 20). Similar P concentrations in the clayey sediments of the Vøringplatået and in the sandy sediments of Kråkenesdjupet/Svinødjupet suggest variable carrier phases of P in different parts of the study area. Organic matter and/or $MnO_x$ may be the carrier phases of P in the fine-grained sediments of Vøringplatået while detrital apatite may be the principal P bearing phase in coarse-grained, organic-poor sediments of Kråkenesdjupet/Svinødjupet.

Relatively high P concentrations in some shore-proximal stations may reflect P input from terrestrial sources such as sewage or agricultural fertilizers.

#### *5.1.2.3. Beryllium, Chromium, Cobalt, Scandium, Vanadium, Zinc, Zirconium, Yttrium*

The similarity of Be, Co, Sc, V and Zn variations with Mg and Fe (Figs. 21-25 vs. Figs. 10-11) indicates that chlorite and/or smectite (i.e. phases rich in Fe and Mg) may control the distribution of these trace elements. Cr and Y on the other hand seem to be carried by illite as they generally correlate with K (Figs. 26-27 vs. Fig. 9). Random distribution of Zr (Fig. 28), which does not correlate with any of the major elements suggests its occurrence in accessory minerals, most probably in detrital zircon crystals. Clear correlation of Sr with Ca and $C_{carb}$ (Fig. 29 vs. Figs. 17-18) indicates that majority of Sr present in these sediments occurs in carbonate lattice.

### 5.1.3. Metal contaminants

#### *5.1.3.1. Mercury*

Hg concentrations are low throughout the investigated area and range typically between 0.01 and 0.03 ppm (Fig. 30). Relatively high Hg concentrations of 0.05 and 0.06 ppm were found in three stations in Skinnadjpet and Trænadjupet. What causes these slightly higher Hg values is not known; there is no significant anomaly in any other parameter at these stations. It is noteworthy that the three stations showing high Hg values occur adjacent to those stations having the lowest Hg values (Fig. 30).

#### *5.1.3.2. Lead*

Several geochemical studies have clearly demonstrated that ore processing since Greek and Roman times has significantly increased the atmospheric emission of Pb, resulting in Pb

contamination of the Earth's surface (Nriagu & Pacyna, 1988; Hong et al., 1994). Atmospheric emissions and the levels of Pb contamination have particularly increased during the middle decades of the last century when Pb was widely used as gasoline additive (Smith & Flegal, 1995). The re-distribution of atmospherically supplied Pb in the marine environment is largely dependent upon interaction of Pb with suspended particles. Scavenging of Pb onto surfaces of suspended organic matter, clay minerals and/or Mn-Fe-oxyhydroxides may aid removal of Pb from the water column. Significant Pb contamination levels can in such a case be found in areas where the preferred Pb substrates selectively accumulate.

The fine-grained sediments of the Norskerenna are somewhat enriched in Pb (42-51 ppm) compared to the rest of the investigation area (20-41 ppm; Fig. 31). Norskerenna is known to act as a natural sediment trap, accounting for the deposition of 50-70% of sediments carried in suspension in the North Sea (Eisma & Kalf, 1987). This long transport path and lasting exposure to scavenging may likely explain the elevated Pb concentrations in the Norskerenna. However, these Pb values are still considerably lower than the values seen in southern and eastern parts of the Norskerenna (average 58 ppm; Sæther et al., 1996).

*5.1.3.3.Cadmium*

Sediments of the Vøringplatået are slightly enriched in Cd compared to the rest of the study area (Fig. 32). This generalisation excludes one erratic station in the Kråkenesdjupet that has very high Cd concentration in contrast to all other stations. The significance of this high Cd value remains to be evaluated. Elevated Cd concentrations at the Vøringplatået may reflect (i) association of Cd with smectite, or (ii) selective fixation of Cd by carbonate. Both, smectite and carbonate are relatively abundant phases in the Vøringplatået (Figs. 5; 17-18).

*5.1.3.4. Arsenic*

The highest concentrations of As were found in sediments of Norskerenna and Vøringplatået (Fig. 33), and the distribution pattern of As is generally in phase with $C_{org}$ (Fig. 15). This

correlation may suggest that significant portion of As in these sediments is of hydrogeneous origin, removed from the water column by organic material. The mechanism of As fixation may include scavenging or complexation with the surface ligands of particulate organic material. The affinity of As for organic particles indicates that the areas with high $C_{org}$ accumulation can be most liable to As contamination.

5.1.4. Other elements – Sodium, Sulphur

Na and S are treated under separate heading because of their relatively high abundance in pore water ($Na^-$ = 10.77 g/l and $SO_4^{2-}$ = 2.712 g/l at salinity 35‰; Wilson, 1975). Since the applied sample preparation procedure did not include removal of salty pore water, considerable amounts of dissolved Na and S were combined with the sediments upon freeze-drying. The calculated contributions of pore water Na and S to total sediment (grain density 2.75 g/cm$^3$) within porosity range between 50 and 90% are shown in Table 5. These calculations show significant pore water influence to the sediment Na and S budgets, particularly in case of cohesive, organic-rich and clayey sediments.

**Table 5. Pore-water contributions of Na and S to freeze-dried sediment, calculated using different porosities (see text for details).**

| porosity % | Na% | S% |
|---|---|---|
| 90 | 0,83 | 0,070 |
| 80 | 0,65 | 0,054 |
| 70 | 0,50 | 0,042 |
| 60 | 0,39 | 0,033 |
| 50 | 0,29 | 0,025 |

Although the geographical distribution patterns of Na and S show good correspondence with porosity (Figs. 34-36), the magnitude of Na and S changes is too large to be solely explained by porosity variations. The geographical distribution of smectite and organic matter (i.e. phases that may carry significant amounts of Na and S, respectively) and their relatively high abundance in cohesive sediments (Figs. 5; 15 vs. Fig. 36) may be, besides porosity, also

influential upon geographical pattern of Na and S. High Na/S ratio in relatively low porosity, coarse-grained sediments of Kråkenesdjupet/Svinødjupet (Fig. 37) presumably reflects significant Na contribution from plagioclase.

## 5.2. Stratigraphical trends

The down-core fluctuations of major elements, except Mn, are largely controlled by variable proportions of detrital (alumino)silicates and carbonate. This is indicated by commonly observed negative correlation between $C_{carb}$ and Ca on one hand and Al, Mg, K on the other hand (Figs. 38-56). The enrichments of Na and S in surface layers are the manifestations of high cohesiveness and significant porewater contribution upon Na and S contents of freeze-dried sediments. Although the primary productivity and related accumulation rate of organic matter may have increased over the past years due to human activities, the post-depositional mineralisation of organic matter is likely the main factor controlling the down-core decrease of $C_{org}$ contents. The break down of organic matter in which a variety of oxidants are used in a sequence (oxygen > nitrate > Mn-oxides > Fe-oxides > sulphate), defined by the energy gained in each specific reaction (Froelich et al., 1979) is the driving mechanism behind diagenetic processes.

The variations in trace element contents are typically within relatively narrow concentration ranges. There is undoubtedly a geologic message in these variations, but their importance in the context of interpreting the changes in sedimentary conditions and/or environmental state may be insignificant. Still, some elements such as Mn, Ba, Pb, and in some instances also As, P and Fe show stratigraphical changes that are interpreted to reflect diagenetic processes and/or pollution history. The fate of these elements is discussed in more detail below.

### 5.2.1. Lead

Pb is the only heavy metal that shows consistent stratigraphical trends in all stations of the study area. Pb concentrations are stable and relatively low in the deeper intervals, but increase gradually upwards from 6-10 cm sediment depth. This increasing trend does not always

continue to the very surface – in some stations the 2-3 cm subsurface interval has the highest Pb concentrations. The profile shape of Pb concentrations with elevated values in surface/near-surface sediments likely indicates recent atmospheric Pb contamination. Slightly declining values in the very top sediments of some stations may signal decreased Pb emissions – consistent with measures introduced during the 1970s controlling the gasoline-related Pb emissions.

### 5.2.2. Barium

Distinct Ba enrichments within surfaces sediments characterise all stations of the Norskerenna (Figs. 53-56). The estimates for the rate of sedimentation (Haas et al., 1996) would date the stabilisation of the Ba profiles to background levels at 2-4 cm sediment depth to the early 1970s, which generally overlaps with the onset of off-shore hydrocarbon exploration. It is therefore quite likely that the recent barite input from discharged drilling mud controls the Ba enrichment in surface sediments of the Norskerenna. General correlation of Ba profiles with Al in areas beside Norskerenna suggest that aluminosilicate matrix minerals carry most of Ba in those areas.

### 5.2.3. Manganese

The break points in the Mn profiles at 2-8 cm sediment depth divide uniformly low background contents in the deeper layers from the higher surface/near-surface contents. Below that break point Mn occurs primarily in diagenetically inert matrix minerals. Surface/near-surface enrichment, as described above, is controlled by an authigenic $MnO_x$ precipitation, resulting from phase changes and re-cycling at the oxic-sub-oxic interface. The highest Mn concentrations within the very surface interval in most of the stations indicate that porewater oxygen is effectively depleted within the first couple of centimetres of the sediment column. Major exception to this very shallow oxygen consumption is provided by station 526 (Fig. 51; Vøringplatået), where a pronounced Mn peak at 6-7 cm depth indicates a considerably thicker oxygenated zone.

Although $MnO_x$ in known to effectively adsorb a variety of trace elements (Hunt & Kelly, 1988, Glasby, 2000), this adsorption appears to be insignificant in sediments of the study area as none of the trace elements (except Ba in Norskerenna that coincides incidentally; Figs. 53-56) show a correlation with Mn.

### *5.2.4. Iron, Arsenic, Phosphorous*

The stratigraphical As and P profiles are likely influenced by Fe diagenesis in sediments of the Vøringplatået. In these sediments elevated Fe concentrations occur just below the Mn peak, i.e. at the position in the diagenetic sequence where oxic precipitation of Fe should take place (Figs. 48; 49; 51). This suggests that a significant portion of Fe participates in diagenetic re-cycling in sediments of the Vøringplatået, separating this area form all other areas where Fe profiles do not bear obvious signs of Fe diagenesis.

The highest concentrations of As and P coincide generally with elevated Fe contents and occur consistently just below the Mn peak (Figs. 48; 50; 51). This suggest immobilisation of As and P by Fe precipitates. Other trace elements, such as Ni (Fig. 49), Co (Fig. 51), Se (Fig. 48) may have occasionally been fixed by Fe precipitates too, but the profile relationships of these elements are not always as consistent as in the case of As and P.

### 5.2.5. Cadmium, Mercury

The stratigraphical distribution of Cd does not indicate increased load of this metal contaminant in the recent sediments. There is no regular pattern in the down-core variations of Cd, and the concentrations in the surface layers are often even lower than in deeper intervals.

The elevated Hg contents within surface sediments, that may signal increased recent contamination, were observed in four stations (Figs. 49, 51, 53, 54). However, most of the stations do not show such surficial enrichment and the Hg profiles are either flat or have highest concentrations in sub-surface intervals. This suggests that Hg contamination, if present, has a limited geographical distribution in the study area.

### 5.2.6. Other elements

A peculiar geochemical anomaly is observed at 5-6 cm sediment depth in a core from station 521 (Fig. 49). Several elements, including Al, Mg, K, Ca, Cu, Zn, V, Cr, Ba, Sr, Zr, Li, Sc, La and Y, show ramped enrichment in this interval. The X-ray imagery of this core (Rise, 2000) has revealed a banded sediment with variable X-ray transparency. The sedimentological mechanism controlling this banding is presently unknown, but the location of this station at the shelf slope may hint at turbidity flow. The geochemically anomalous layer may under these circumstances represent effectively sorted deposit (base of turbitite?) where minerals rich in the above-listed elements may have been concentrated.

## 6. SUMMARY

The geographical variability of the geochemical character of the sediments in the study area is largely determined by differences in sedimentological regime, texture and mineralogy. This matrix related variability is apparently the main control influencing the geographical distribution of most of the trace elements.

Pb is the only metal whose geographical and stratigraphical distribution patterns indicate a supply from pollution sources. Pb concentrations are highest either in the surface samples or in 2-4 cm sediment depth and decrease gradually down core, consistent with gasoline related recent atmospheric fallouts. Surface enrichments of Pb are strongest in sediments of the Norskerenna reflecting high Pb input from the North Sea. The elevated Ba concentrations within top 6 cm of sediments at some stations, particularly in the Norskerenna, reflect recent barite discharge from oil exploration sites where barite is used as a component of the drilling mud. Stratigraphical profiles of other trace metals and metal contaminants are generally flat or vary within narrow range in a non-systematic manner, and do not signal an increased load of pollutants in recent sediments.

Diagenetic processes do generally not influence the down-core profiles of trace elements. One major exception to this diagenetic insignificance is provided by the sediments of the Vøringplatået where oxic Fe precipitates effectively scavenge P and As, and occasionally also Ni, Co and Se.

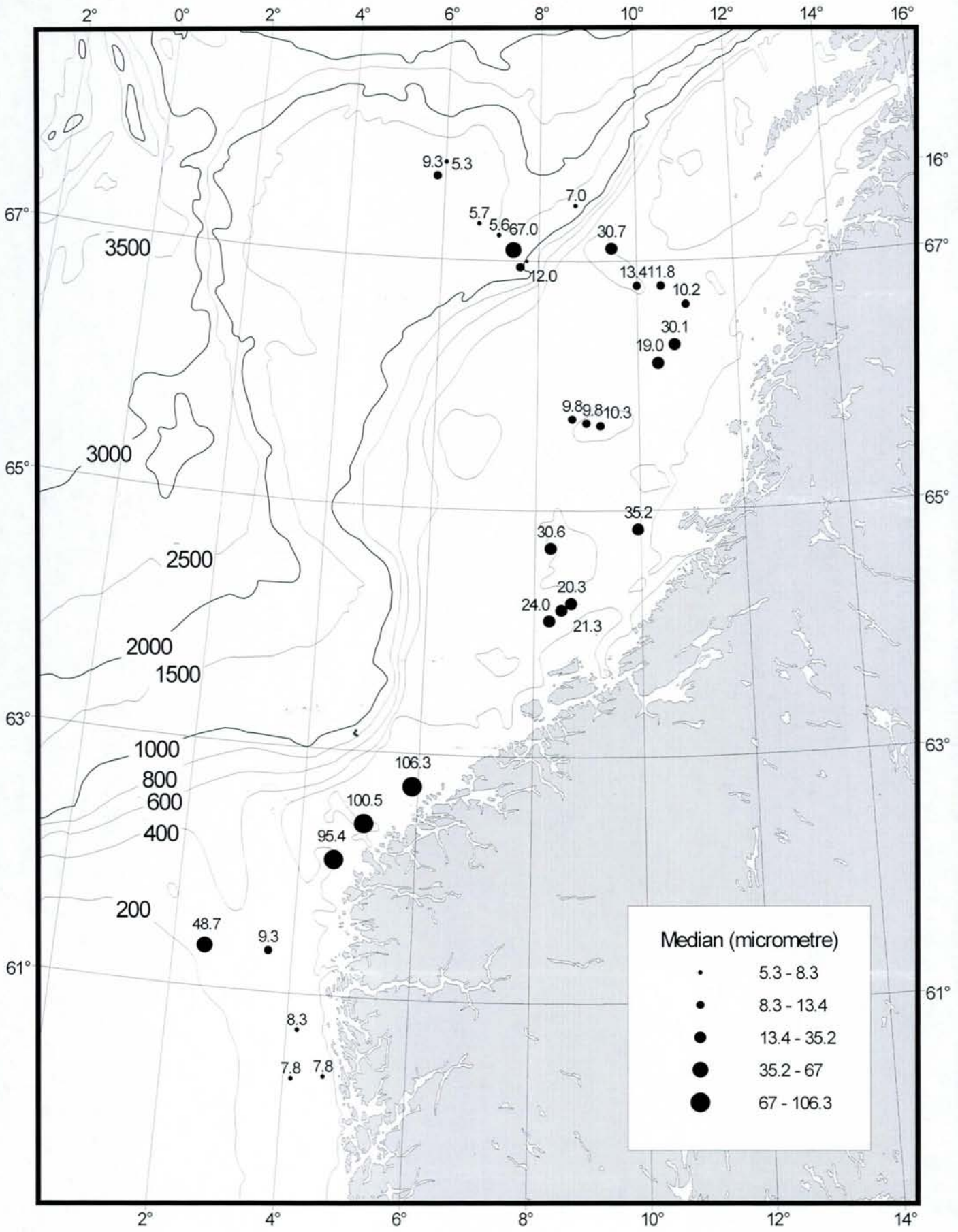


*Fig. 2. Median diameter (μm) of the surface sediments.*

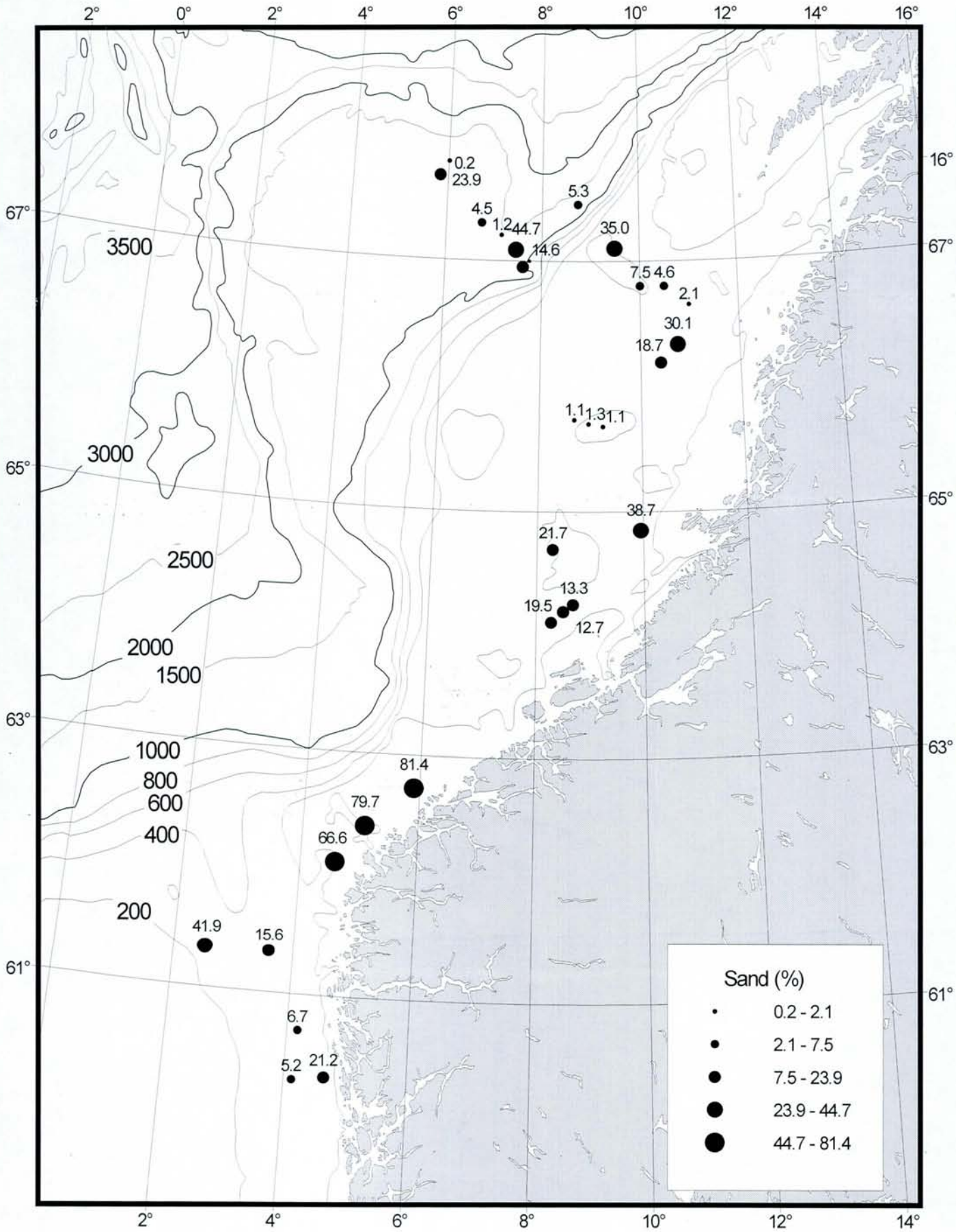


*Fig. 3. Sand (63-2000 μm) contents in the surface sediments.*

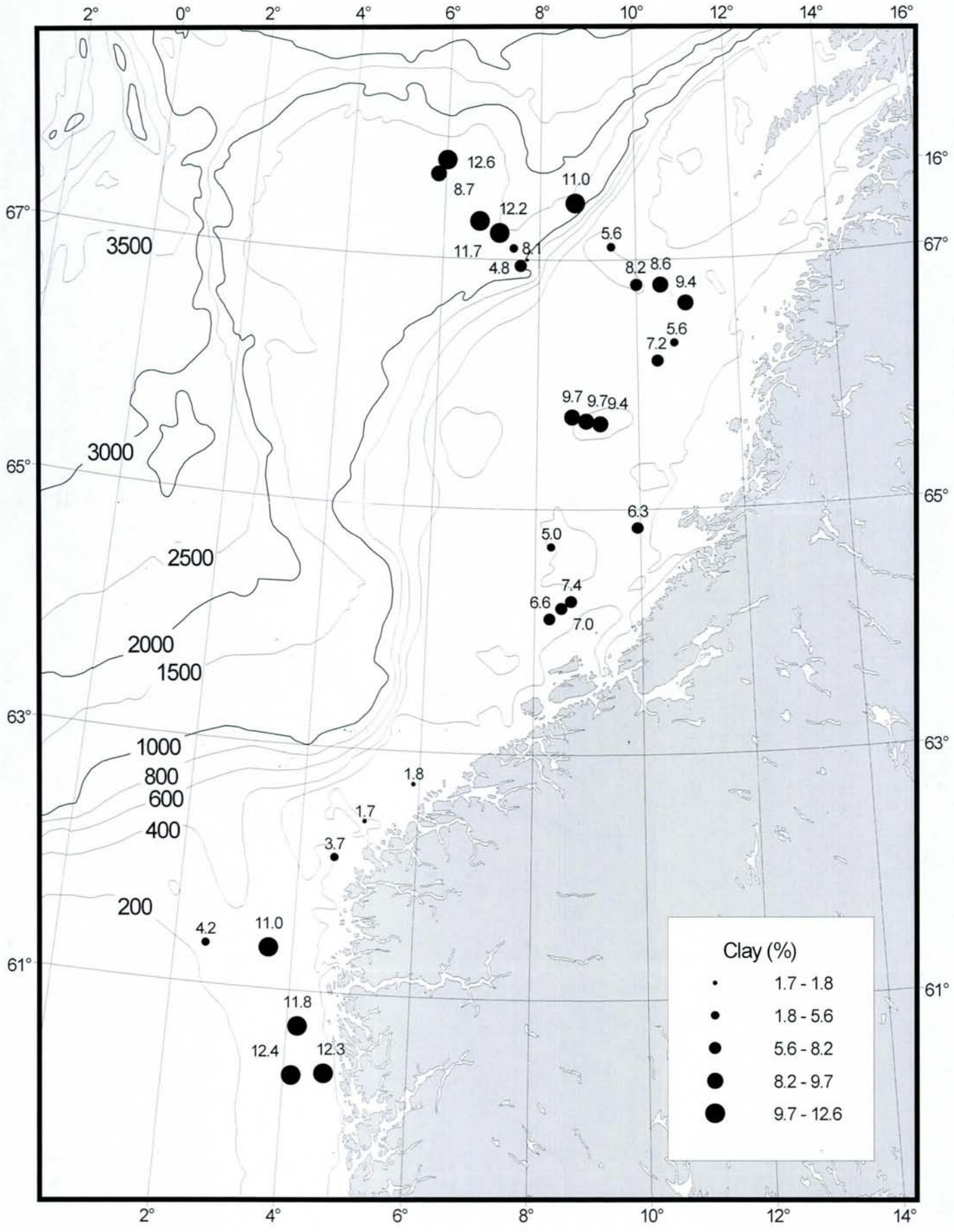


*Fig. 4. Clay (< 2 μm) contents in the surface sediments.*

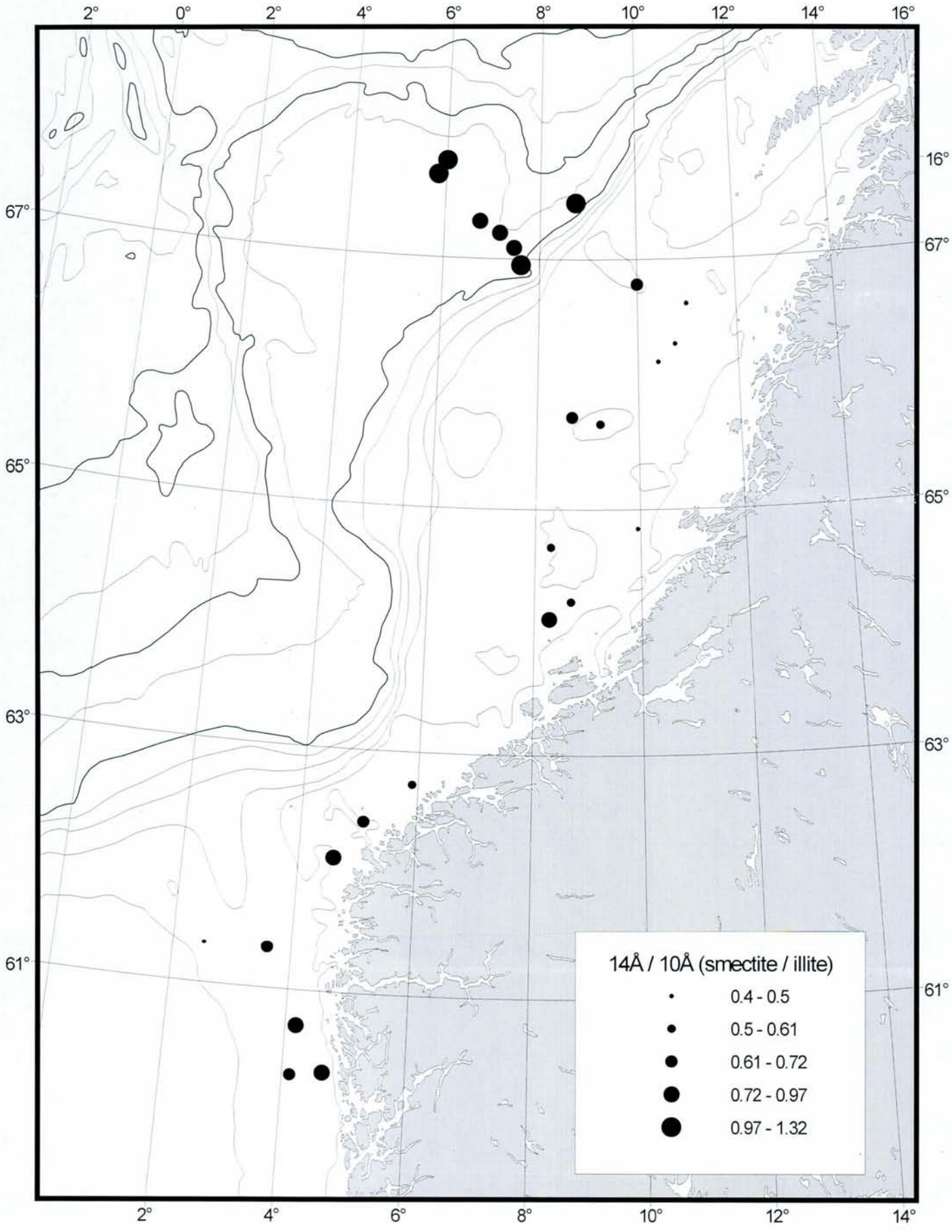


*Fig. 5. Ratios of background corrected peak heights at 14 Å and 10 Å using X-ray diffraction pattern of untreated clay fraction. This ratio reflects relative abundance of smectite (14 Å) and illite (10 Å) in sediments.*

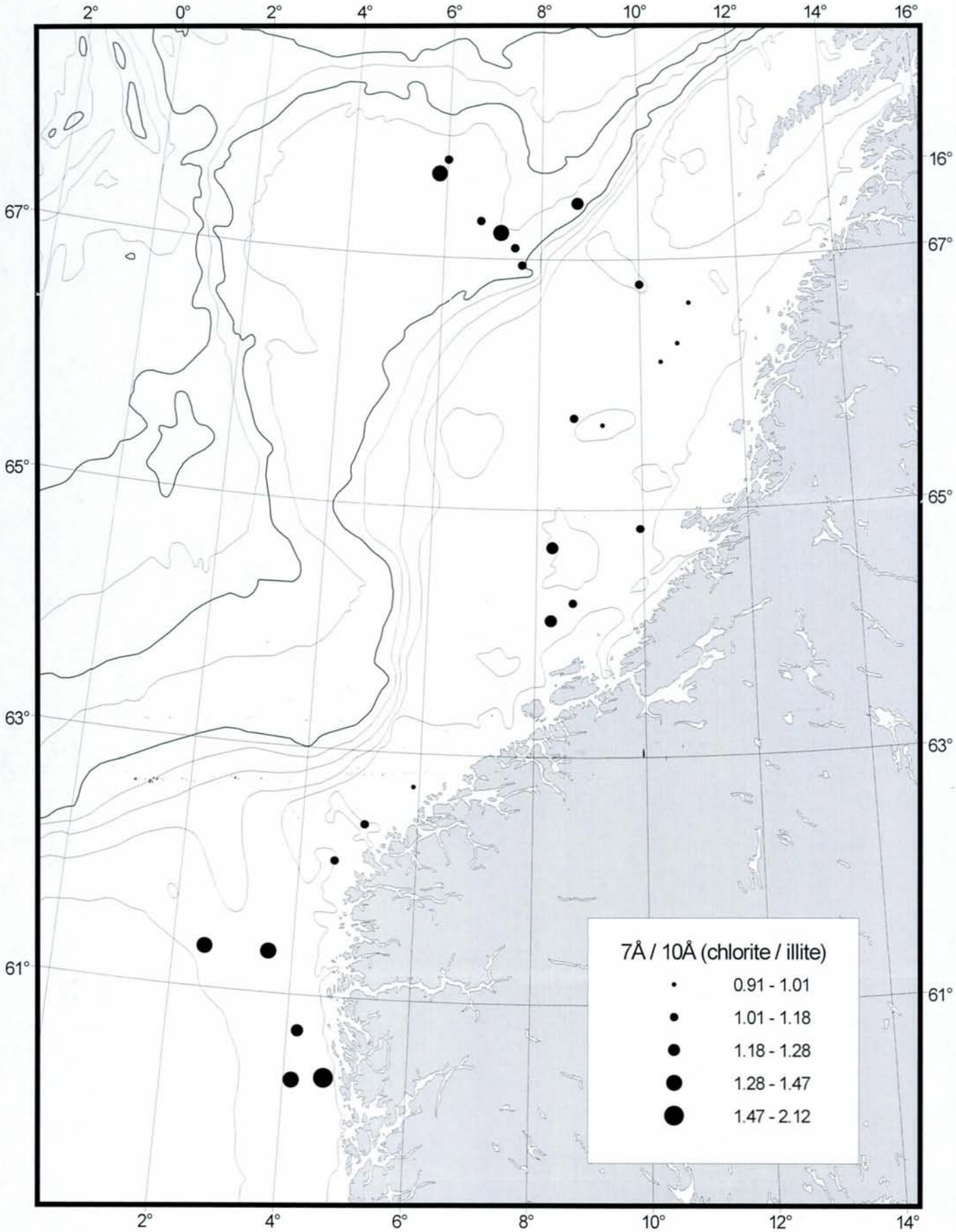


*Fig. 6. Ratios of background corrected peak heights at 7 Å and 10 Å using X-ray diffraction pattern of untreated clay fraction. This ratio reflects relative abundance of chlorite (7 Å) and illite (10 Å) in sediments.*

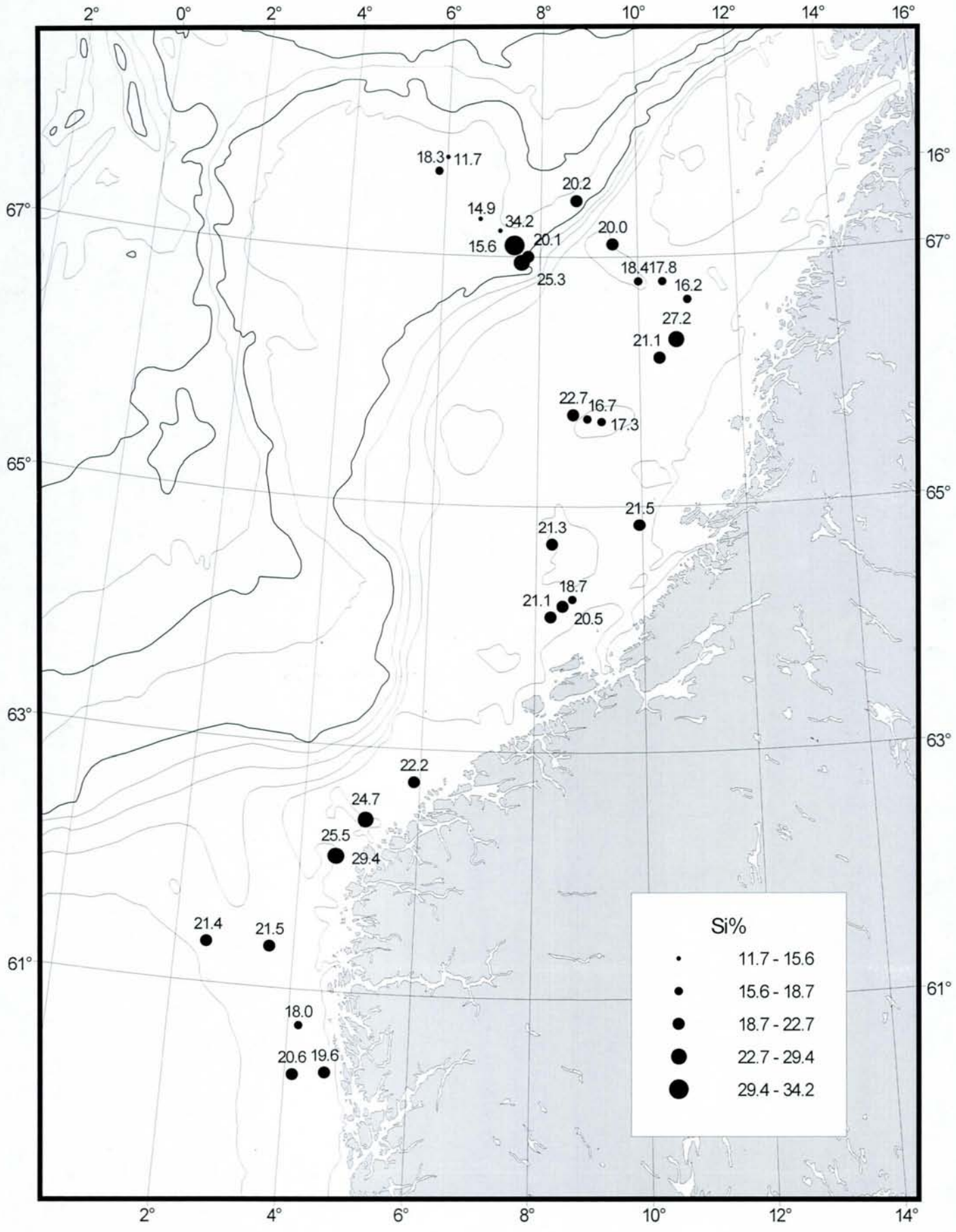


*Fig. 7. Silicon concentrations (%) in the surface sediments.*

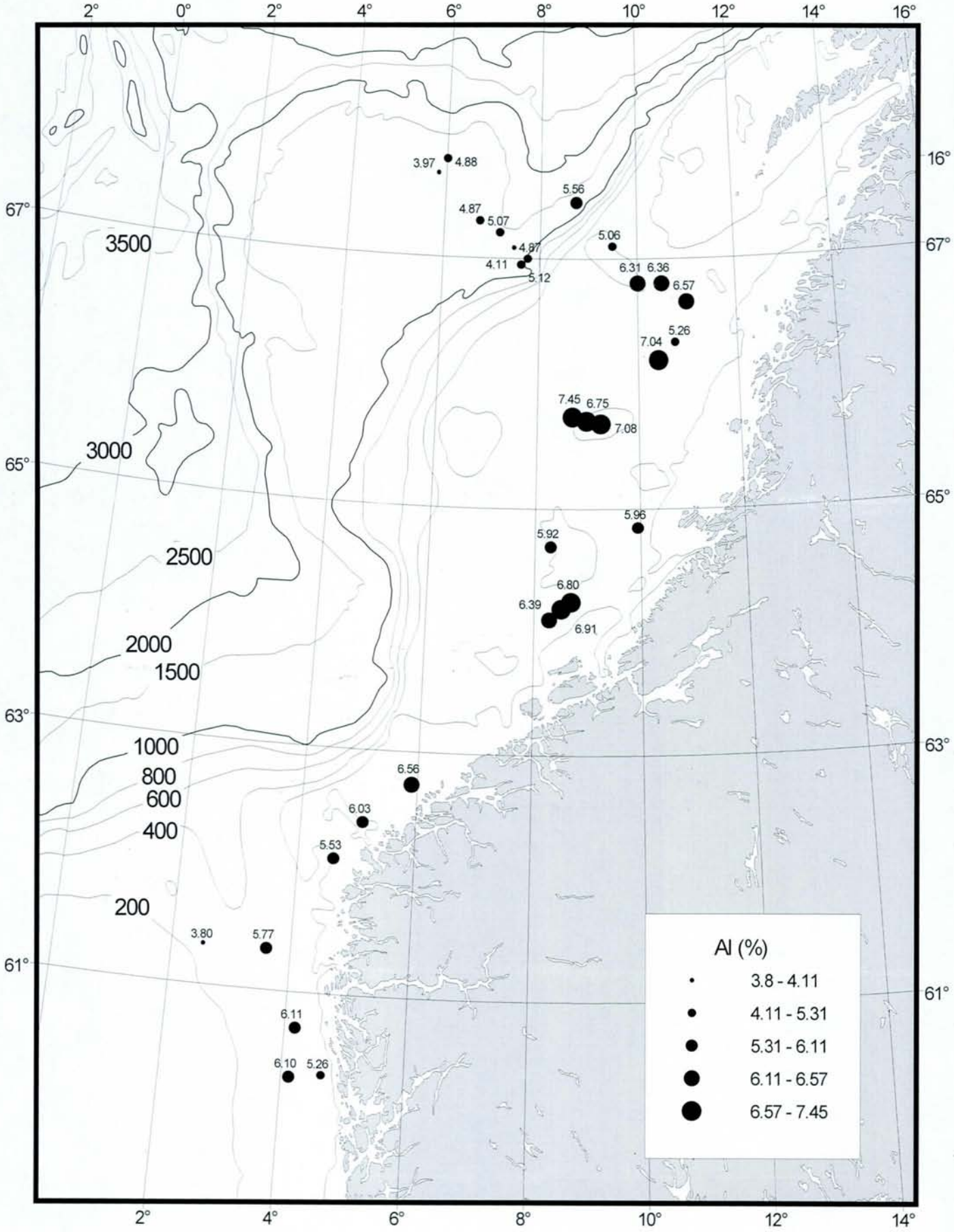


*Fig. 8. Aluminum concentrations (%) in the surface sediments.*

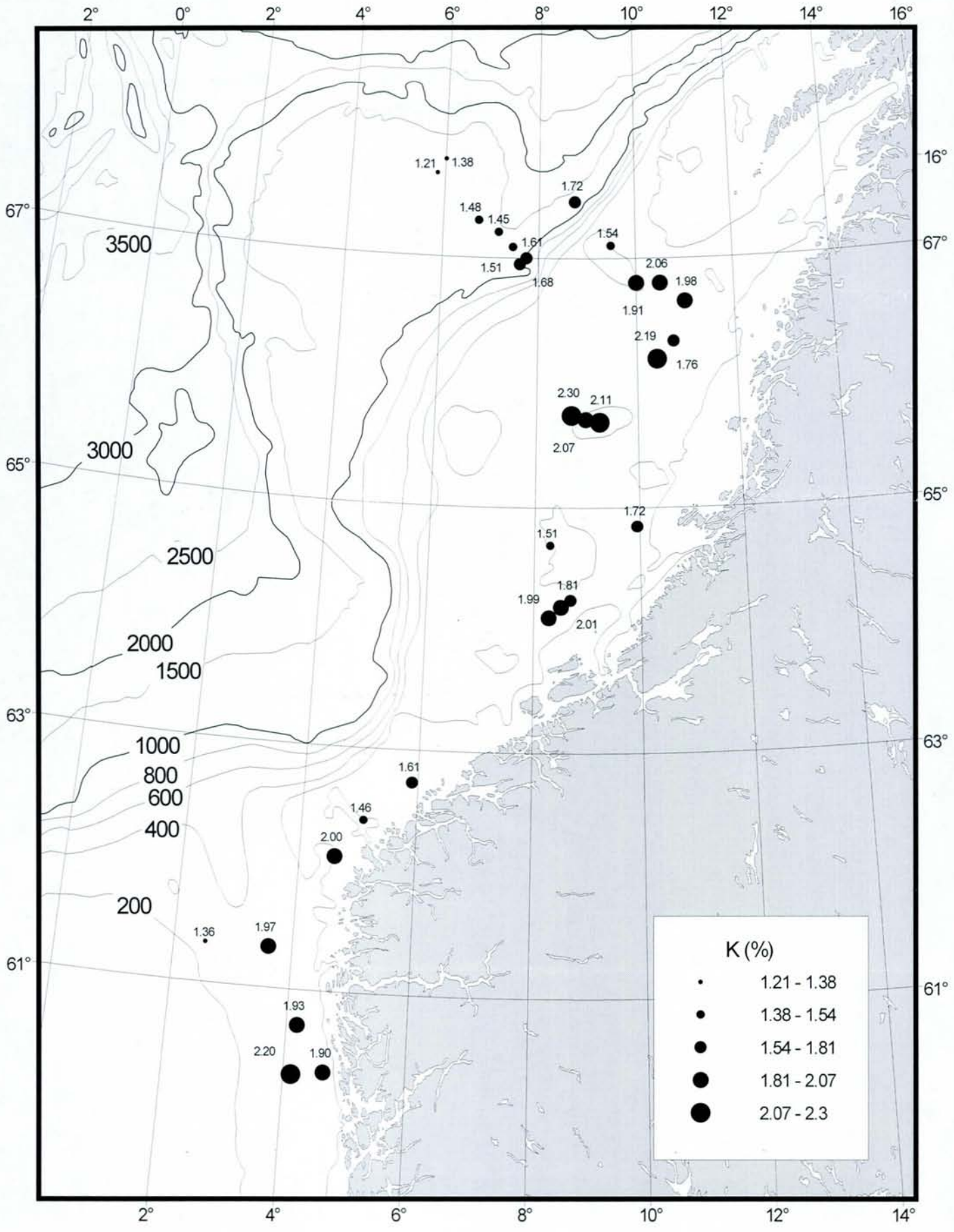


*Fig. 9. Potassium concentrations (%) in the surface sediments.*

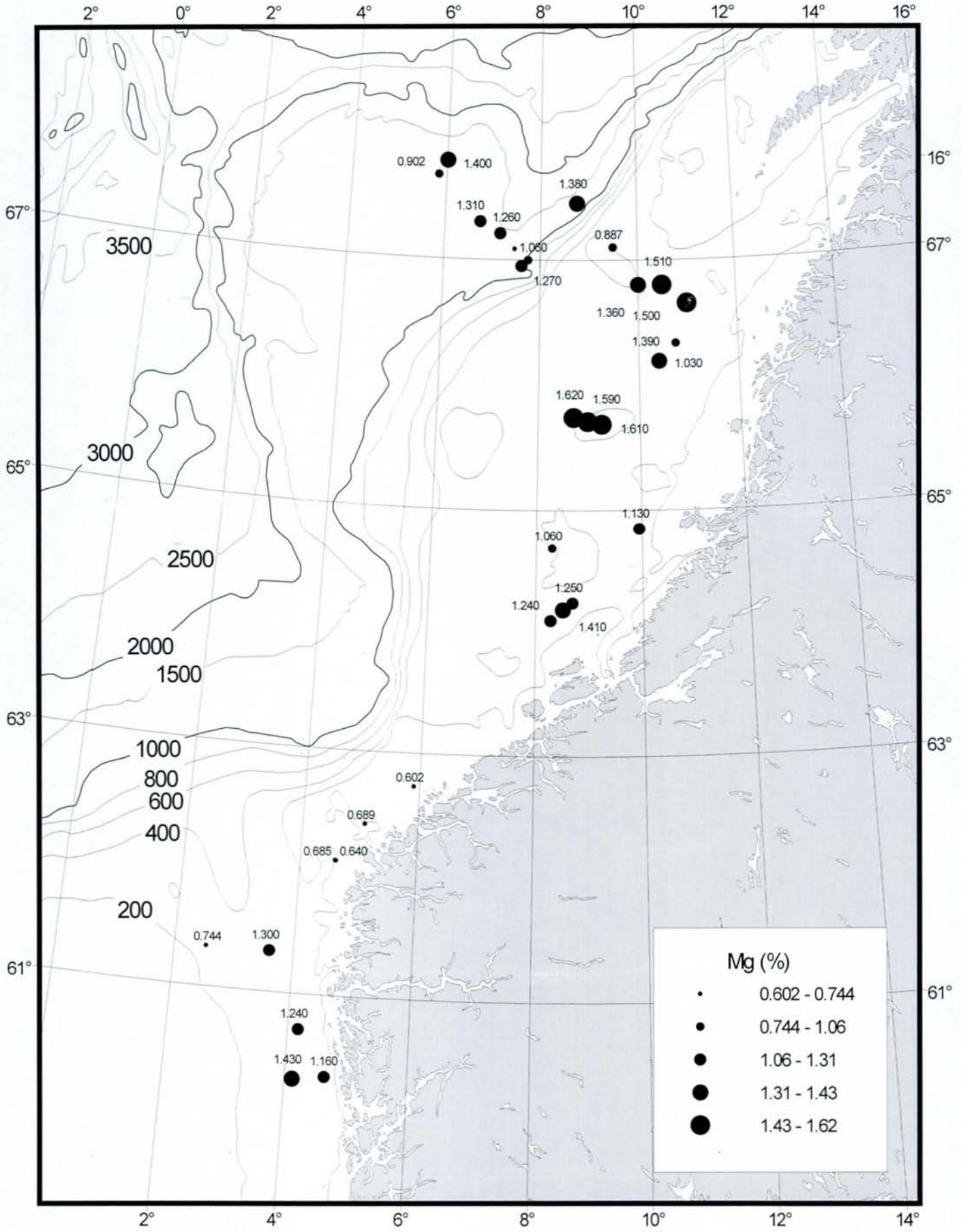


*Fig. 10. Magnesium concentrations (%) in the surface sediments.*

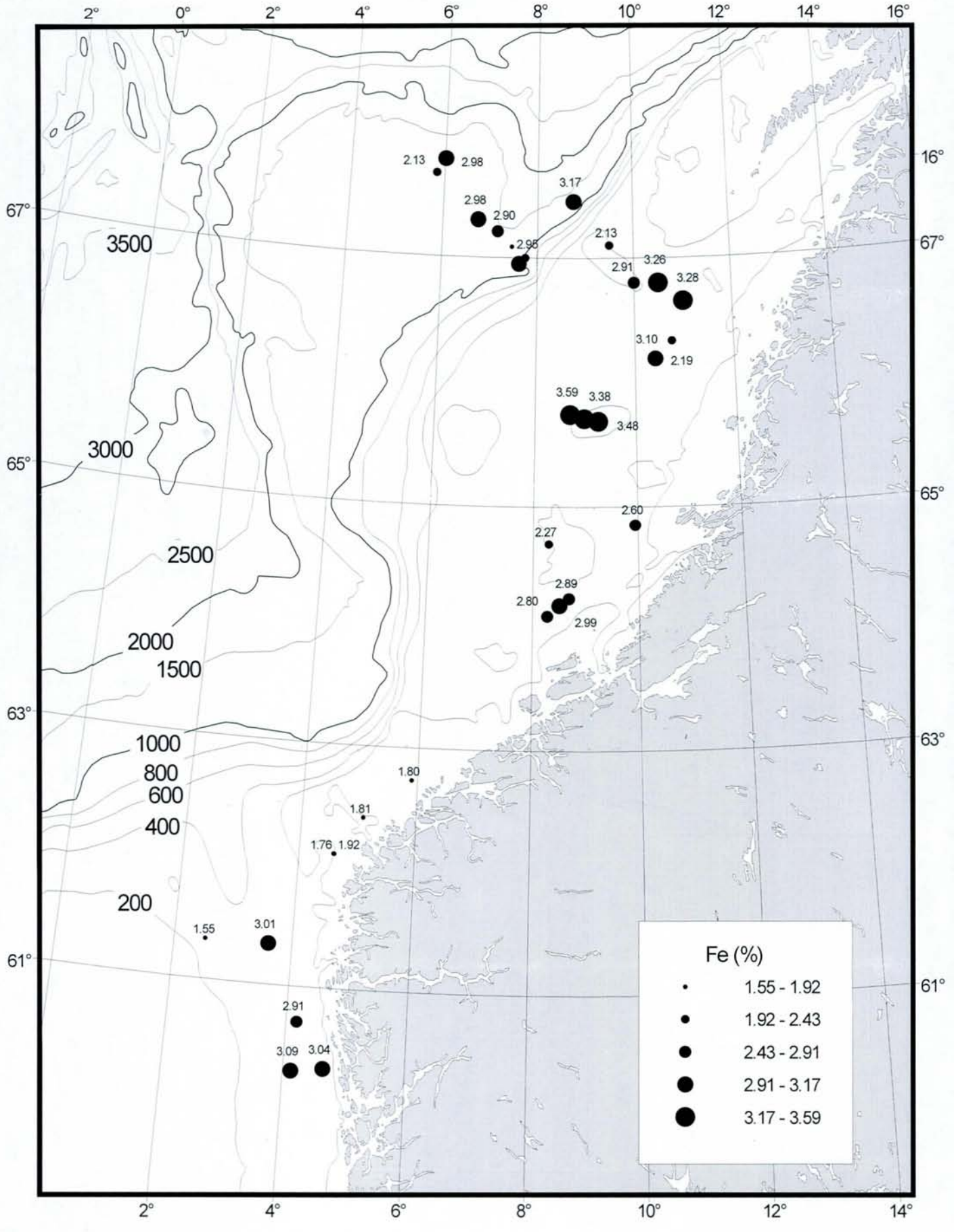


*Fig. 11. Iron concentrations (%) in the surface sediments.*

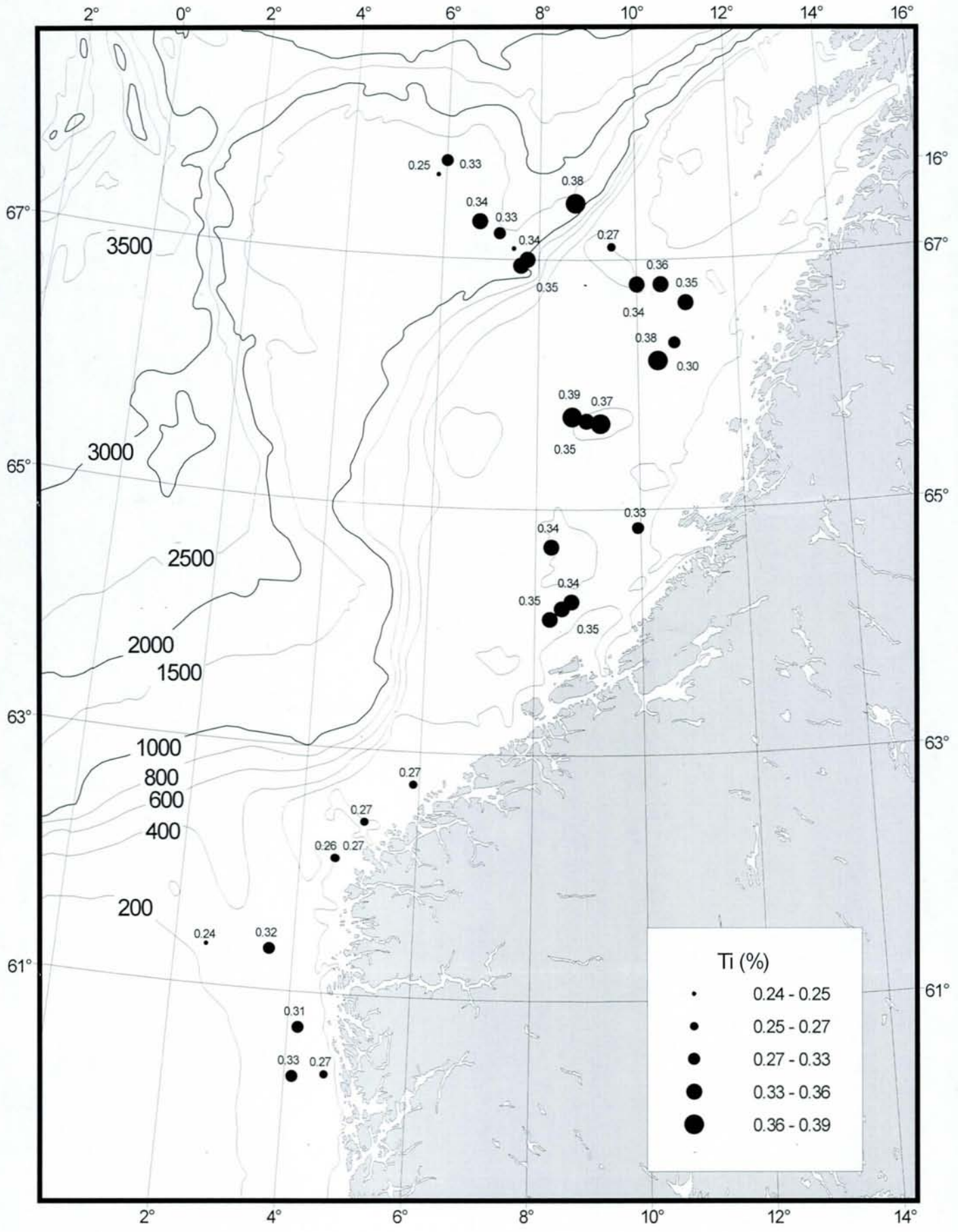


*Fig. 12. Titanium concentrations (%) in the surface sediments.*

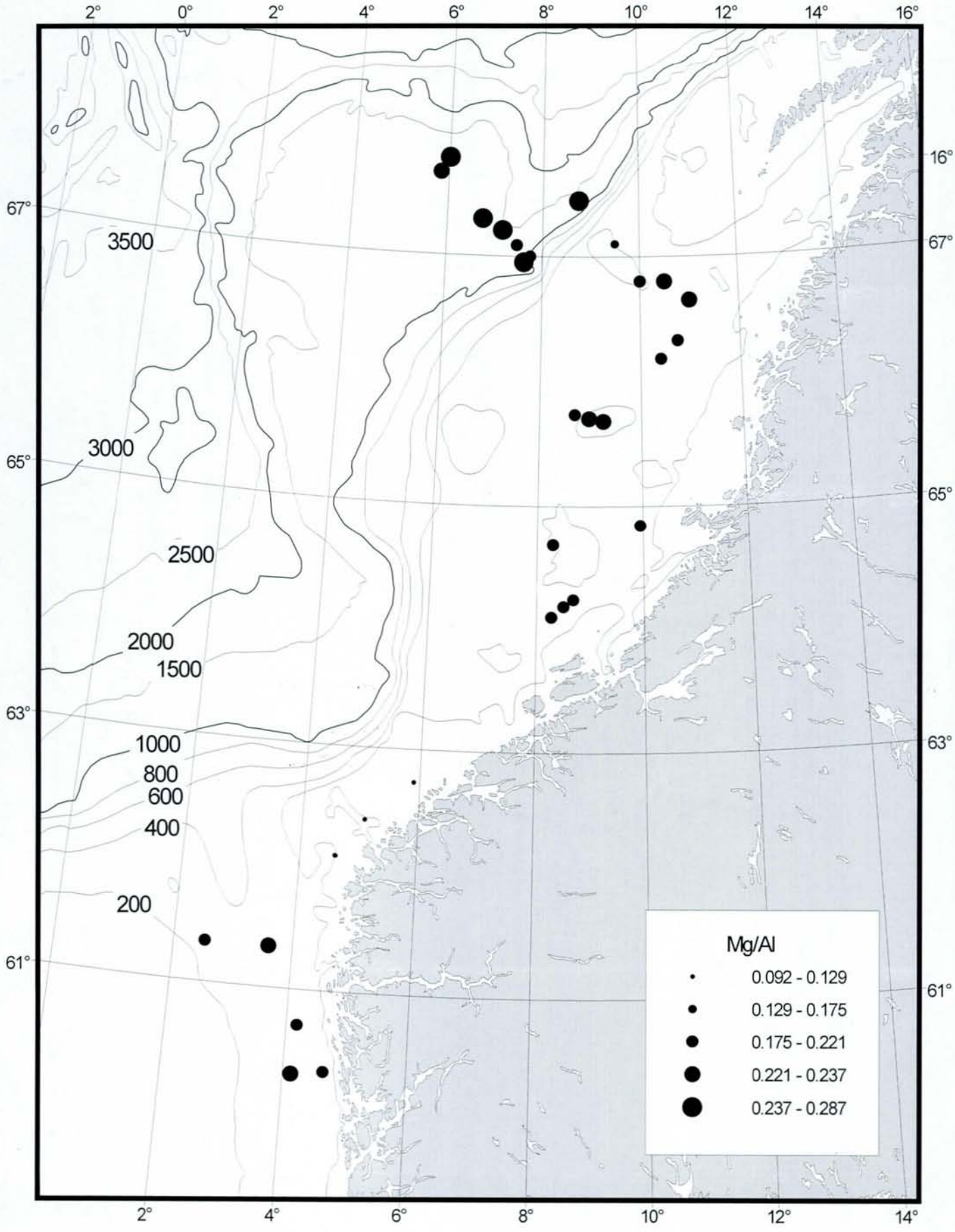


*Fig. 13. Mg/Al ratios in the surface sediments.*

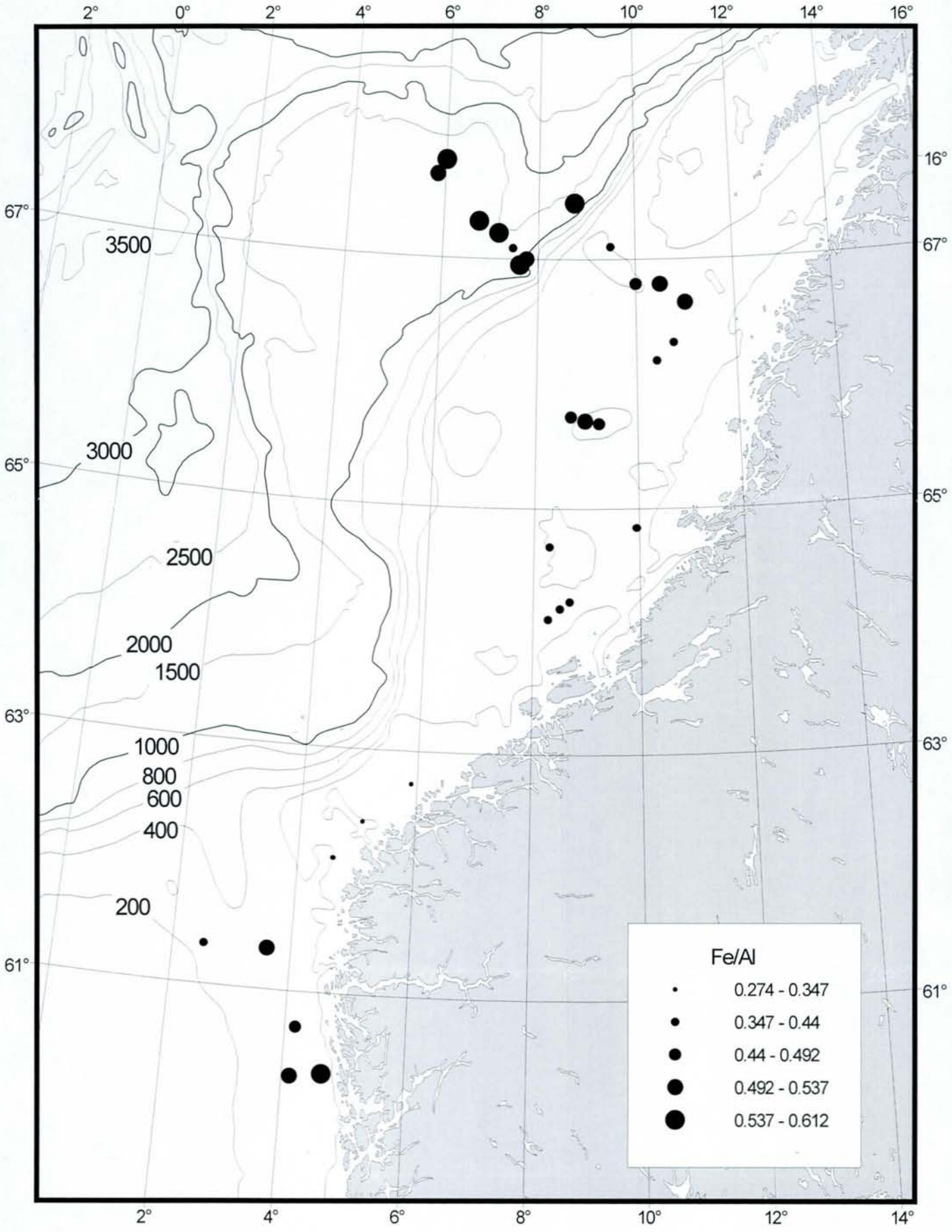


*Fig. 14. Fe/Al ratios in the surface sediments.*

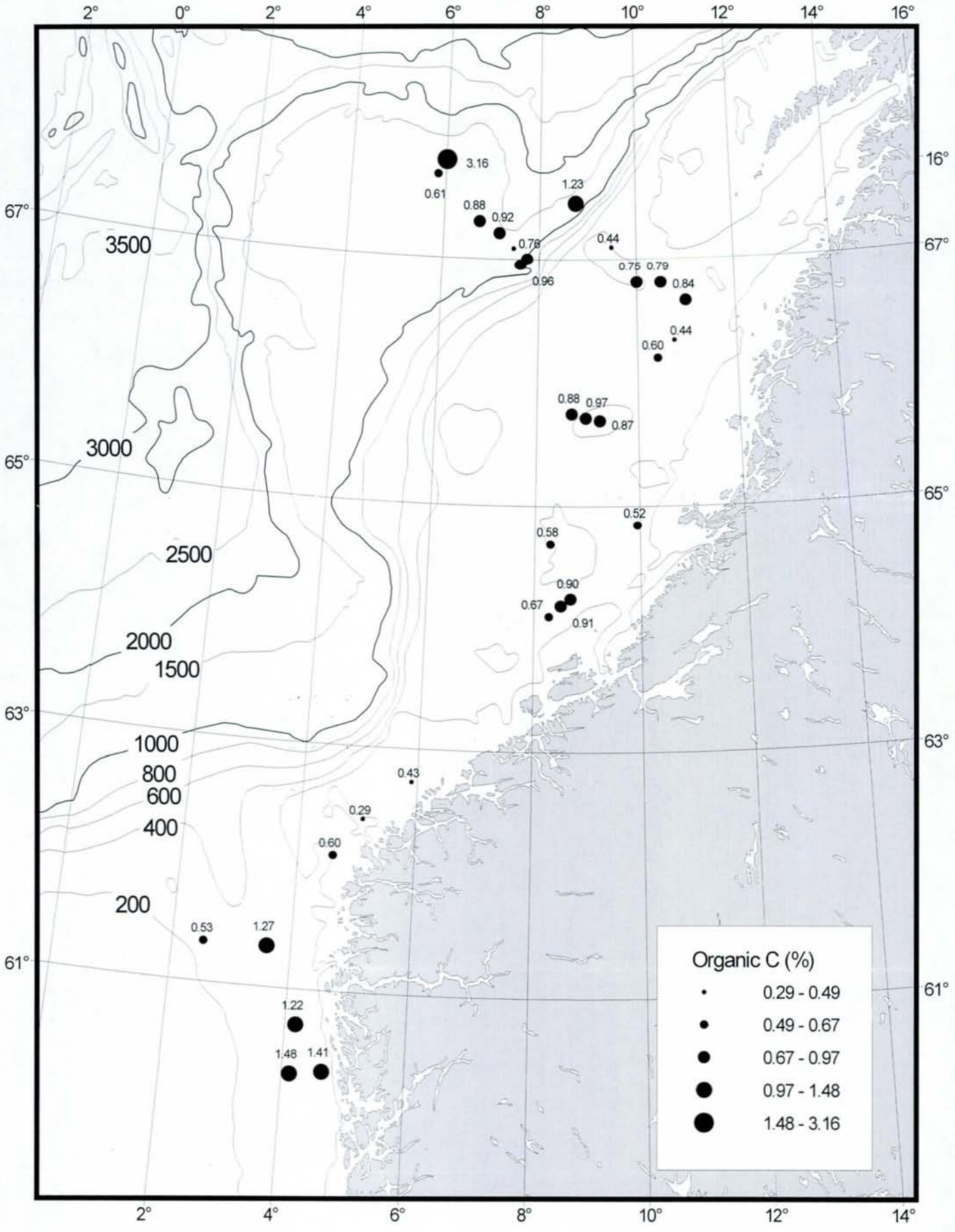


*Fig. 15. Organic Carbon concentrations (%) in the surface sediments.*

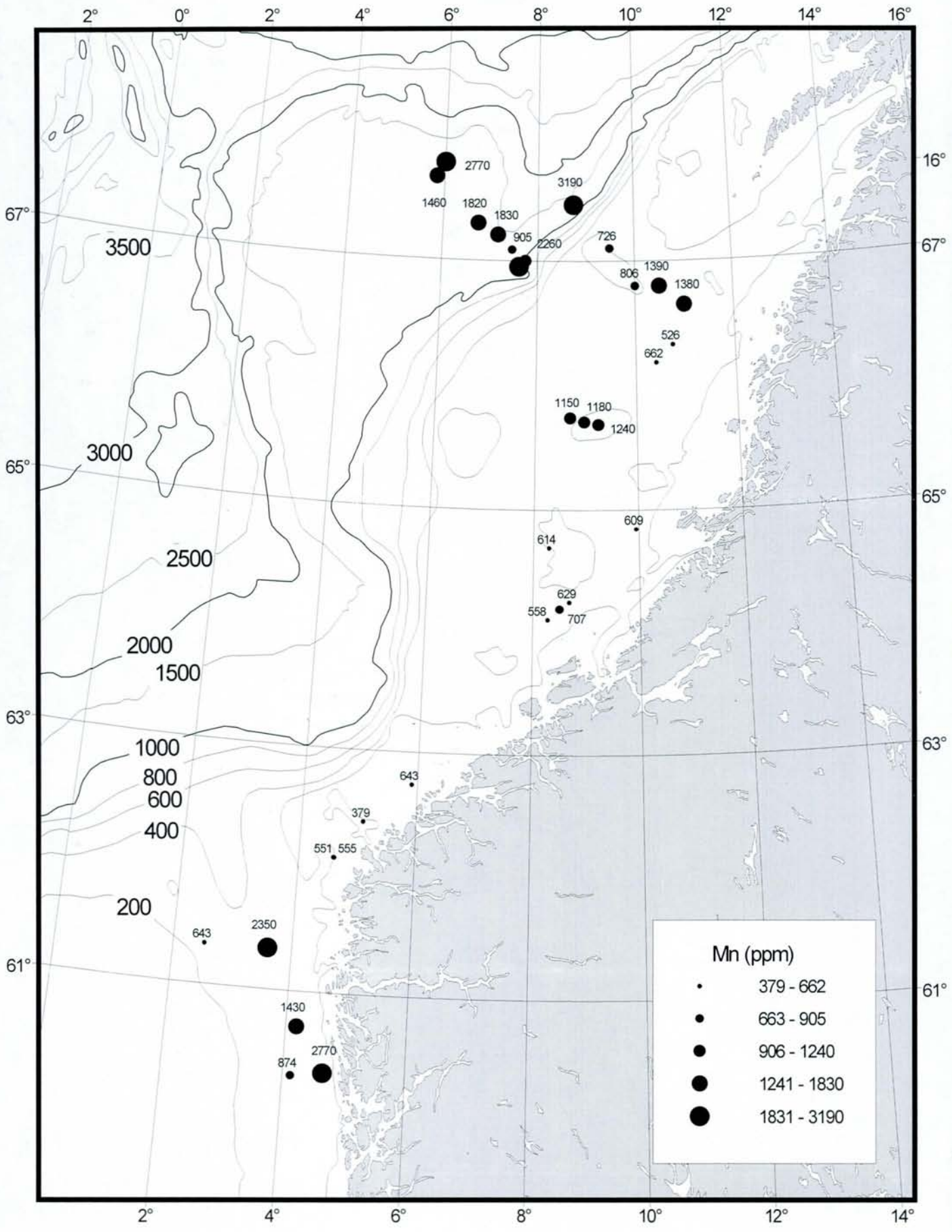


*Fig. 16. Manganese concentrations (ppm) in the surface sediments.*

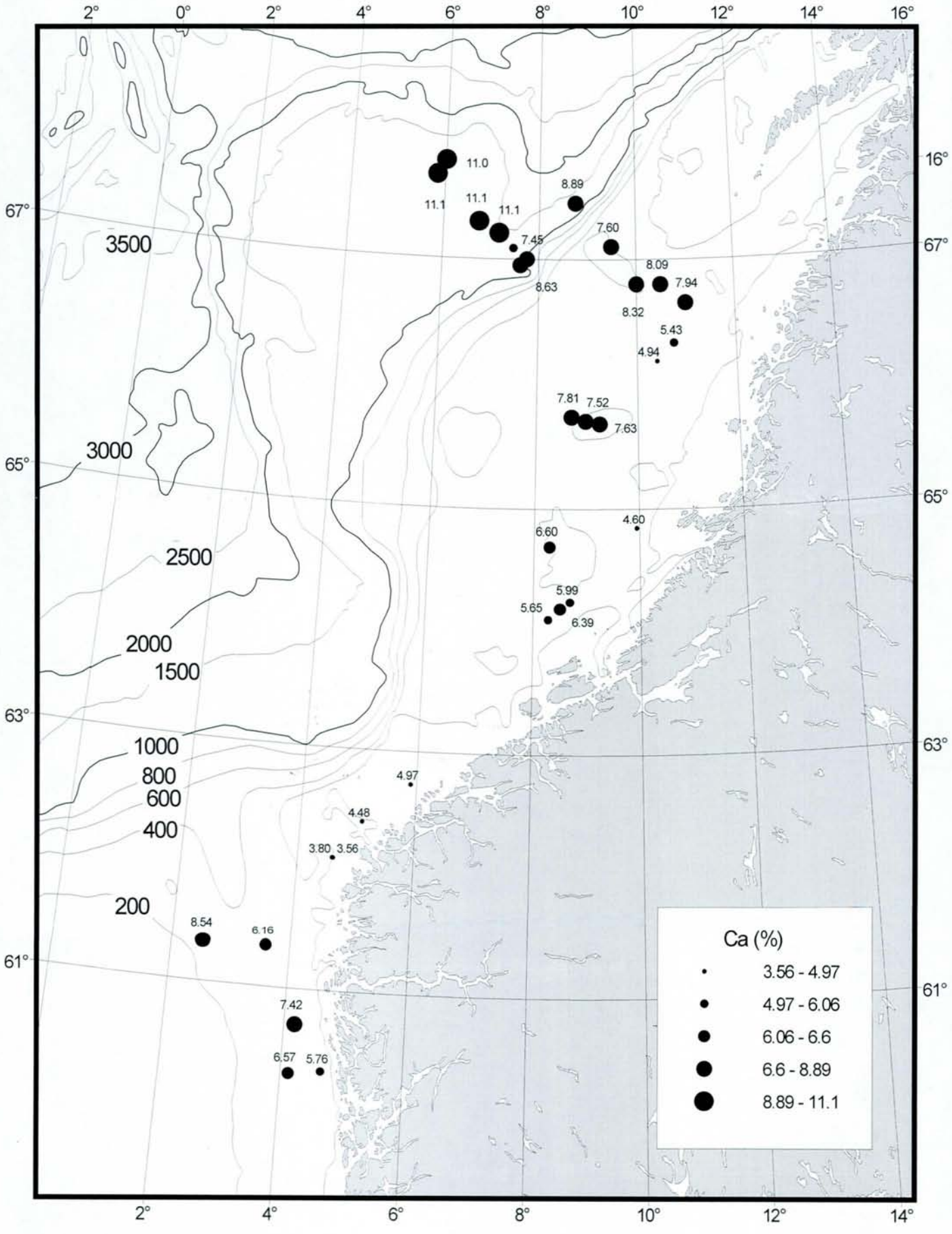


*Fig. 17. Calcium concentrations (%) in the surface sediments.*

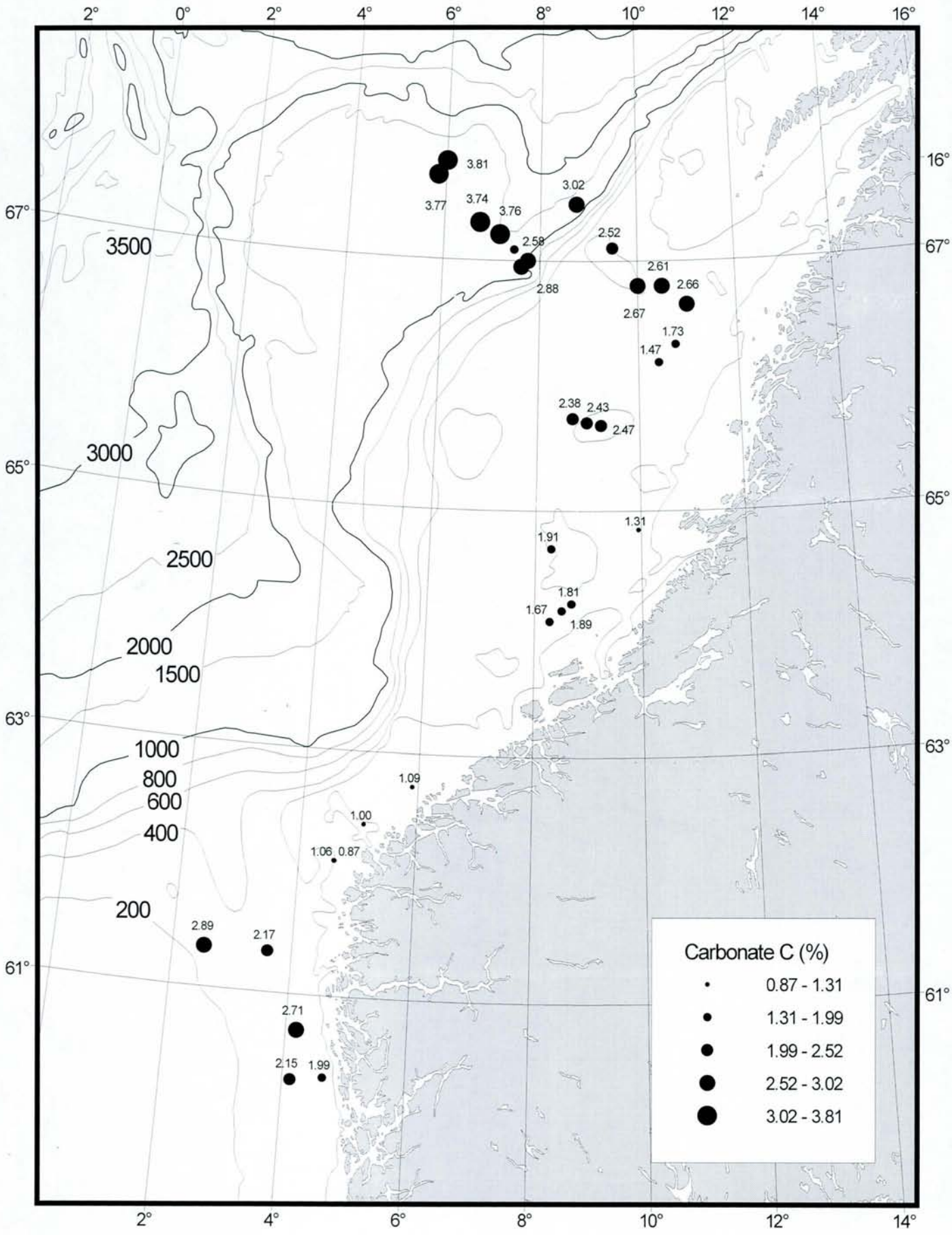


*Fig. 18. Carbonate Carbon concentrations (%) in the surface sediments.*

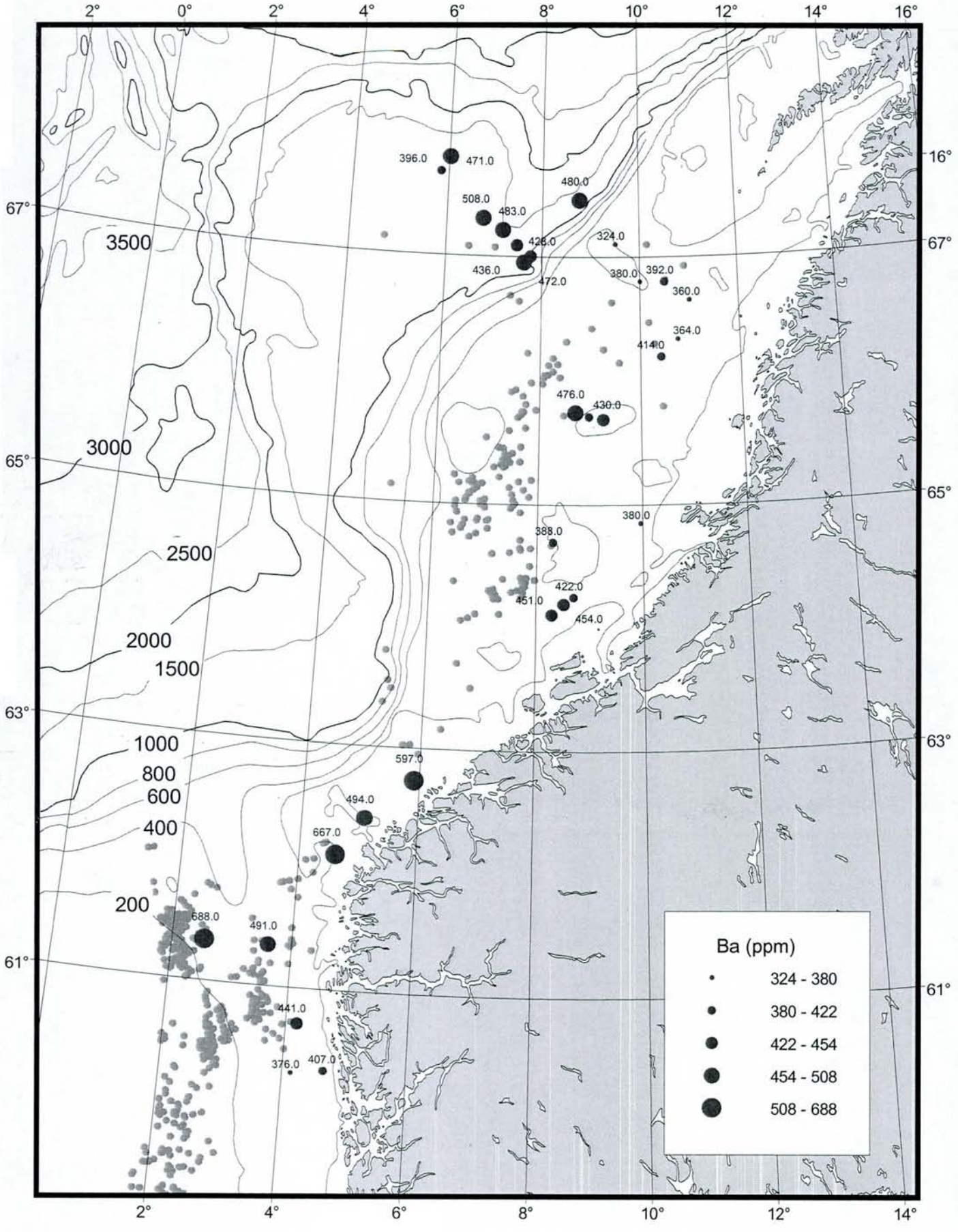


*Fig. 19. Barium concentrations (ppm) in the surface sediments. The drilling sites of off-shore hydrocarbon exploration (NPD database) are indicated in gray. Note that highest Ba concentrations occur in immediate vicinity of drilling sites.*

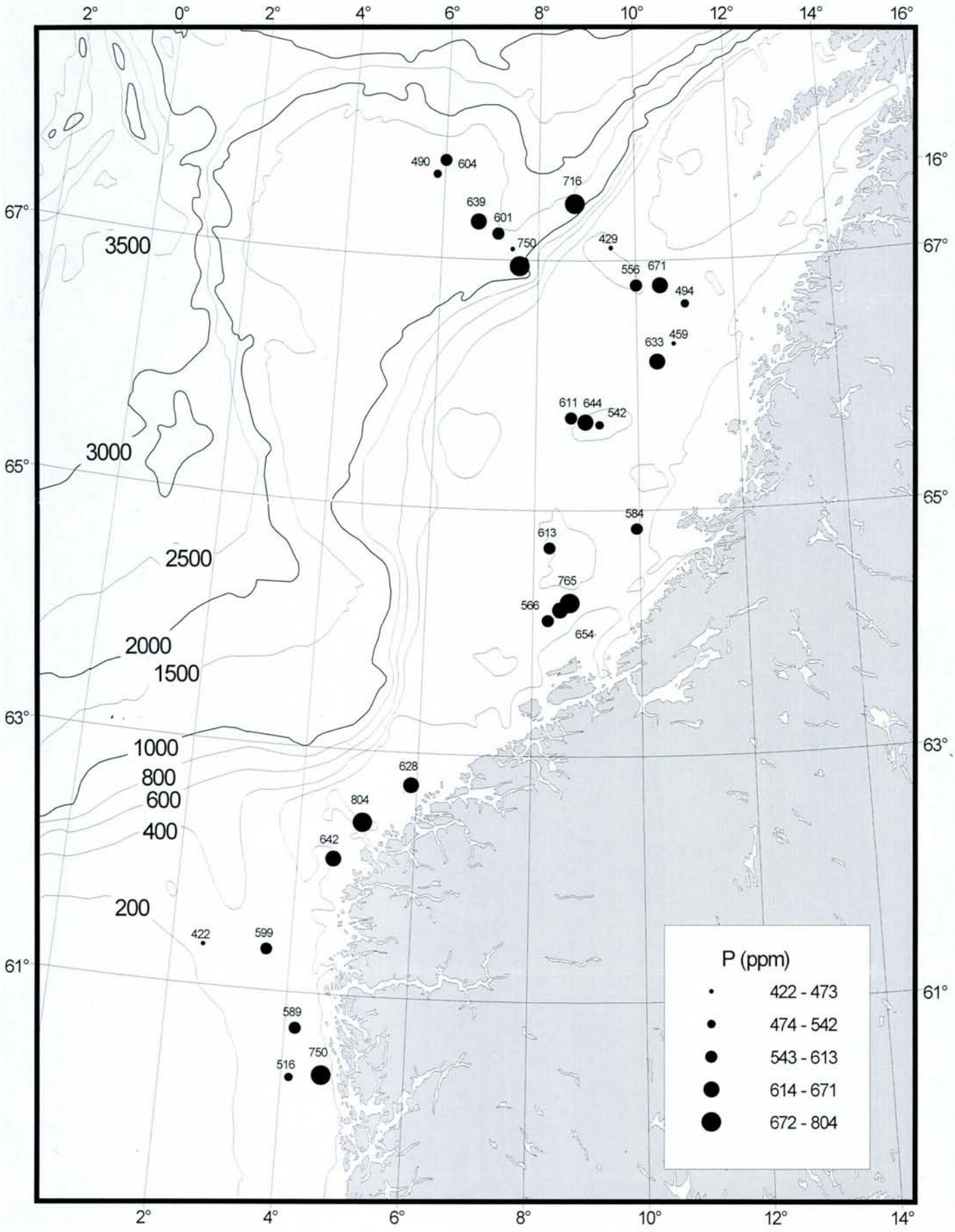


*Fig. 20. Phosphorous concentrations (ppm) in the surface sediments.*

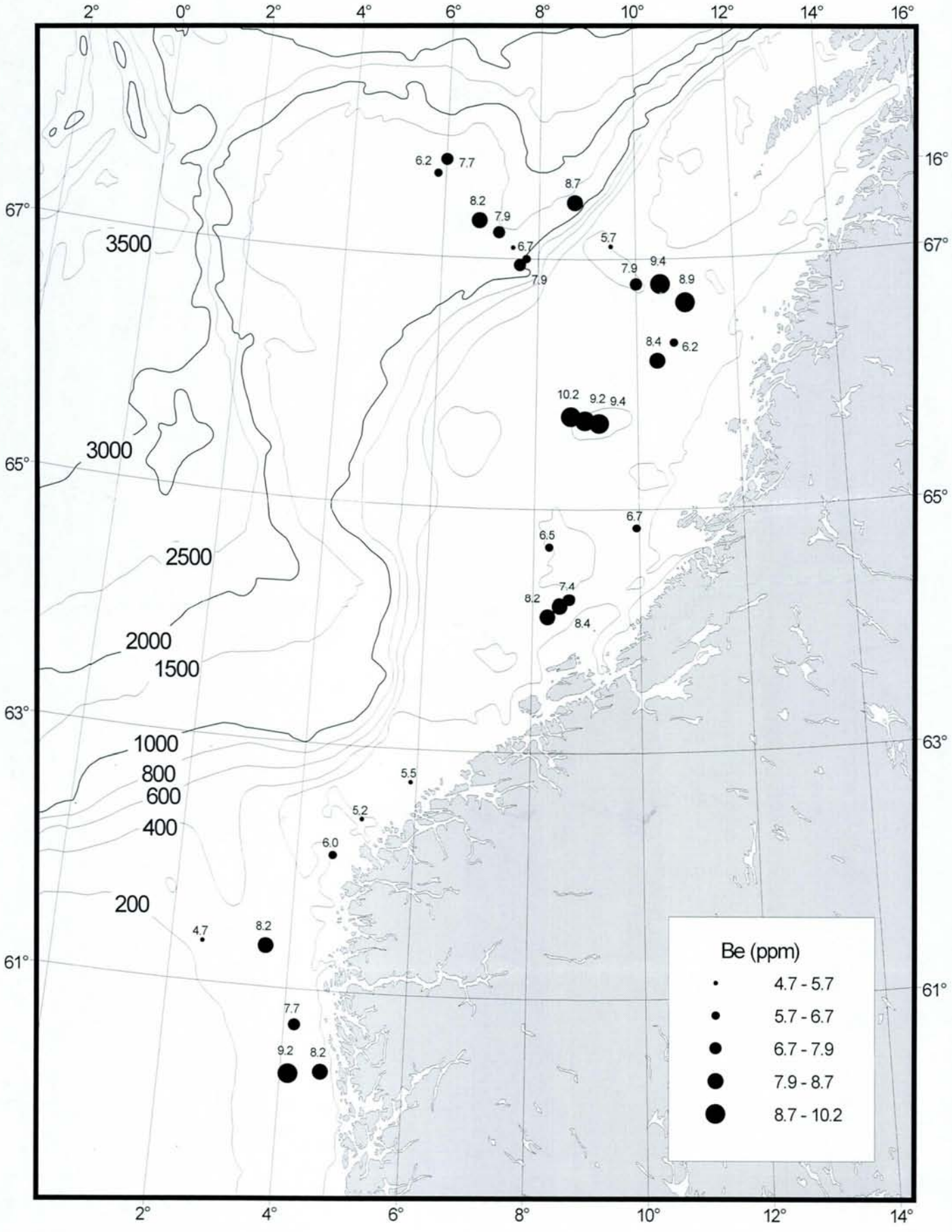


*Fig. 21. Beryllium concentrations (ppm) in the surface sediments.*

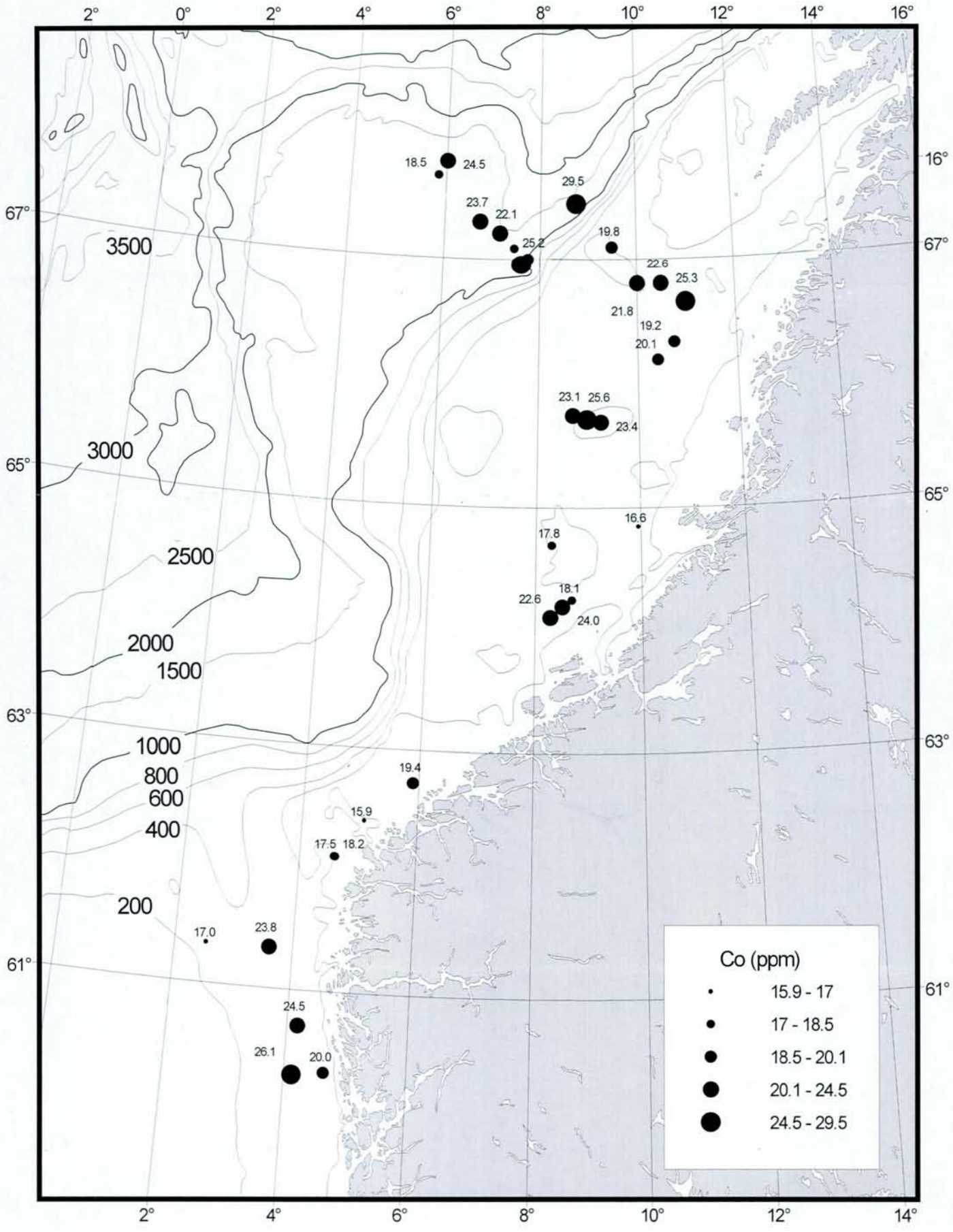


*Fig. 22. Cobalt concentrations (ppm) in the surface sediments.*

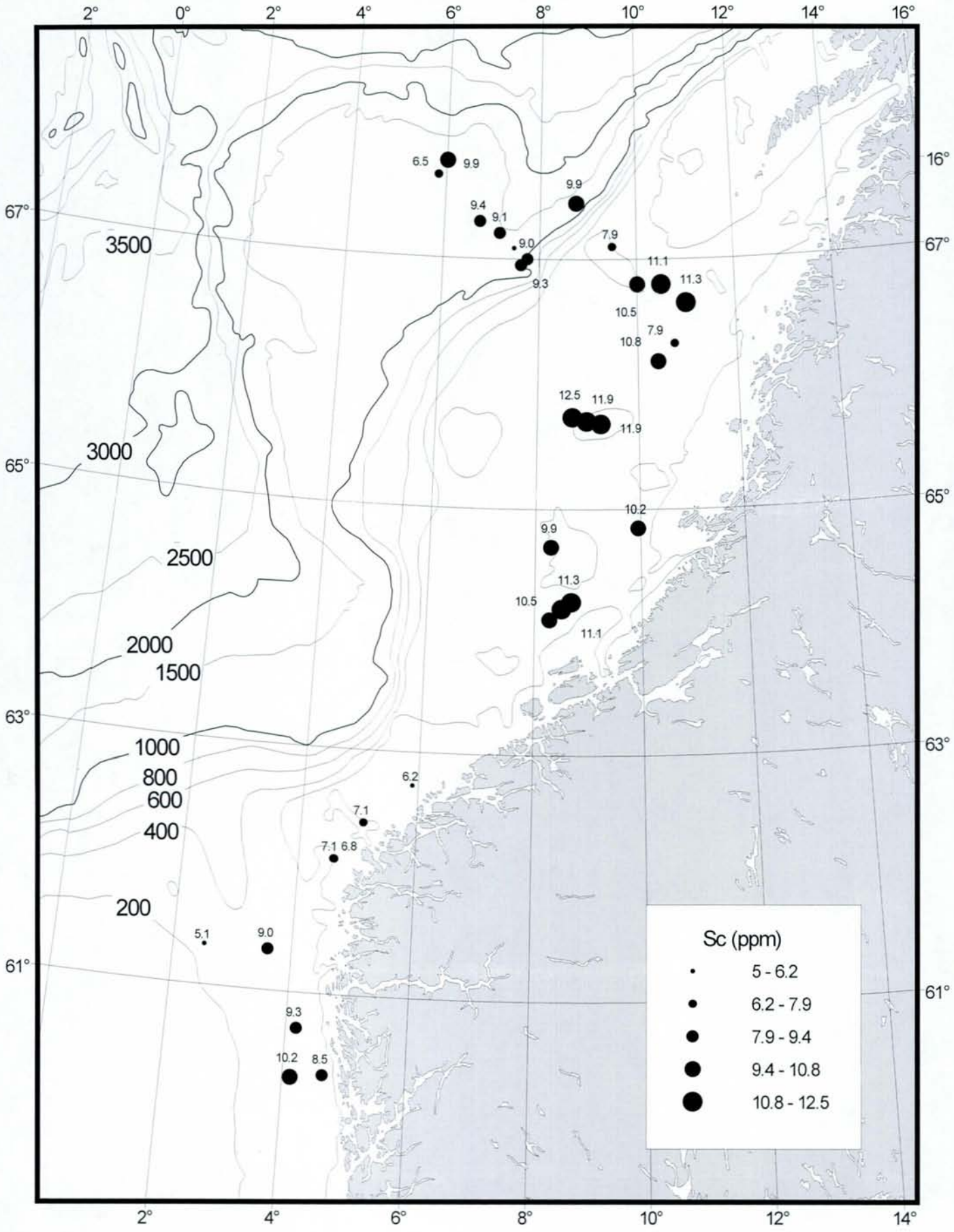


*Fig. 23. Scandium concentrations (ppm) in the surface sediments.*

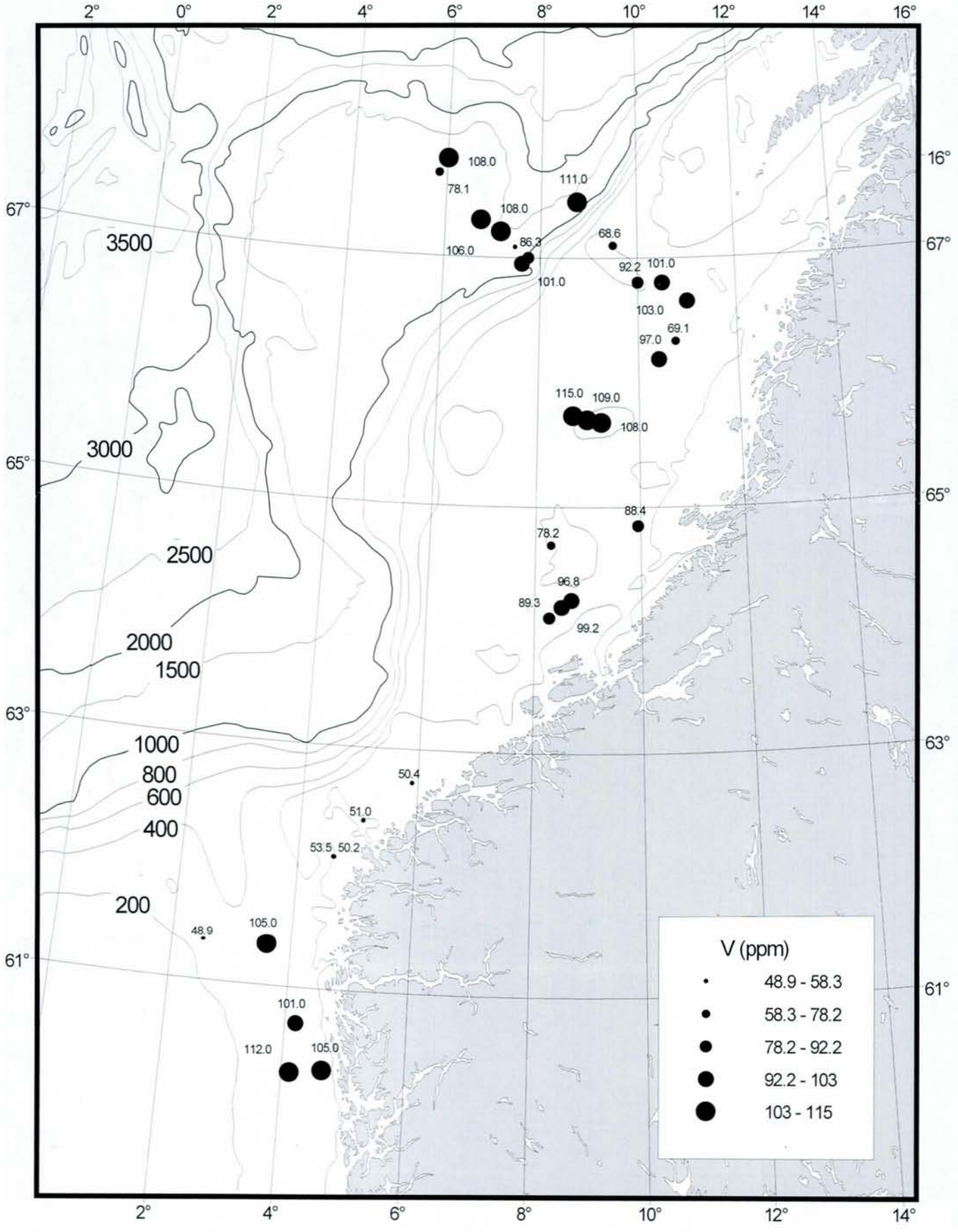


*Fig. 24. Vanadium concentrations (ppm) in the surface sediments.*

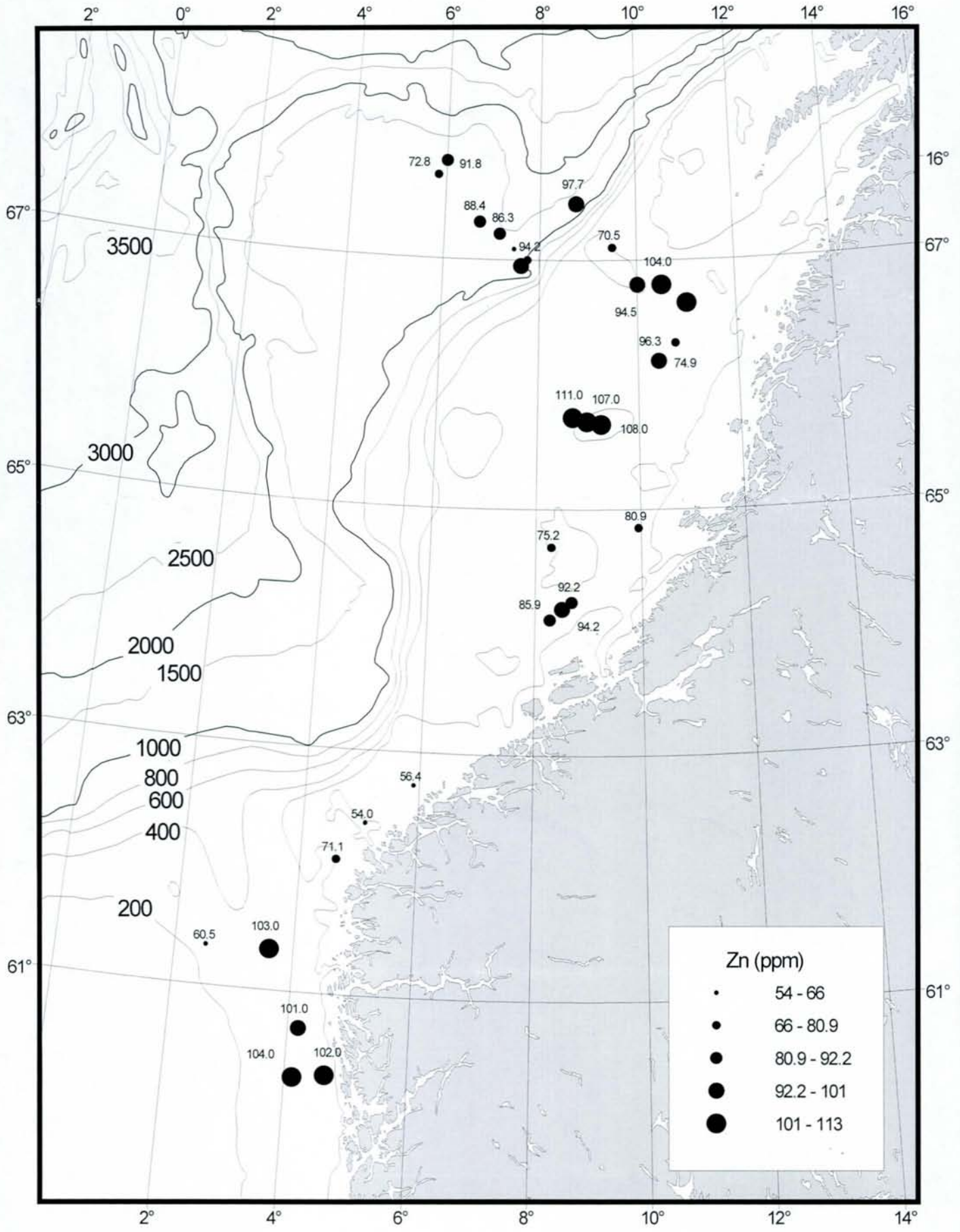


*Fig. 25. Zinc concentrations (ppm) in the surface sediments.*

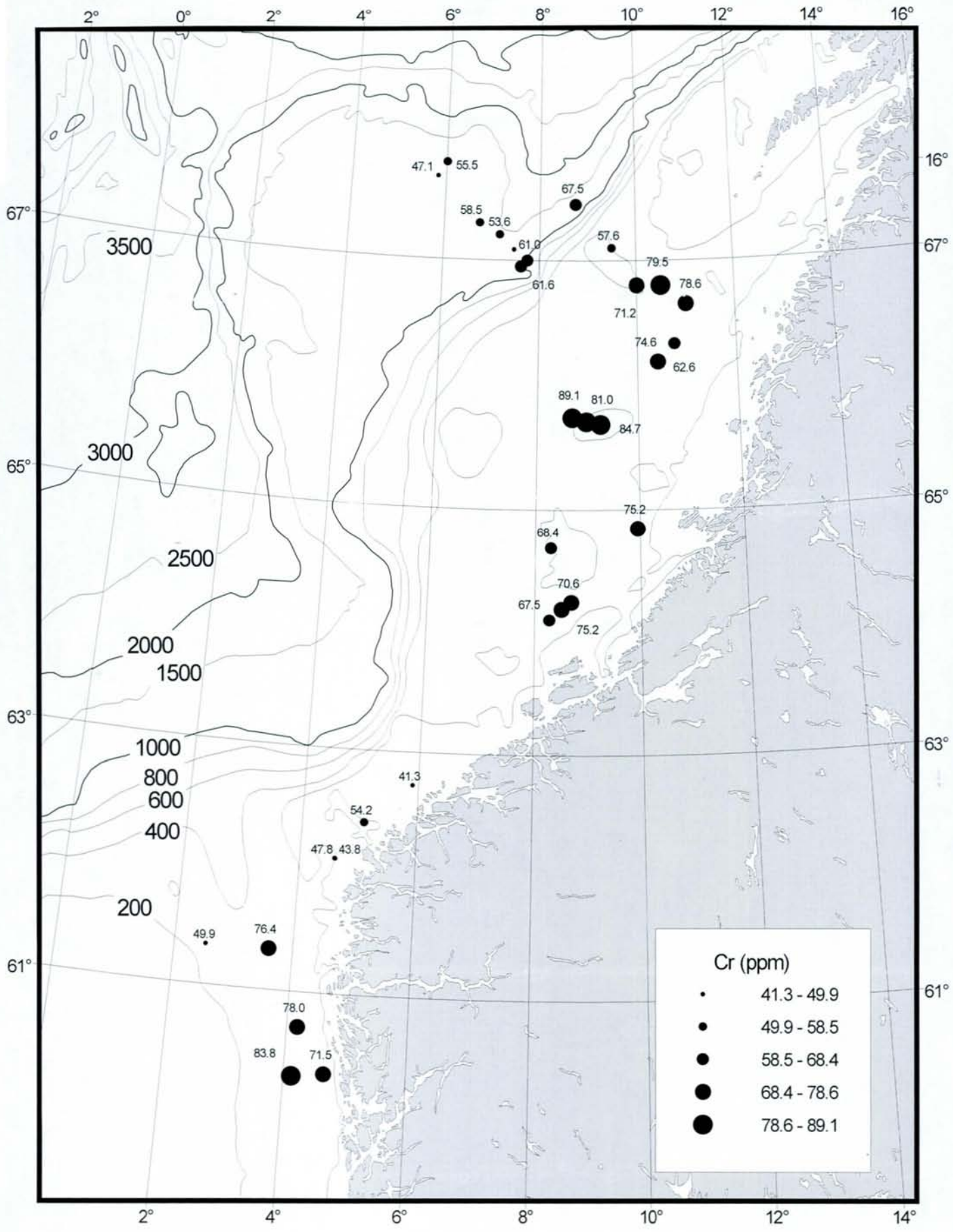


*Fig. 26. Chromium concentrations (ppm) in the surface sediments.*

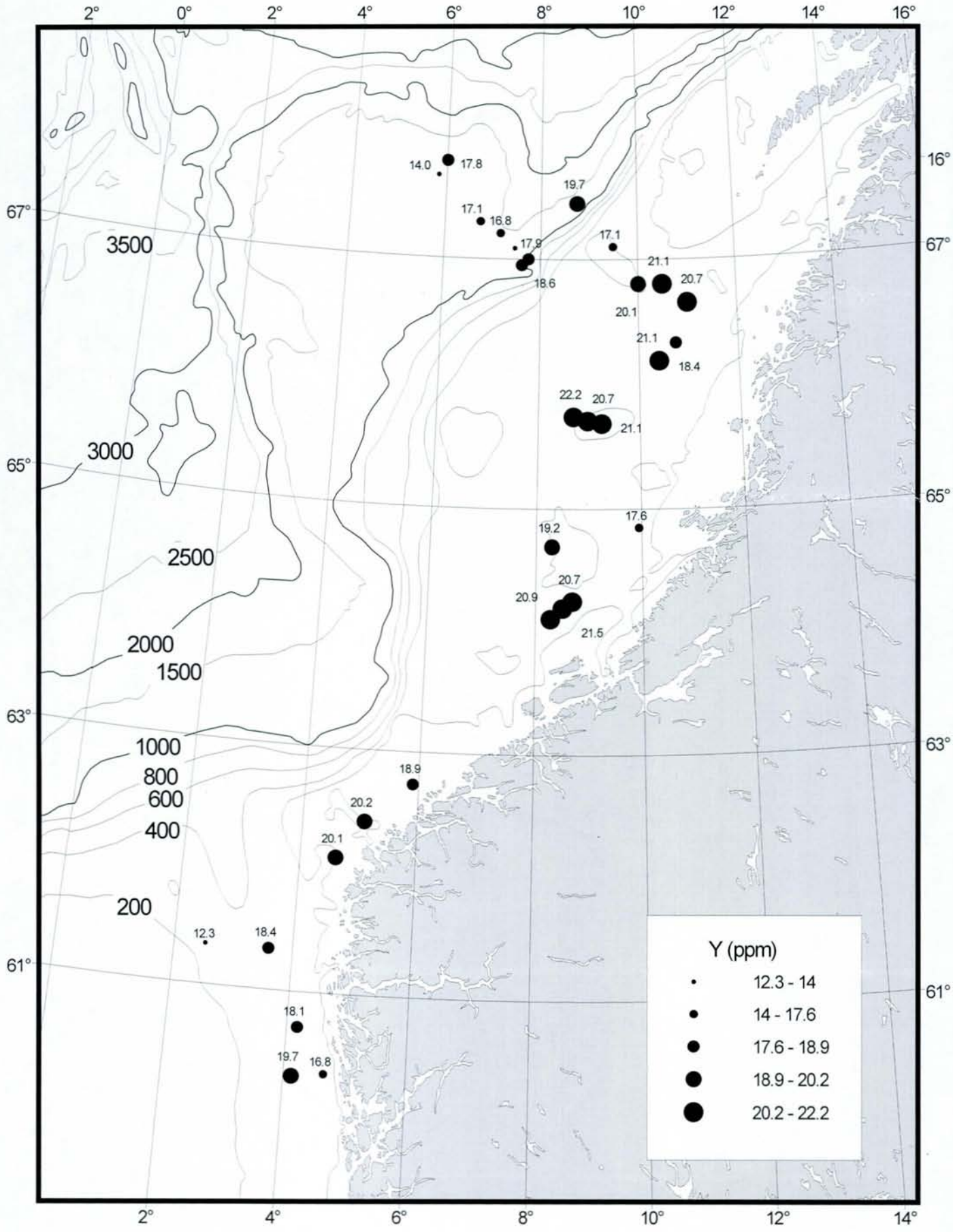


*Fig. 27. Yttrium concentrations (ppm) in the surface sediments.*

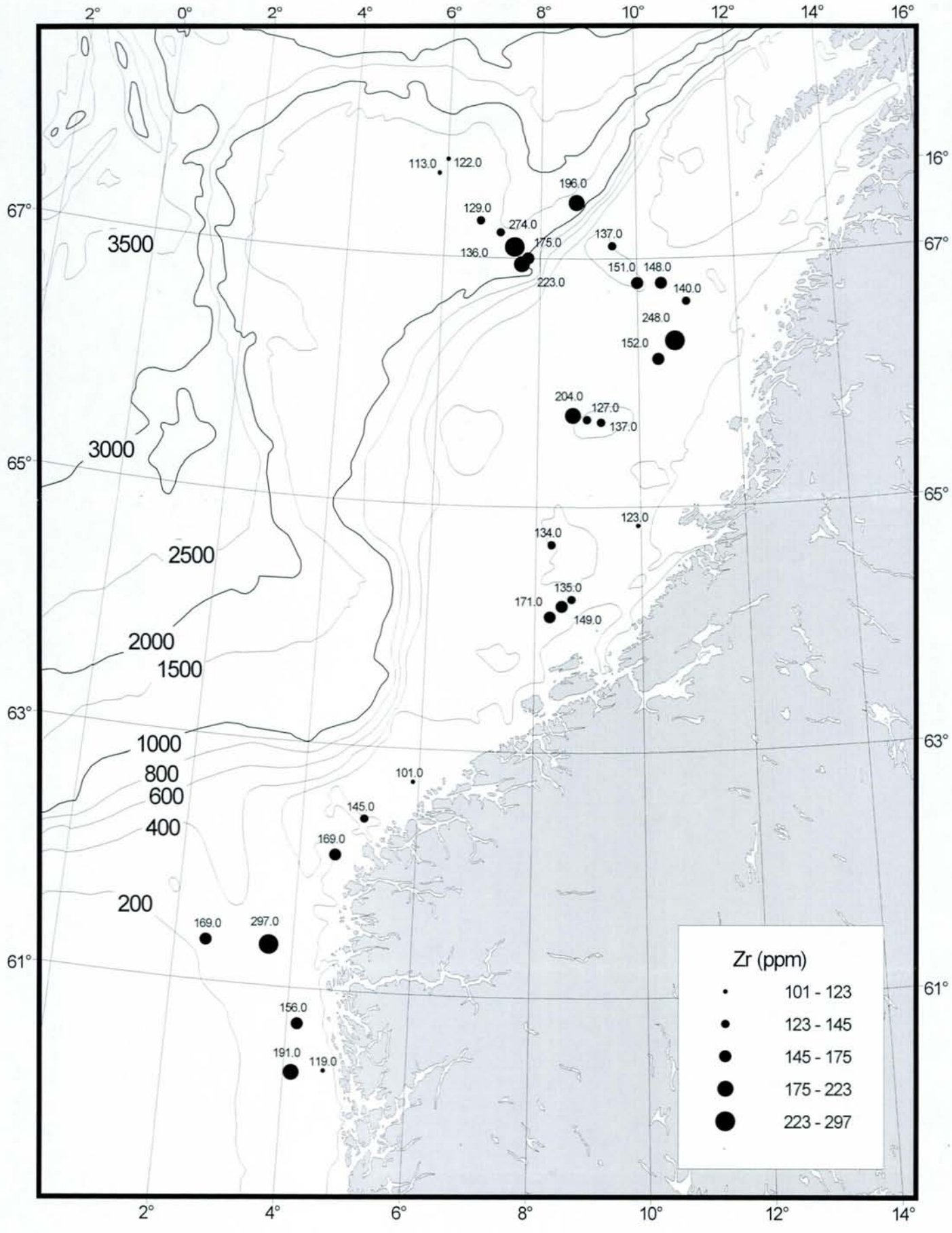


*Fig. 28. Zirconium concentrations (ppm) in the surface sediments.*

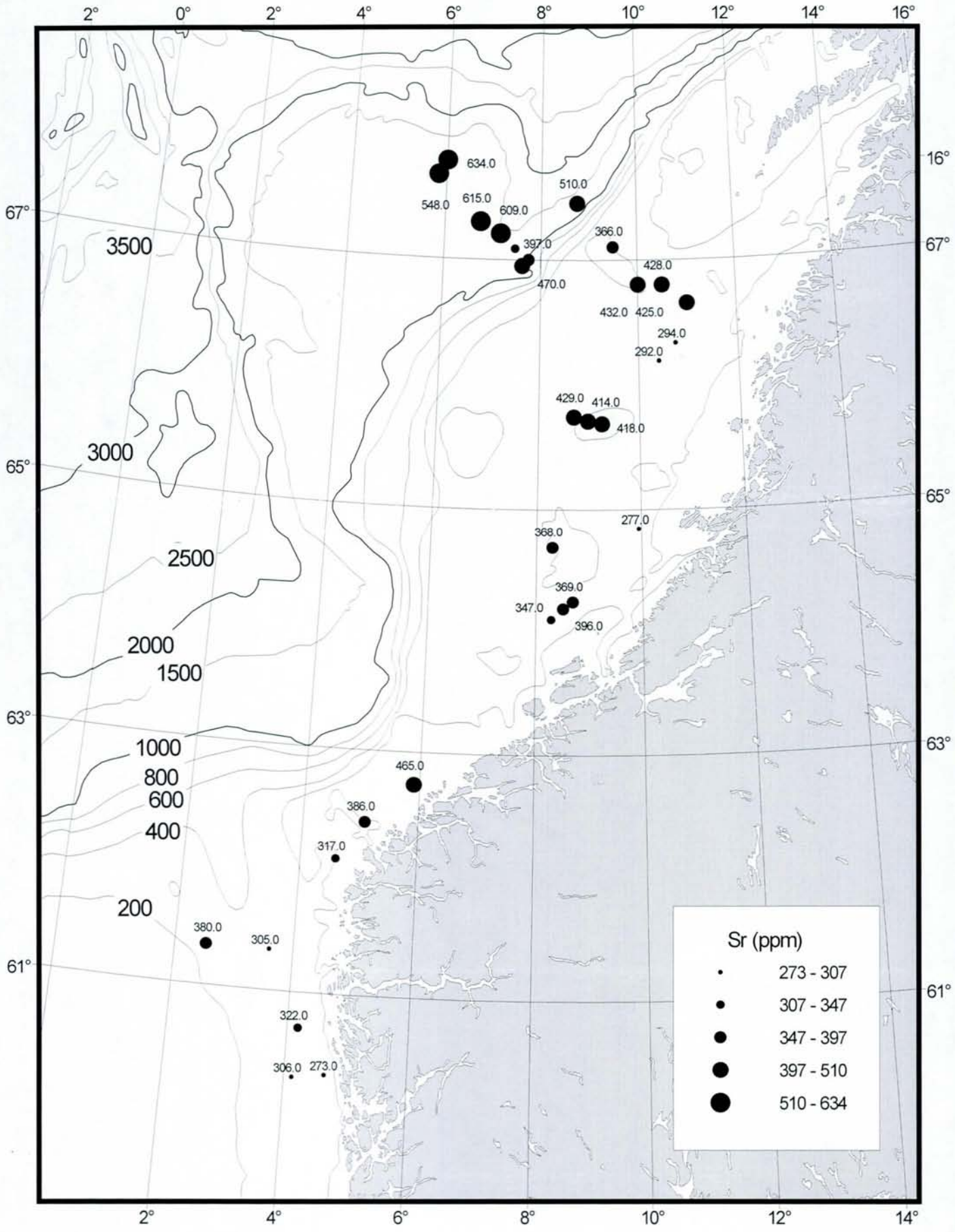


*Fig. 29. Strontium concentrations (ppm) in the surface sediments.*

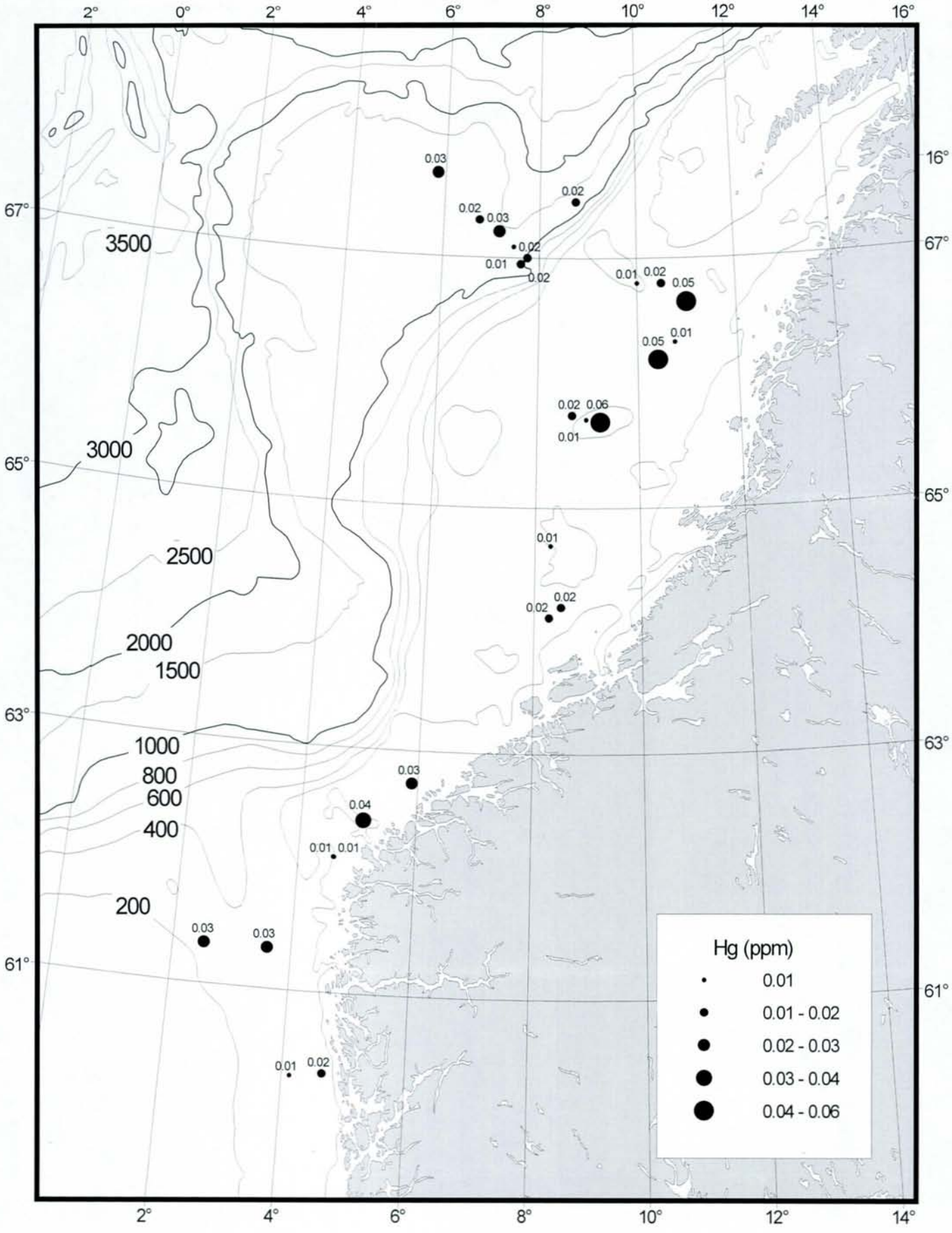


*Fig. 30. Mercury concentrations (ppm) in the surface sediments.*

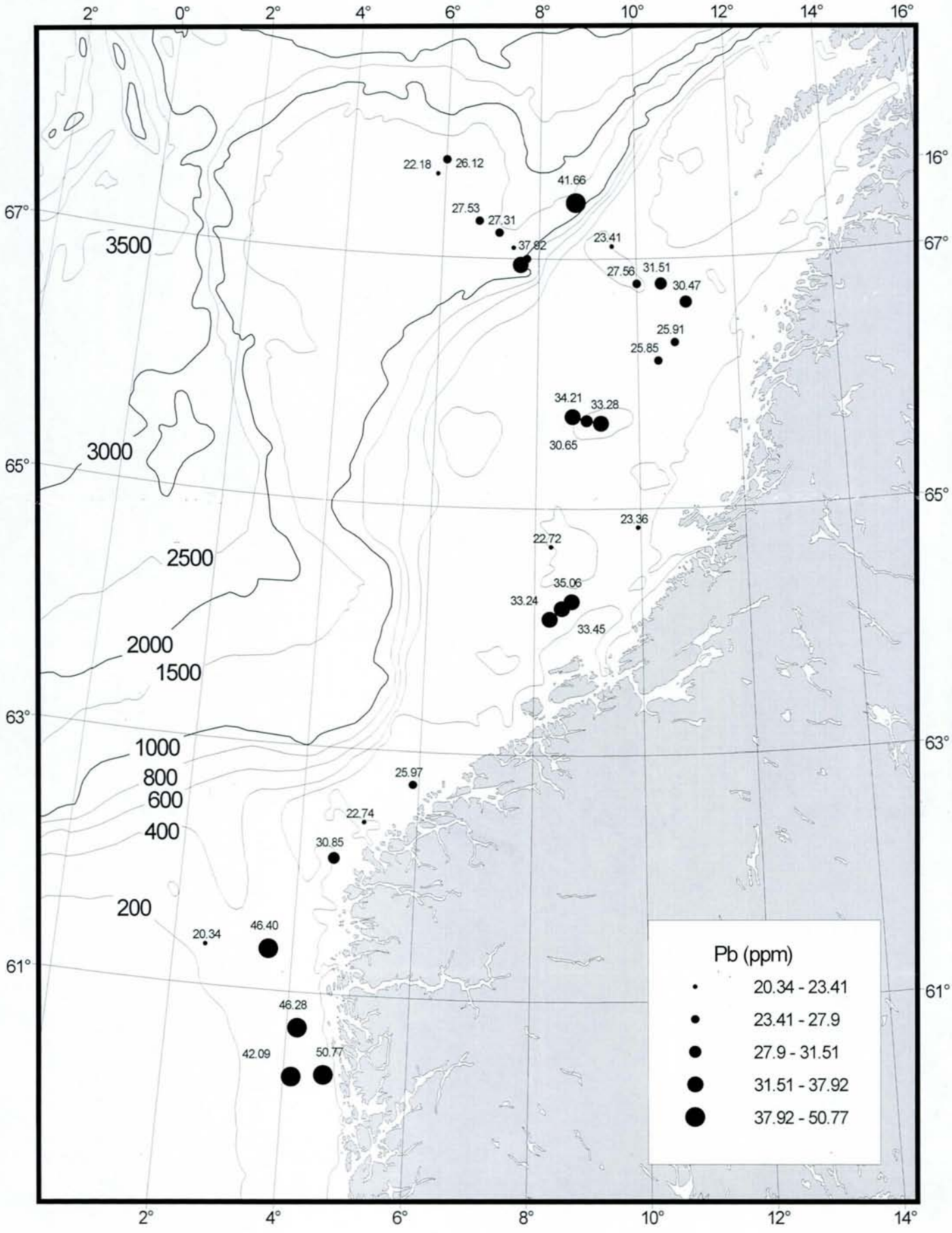


*Fig. 31. Lead concentrations (ppm) in the surface sediments.*

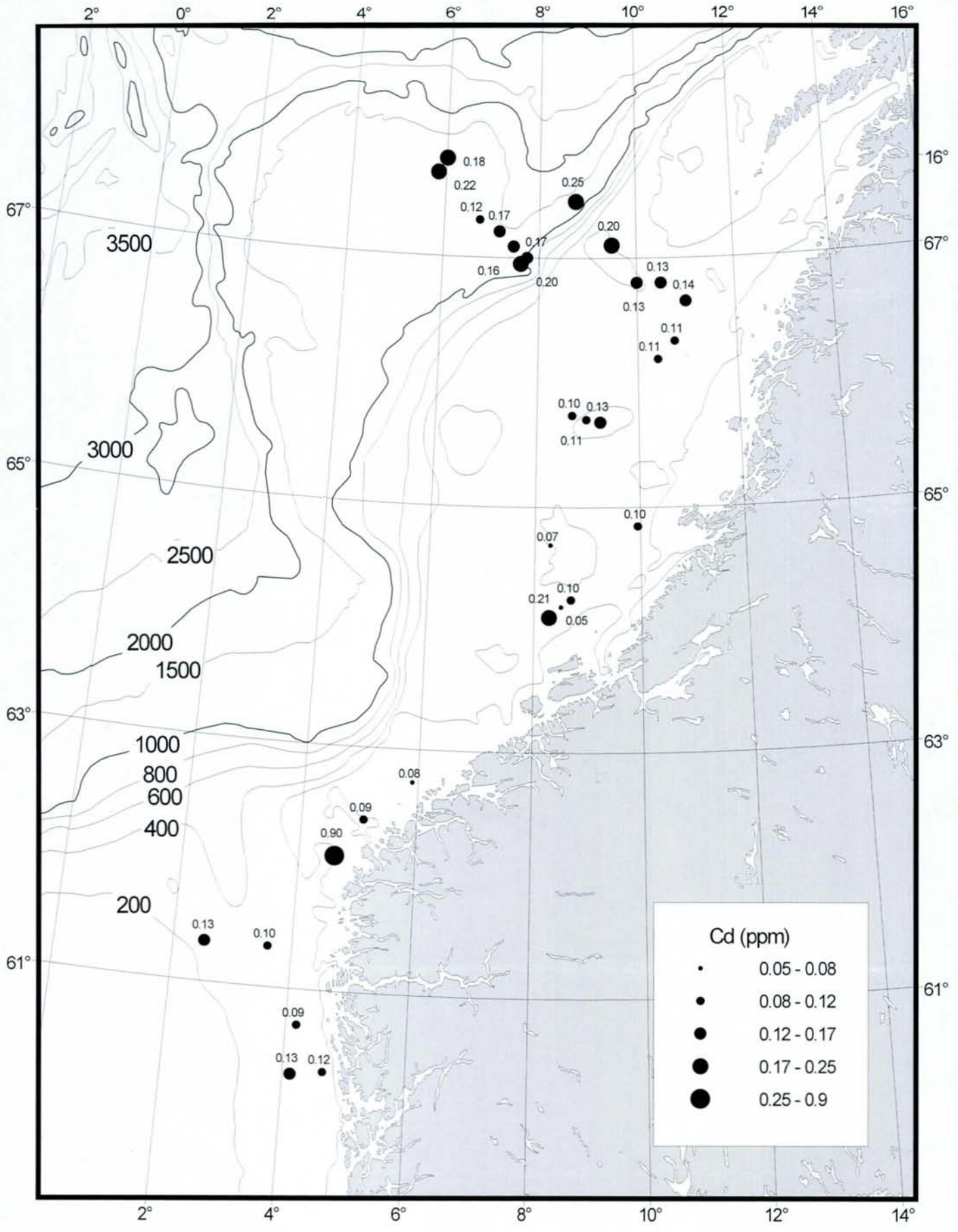


*Fig. 32. Cadmium concentrations (ppm) in the surface sediments.*

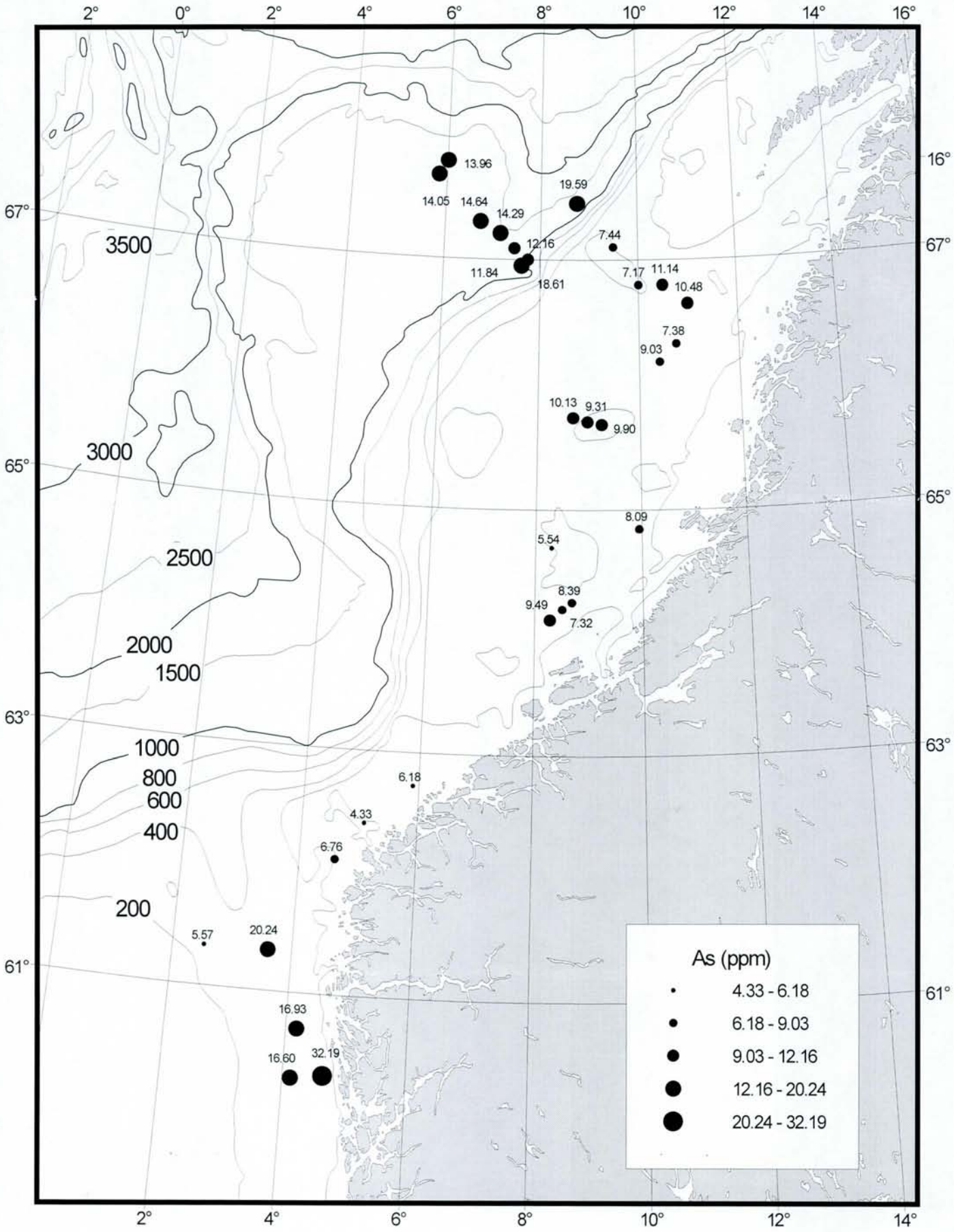


*Fig. 33. Arsenic concentrations (ppm) in the surface sediments.*

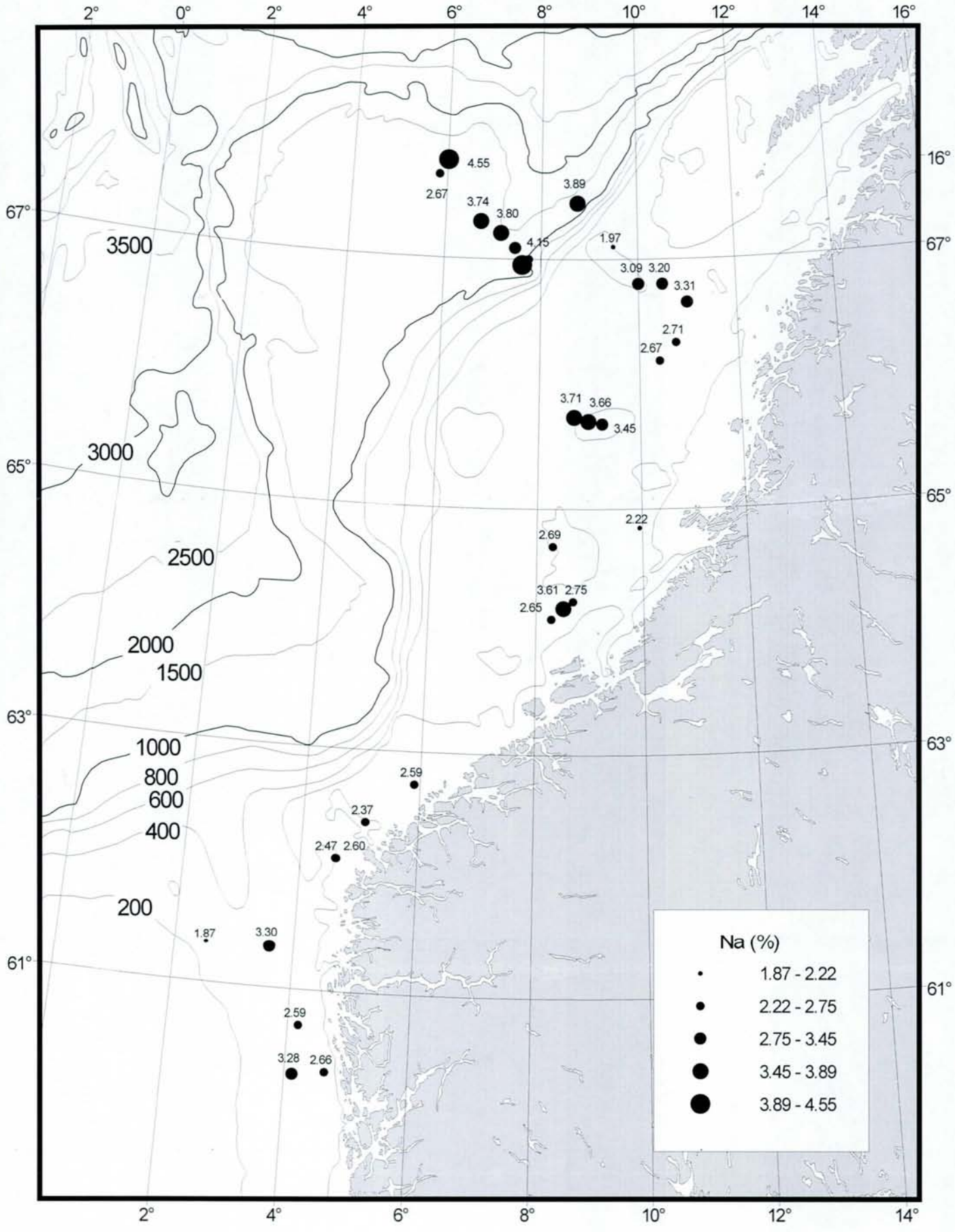


*Fig. 34. Sodium concentrations (%) in the surface sediments.*

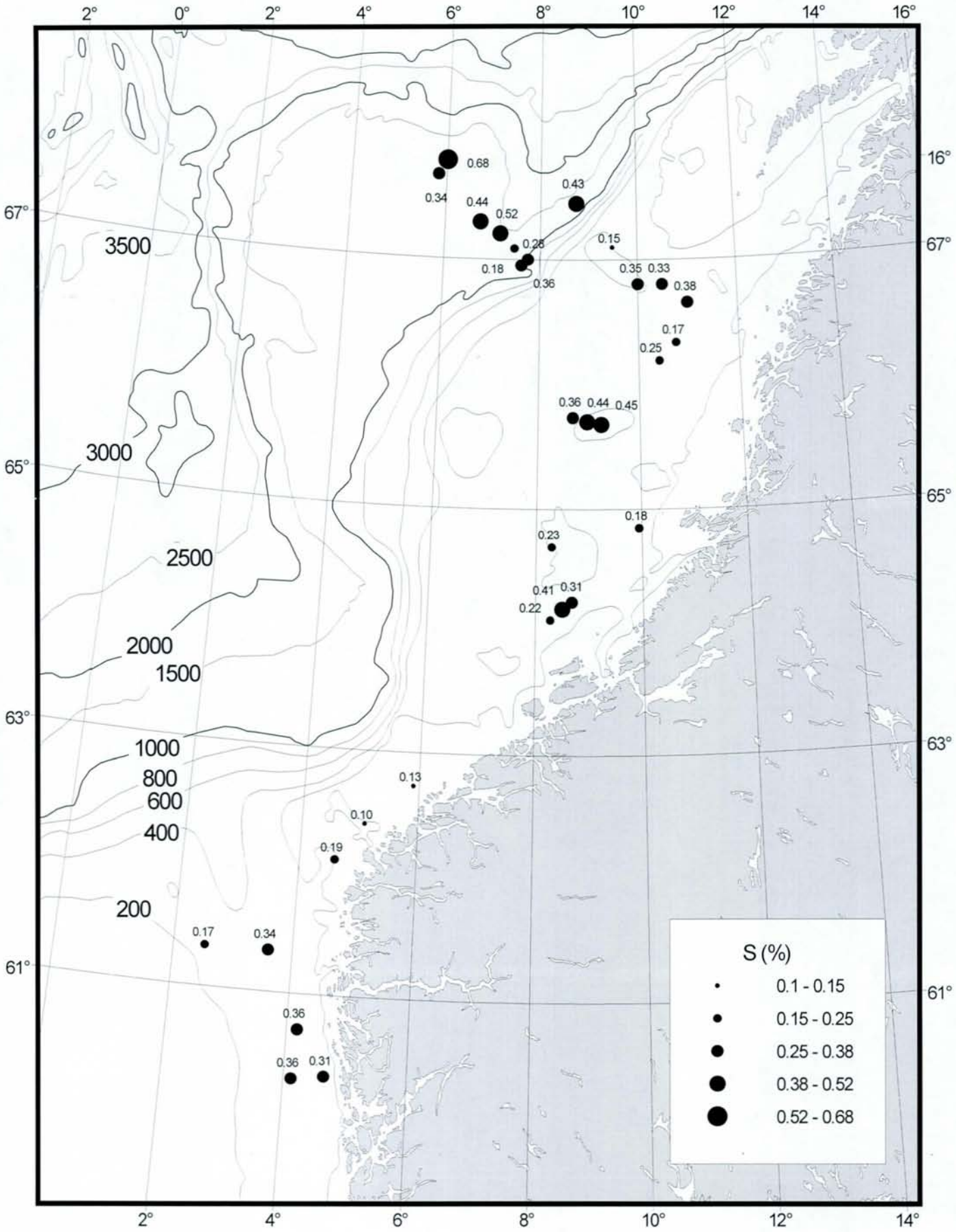


*Fig. 35. Sulphur concentrations (%) in the surface sediments.*

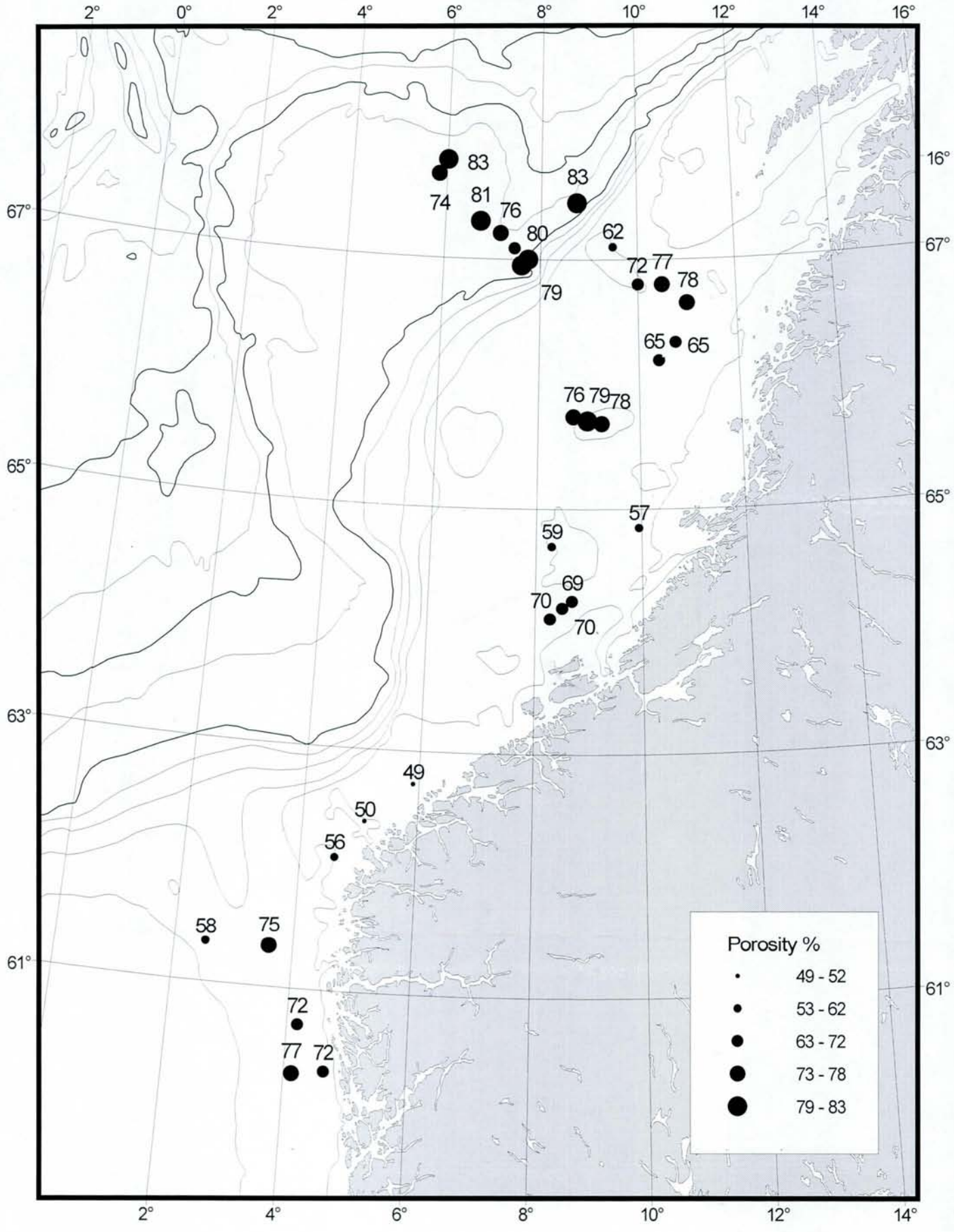


*Fig. 36. Porosity (%) of the surface sediments.*

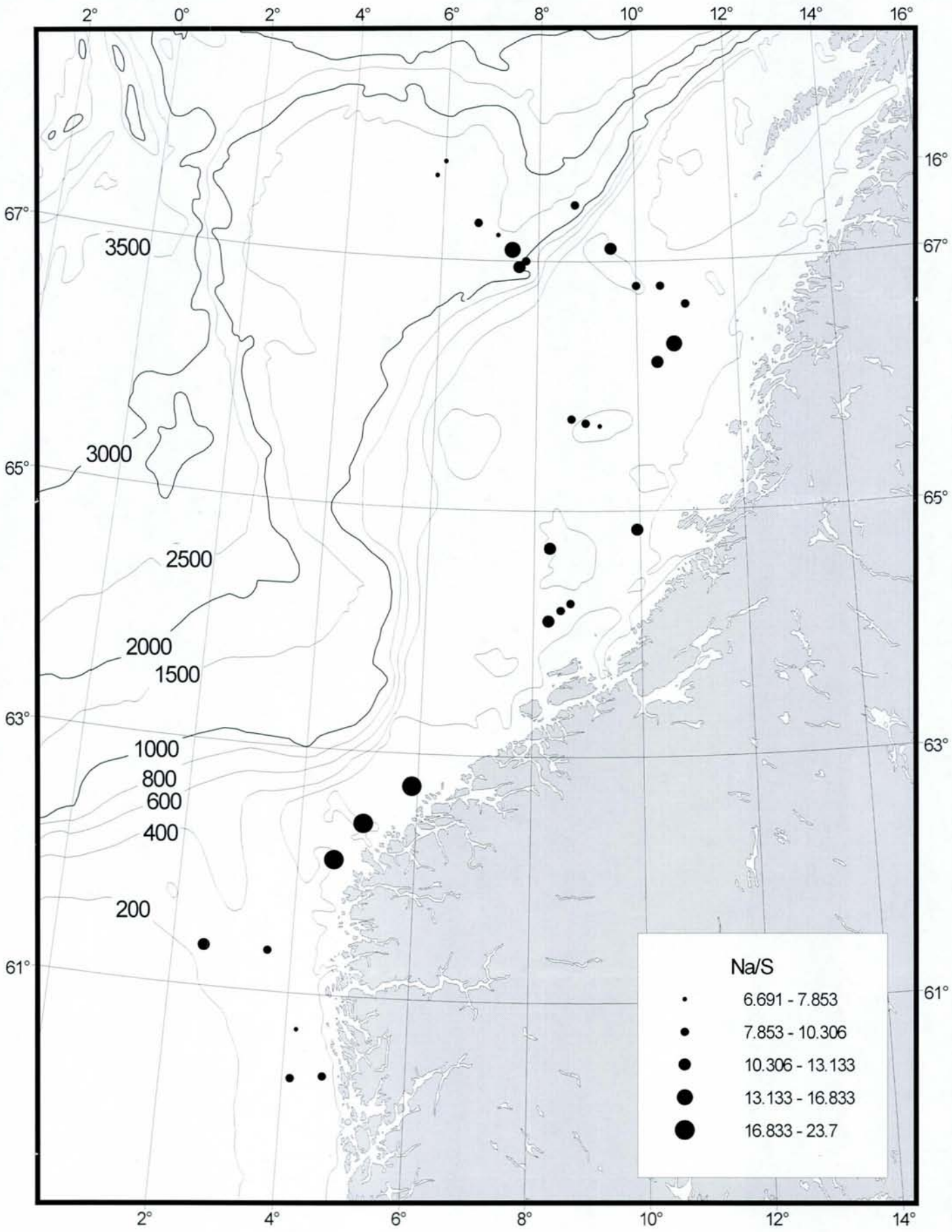


*Fig. 37. Na/S ratios in the surface sediments.*

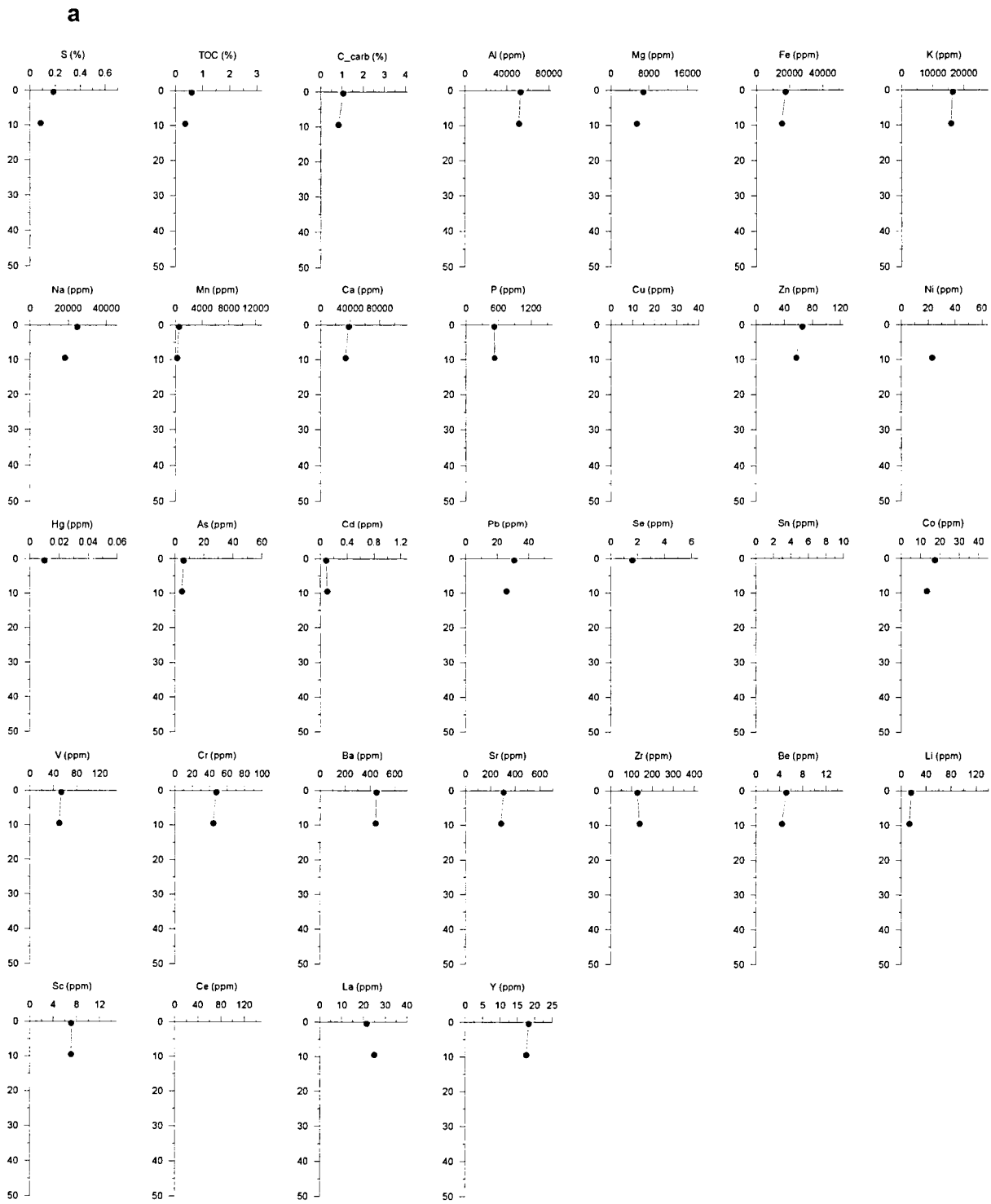


*Fig. 38. Concentration versus depth profiles of elements in the sediments of station 502: (a) constant x-axes of individual parameters at all stations; (b) variable x-axes, defined according to concentration ranges of individual parameters at each station.*

**b**

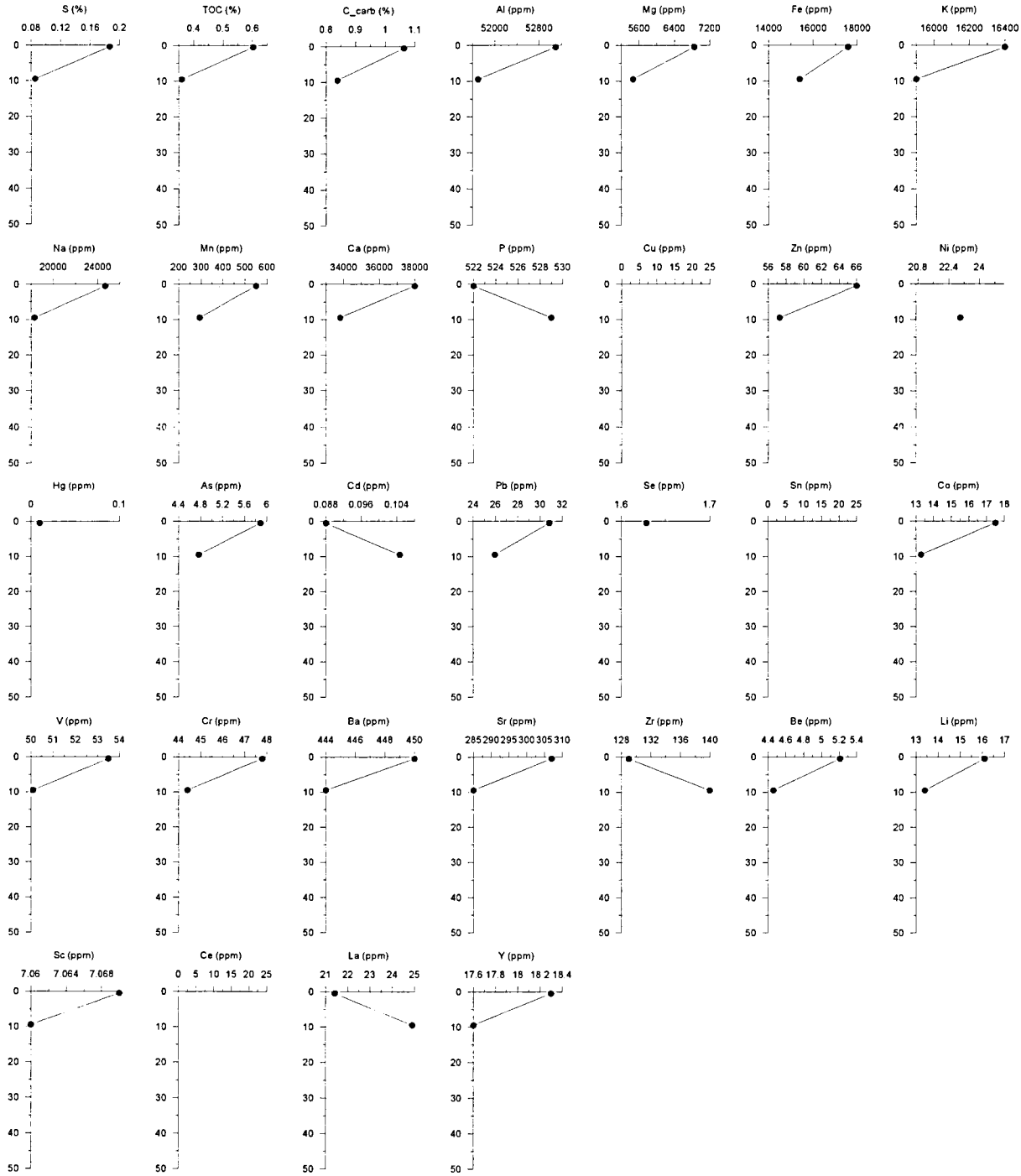


*Fig. 38. (continued).*


*Fig. 39. Concentration versus depth profiles of elements in the sediments of station 503: (a) constant x-axes of individual parameters at all stations; (b) variable x-axes, defined according to concentration ranges of individual parameters at each station.*

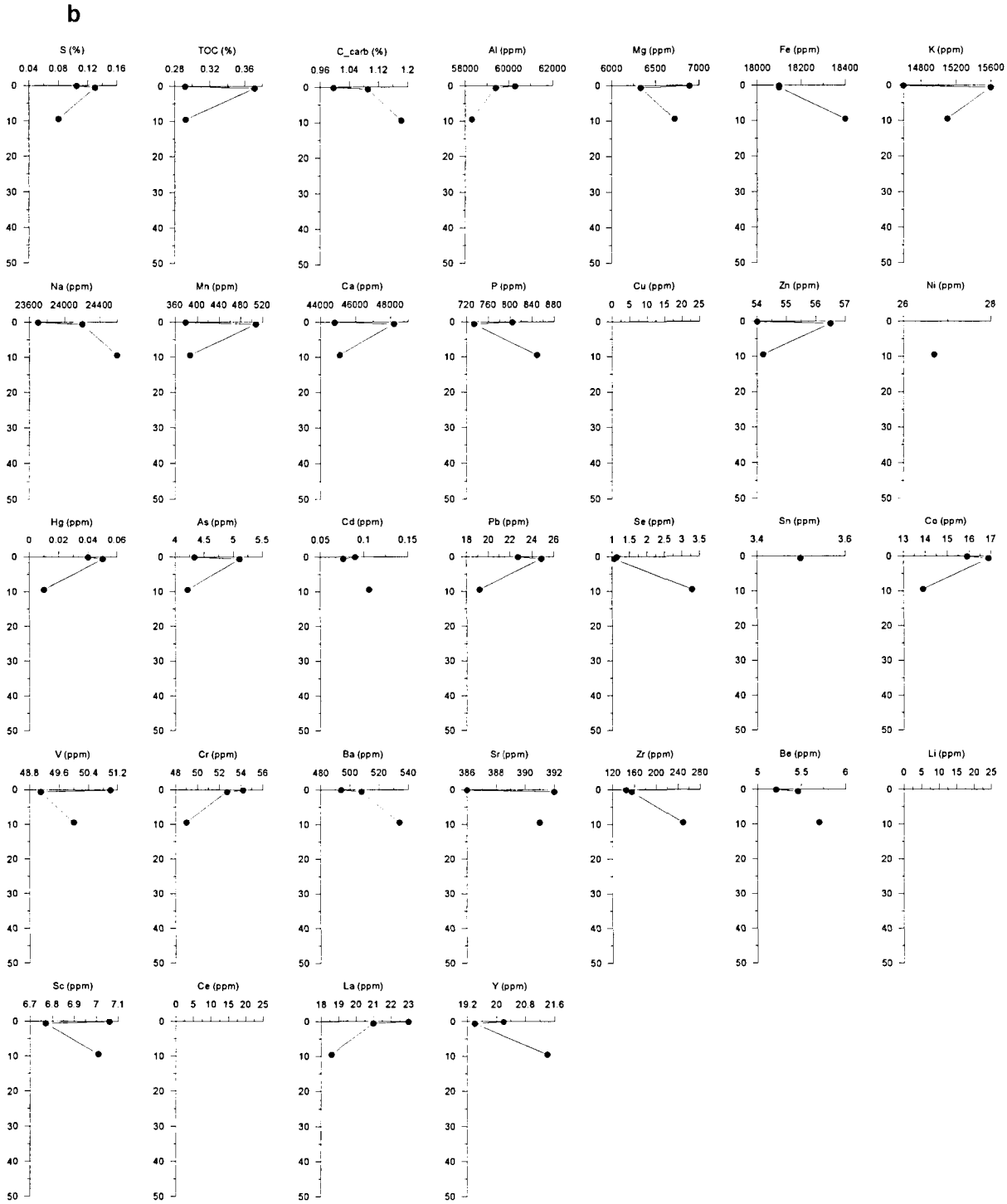


*Fig. 39. (continued).*

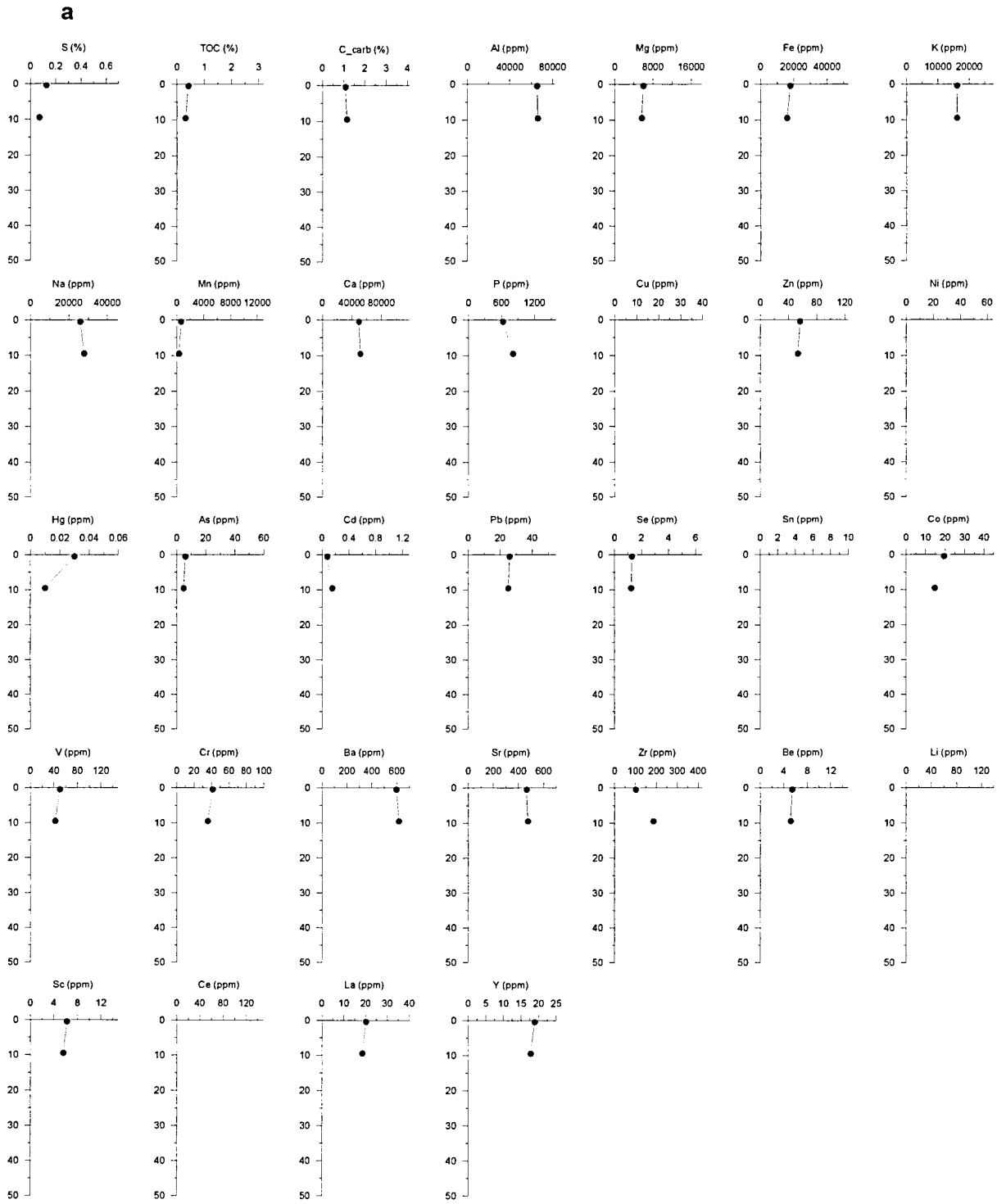


*Fig. 40. Concentration versus depth profiles of elements in the sediments of station 506: (a) constant x-axes of individual parameters at all stations; (b) variable x-axes, defined according to concentration ranges of individual parameters at each station.*

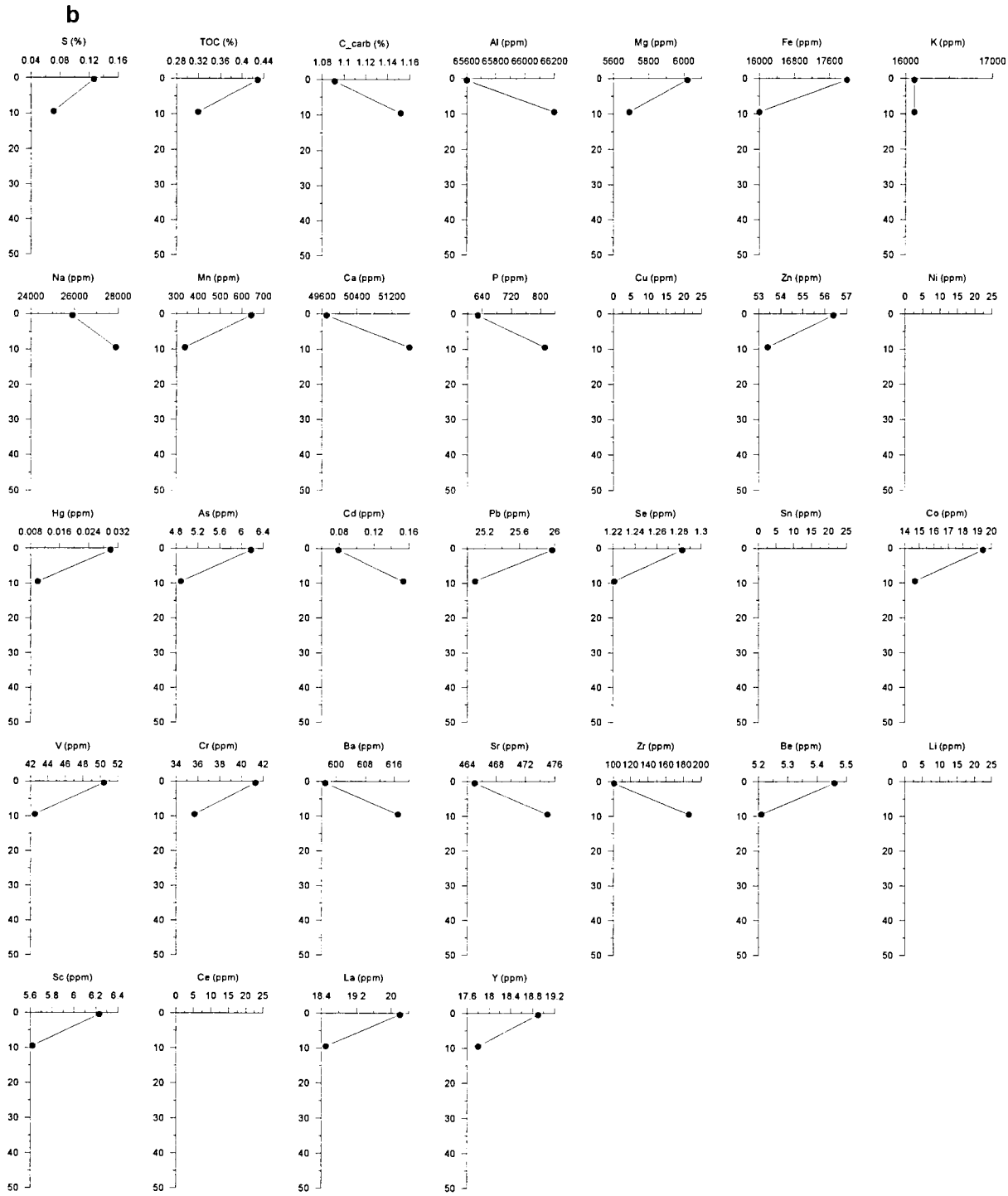


*Fig. 40. (continued).*

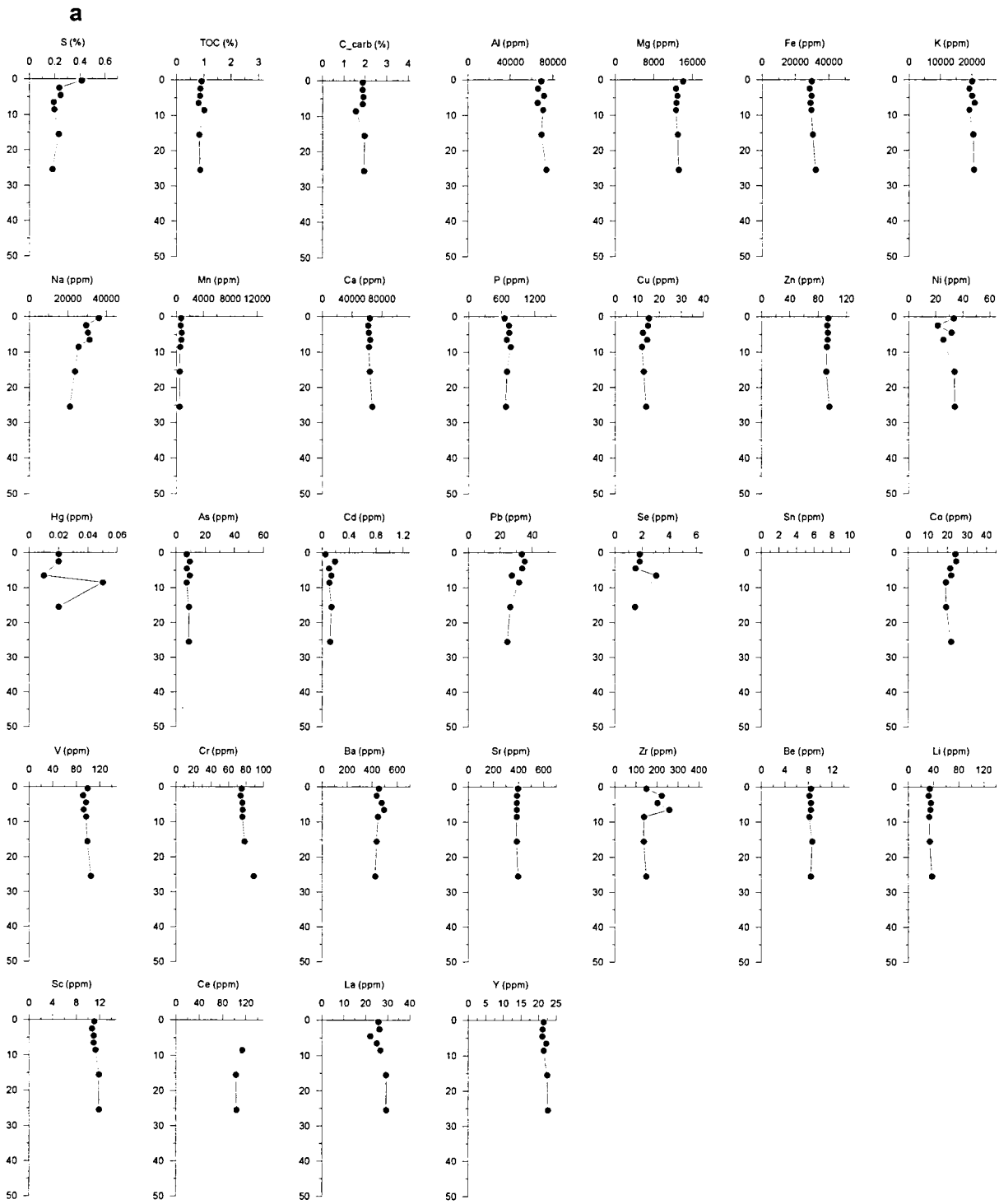


*Fig. 41. Concentration versus depth profiles of elements in the sediments of station 508: (a) constant x-axes of individual parameters at all stations; (b) variable x-axes, defined according to concentration ranges of individual parameters at each station.*

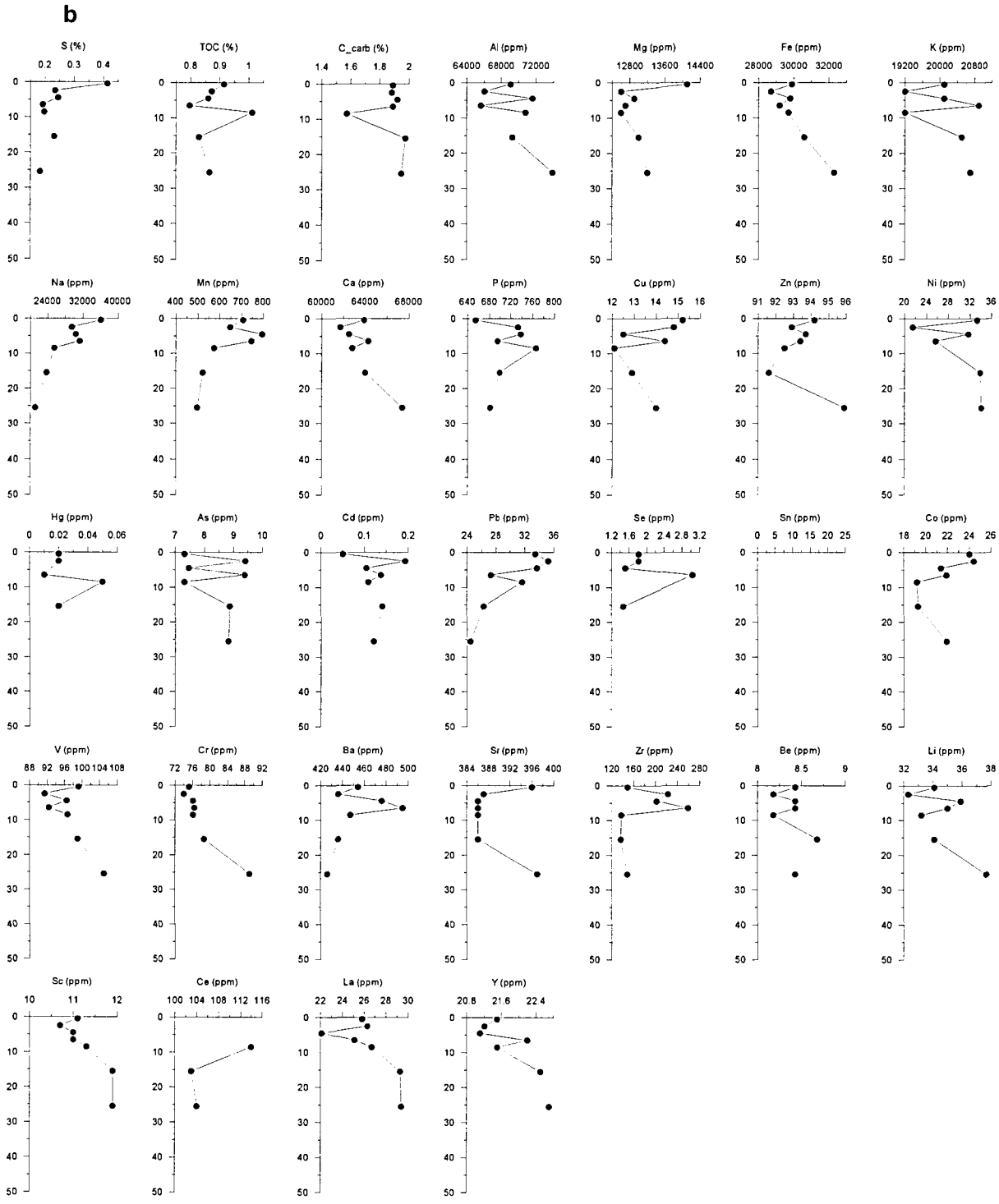


*Fig. 41. (continued).*

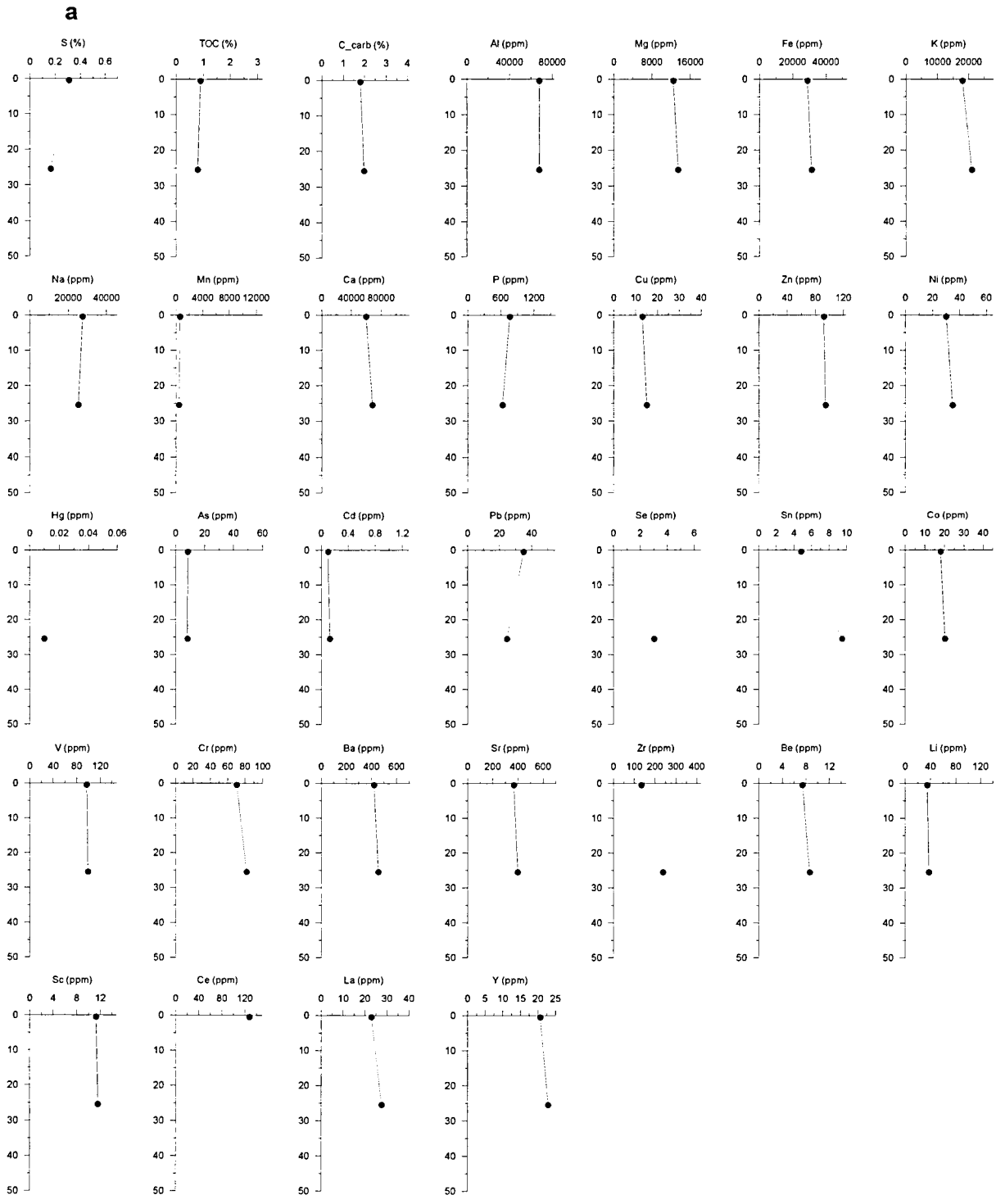


*Fig. 42. Concentration versus depth profiles of elements in the sediments of station 509: (a) constant x-axes of individual parameters at all stations; (b) variable x-axes, defined according to concentration ranges of individual parameters at each station.*

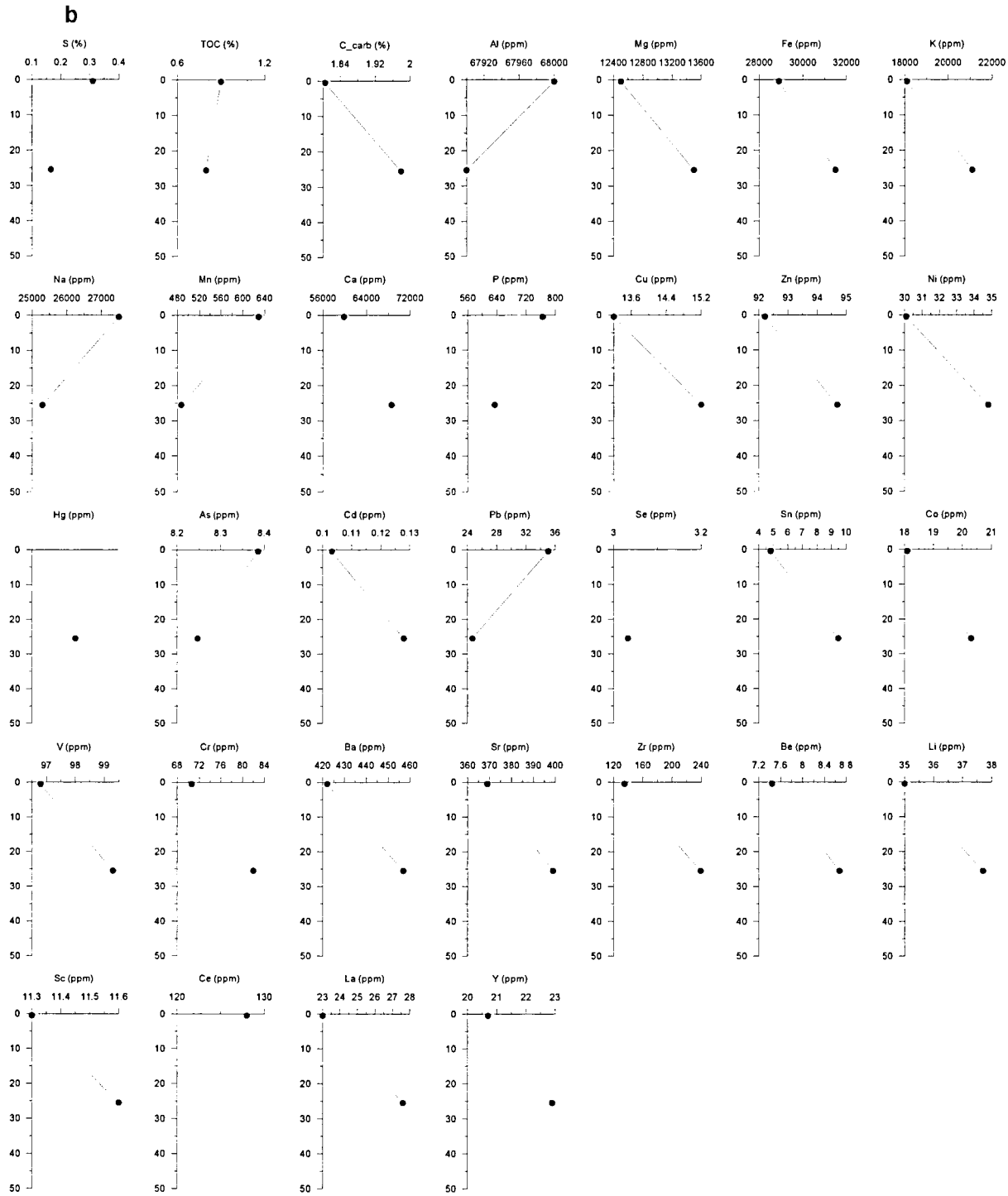


*Fig. 42. (continued).*

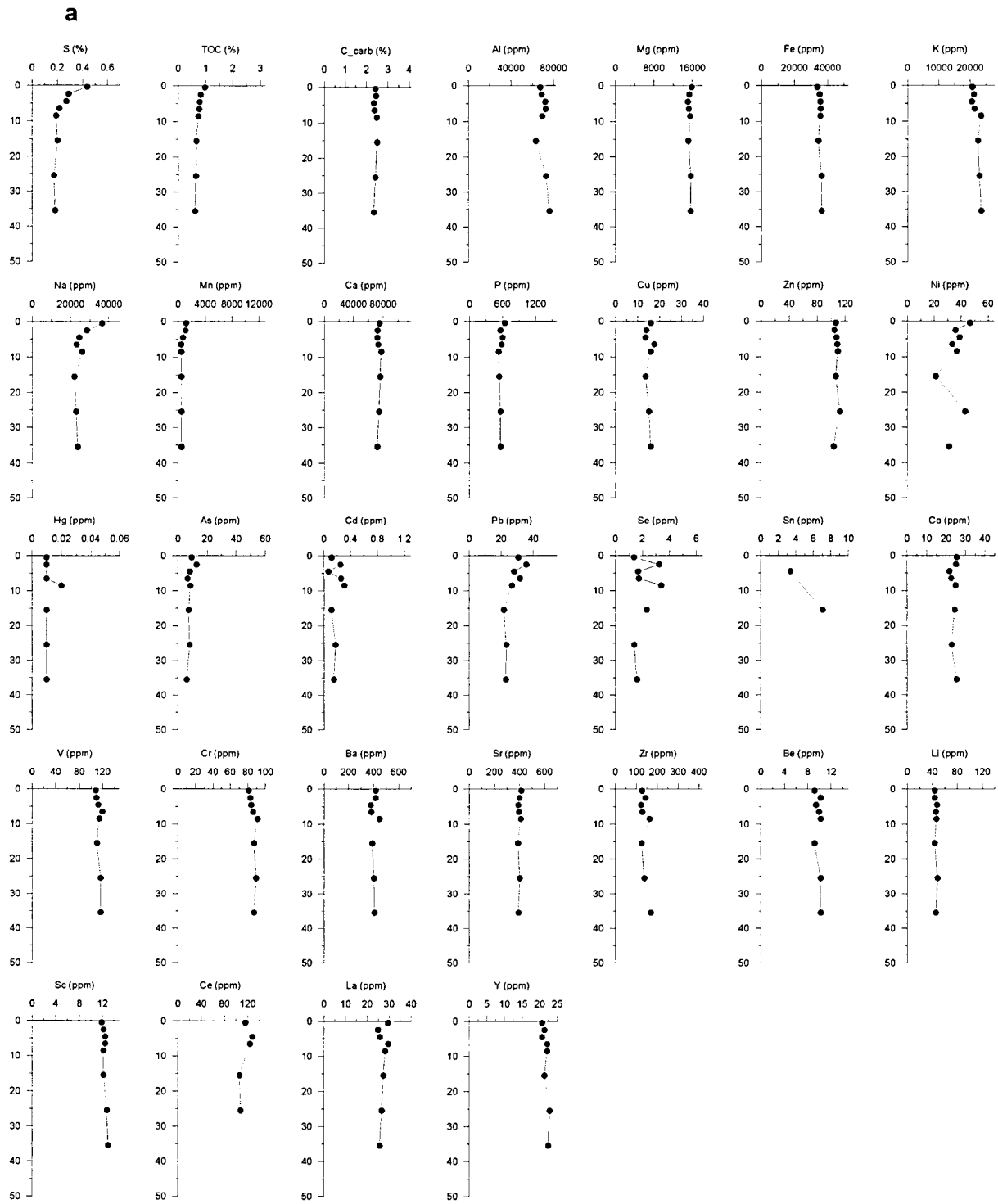


*Fig. 43. Concentration versus depth profiles of elements in the sediments of station 511: (a) constant x-axes of individual parameters at all stations; (b) variable x-axes, defined according to concentration ranges of individual parameters at each station.*

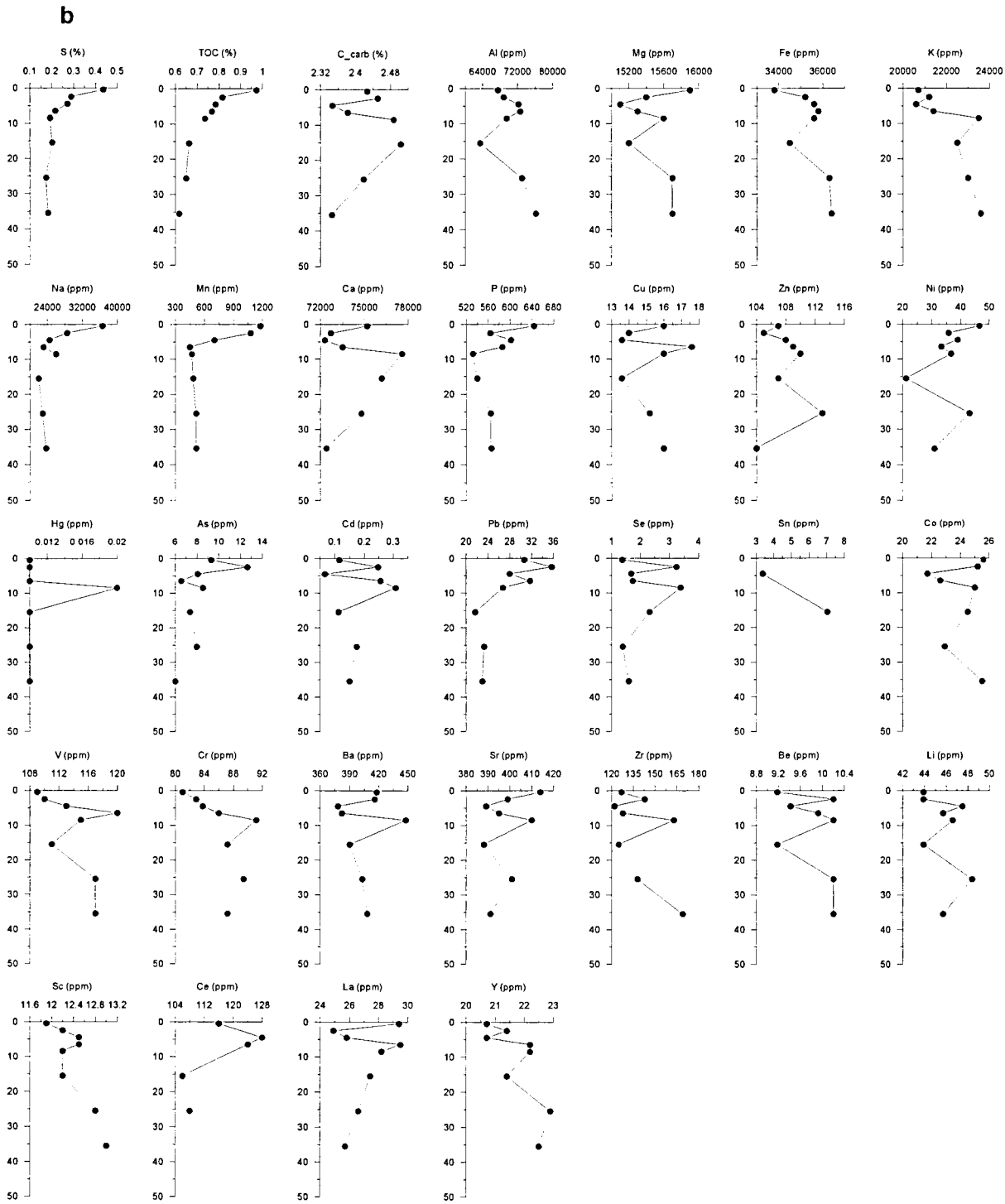


*Fig. 43. (continued).*

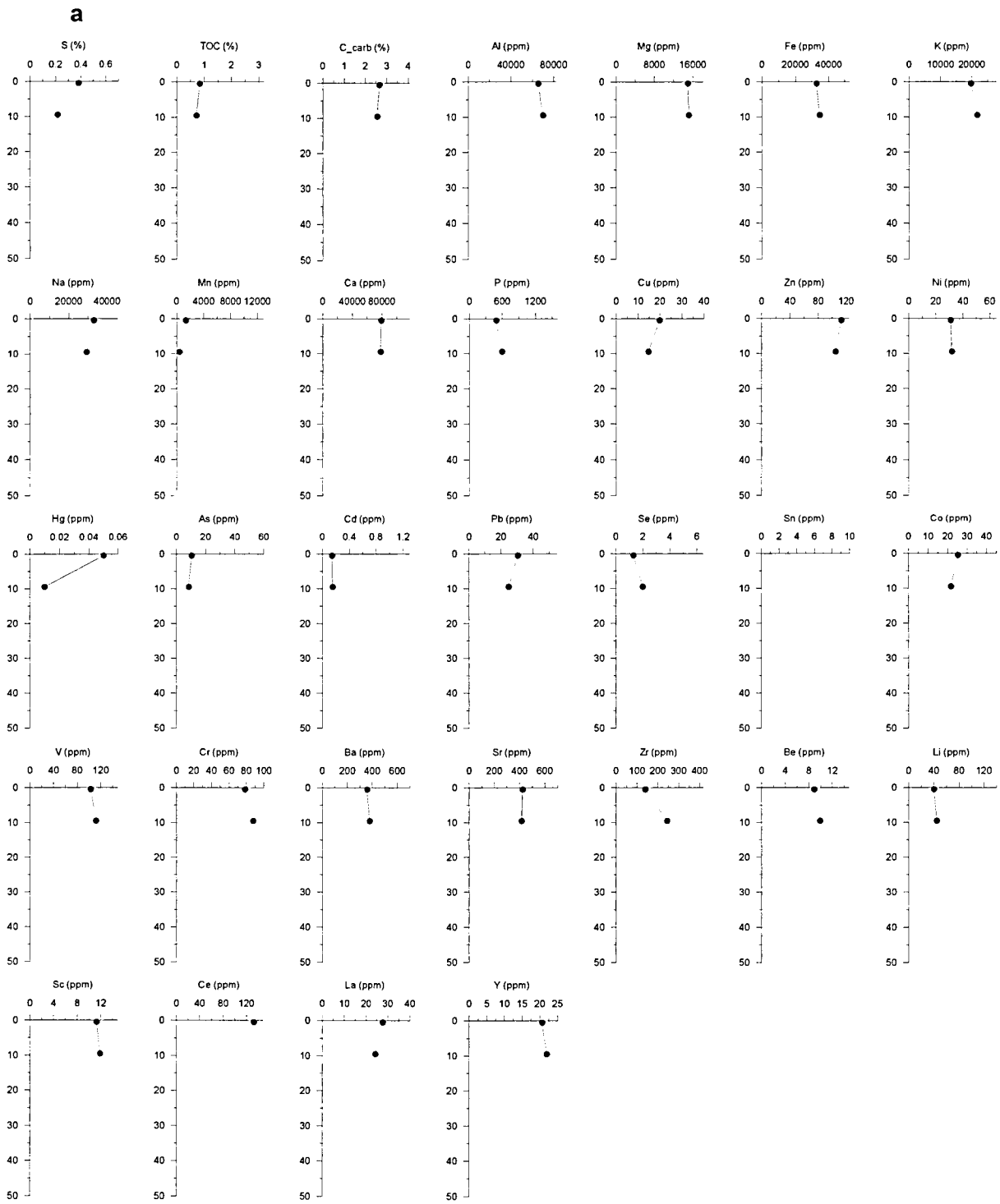


*Fig. 44. Concentration versus depth profiles of elements in the sediments of station 515: (a) constant x-axes of individual parameters at all stations; (b) variable x-axes, defined according to concentration ranges of individual parameters at each station.*

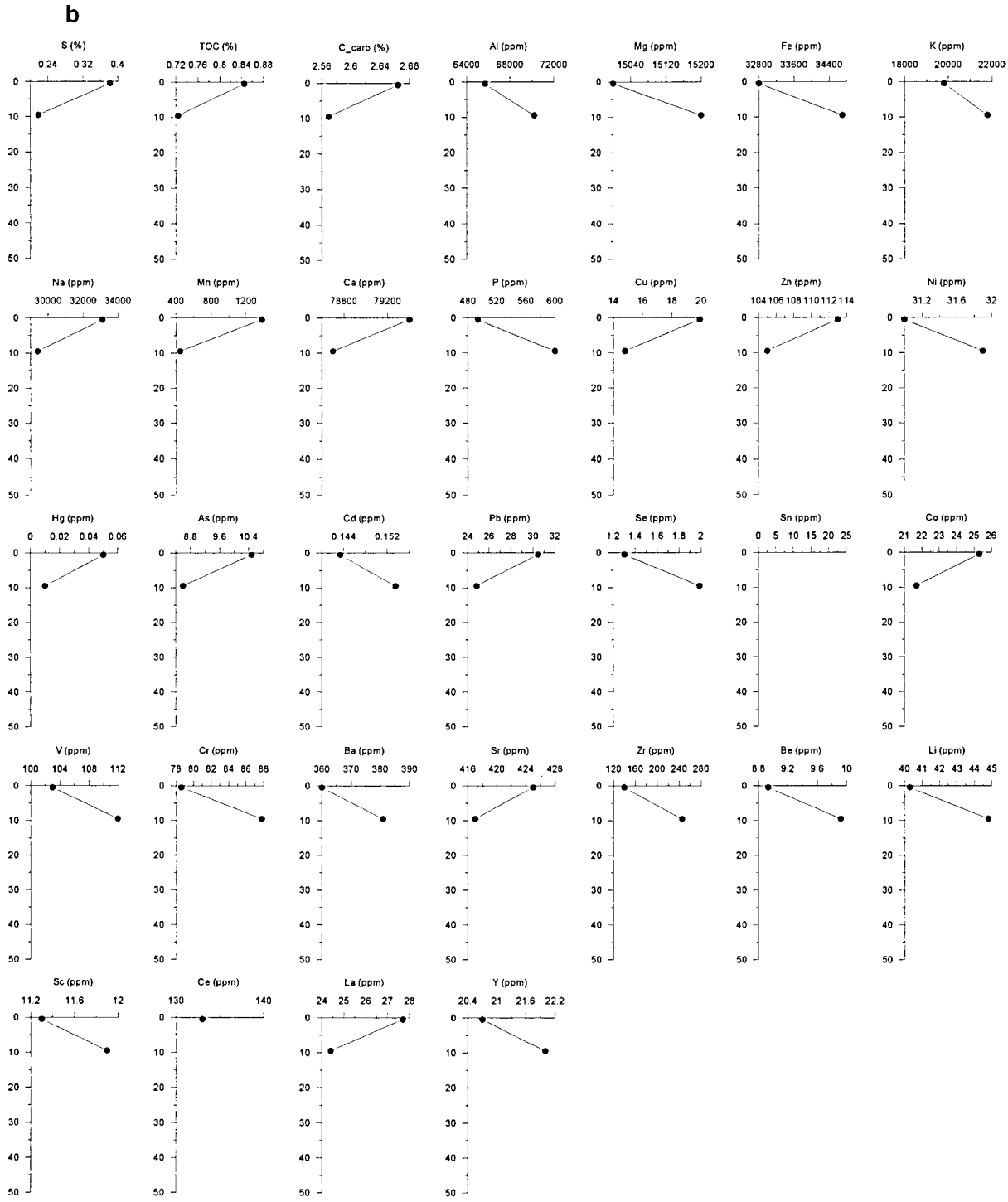


*Fig. 44. (continued).*

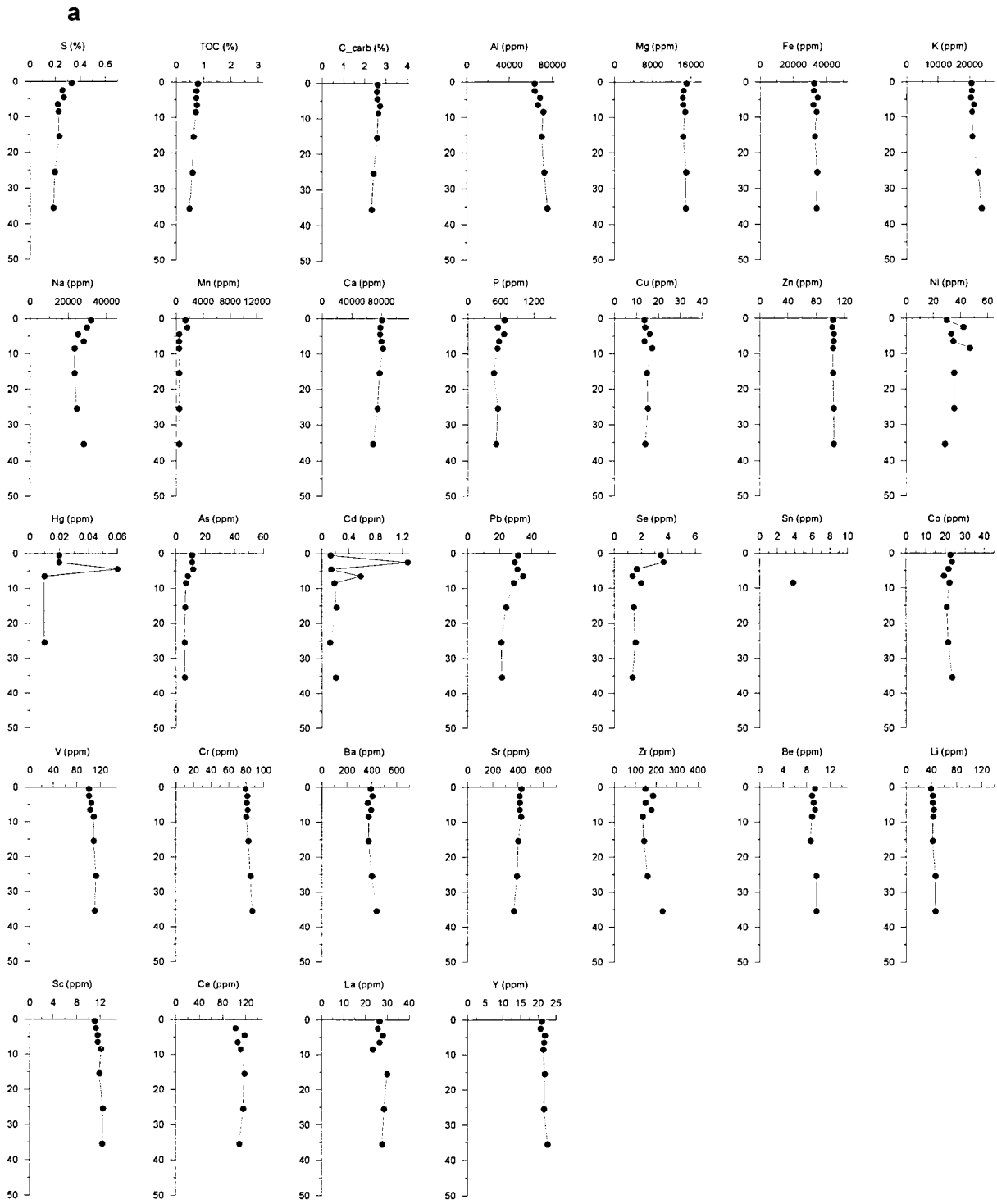


*Fig. 45. Concentration versus depth profiles of elements in the sediments of station 516: (a) constant x-axes of individual parameters at all stations; (b) variable x-axes, defined according to concentration ranges of individual parameters at each station.*

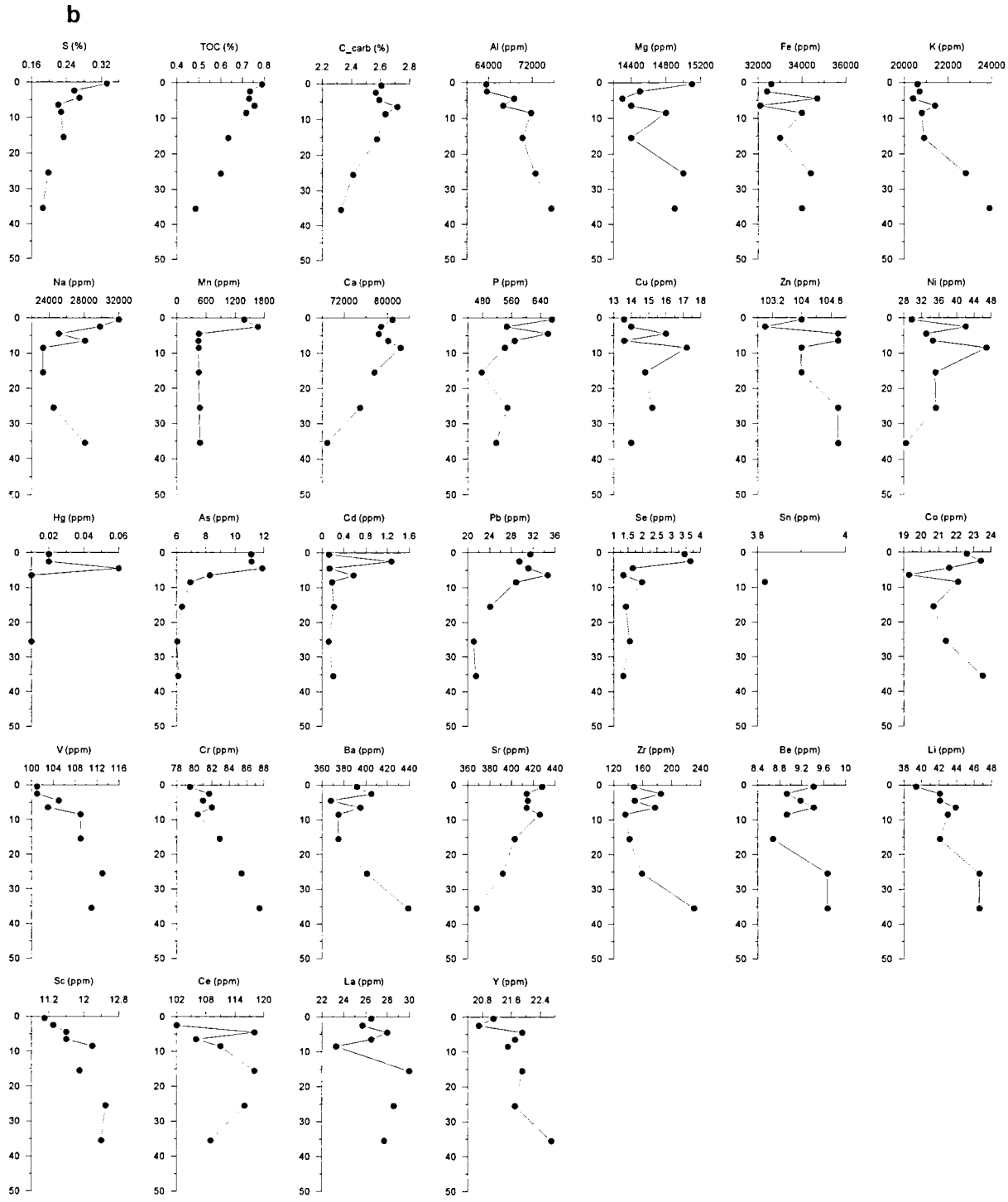


*Fig. 45. (continued).*

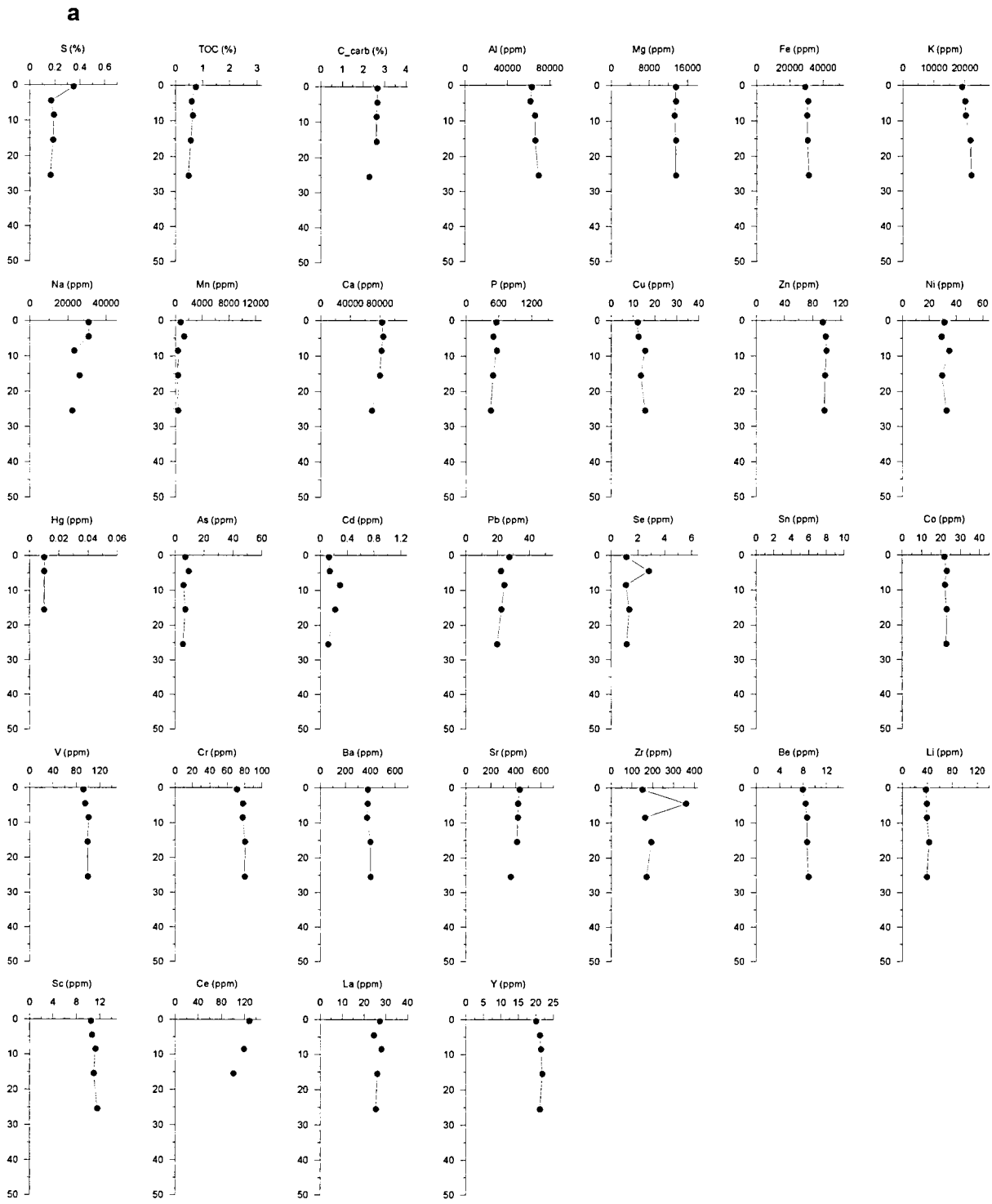


*Fig. 46. Concentration versus depth profiles of elements in the sediments of station 517: (a) constant x-axes of individual parameters at all stations; (b) variable x-axes, defined according to concentration ranges of individual parameters at each station.*

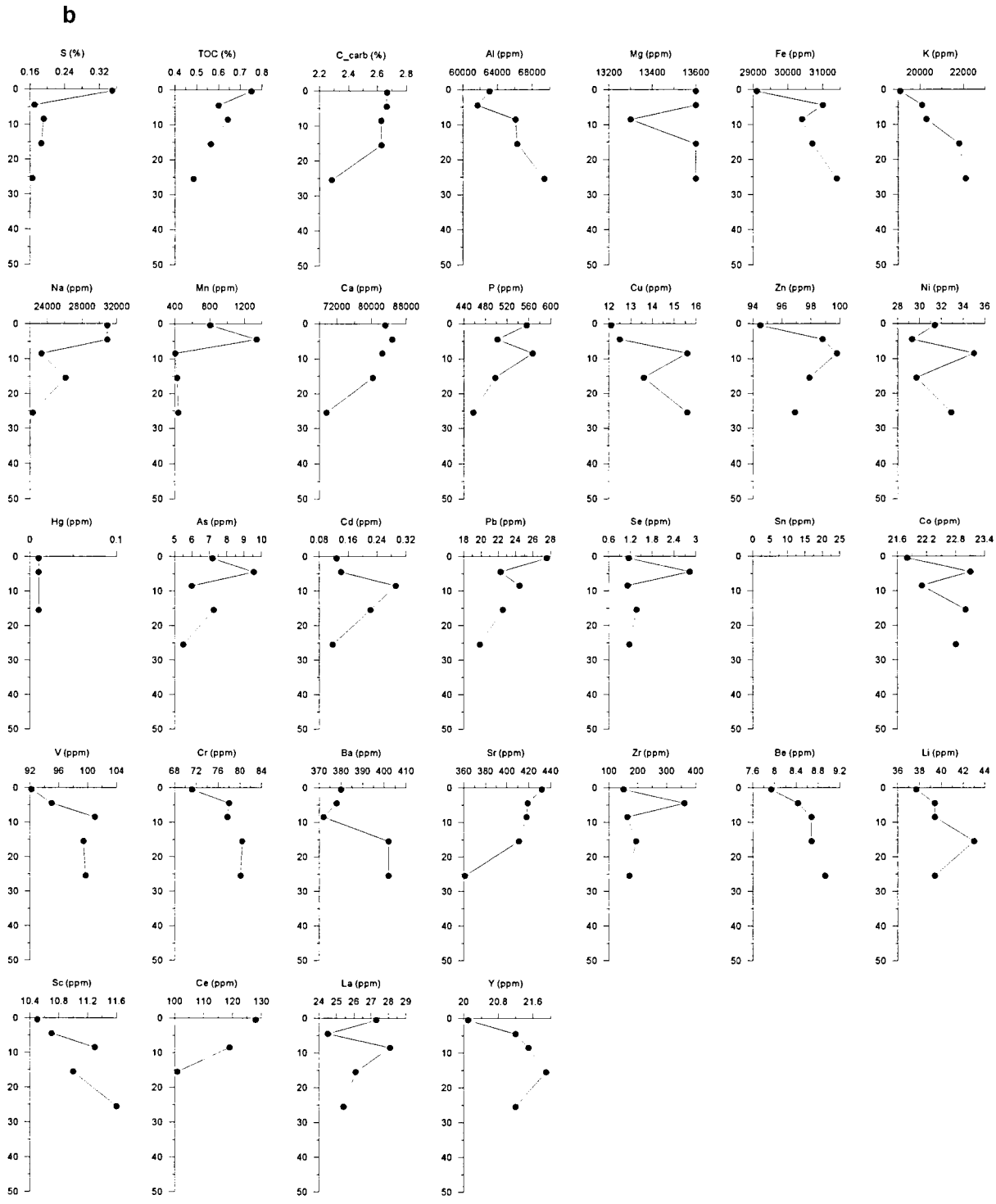


*Fig. 46. (continued).*

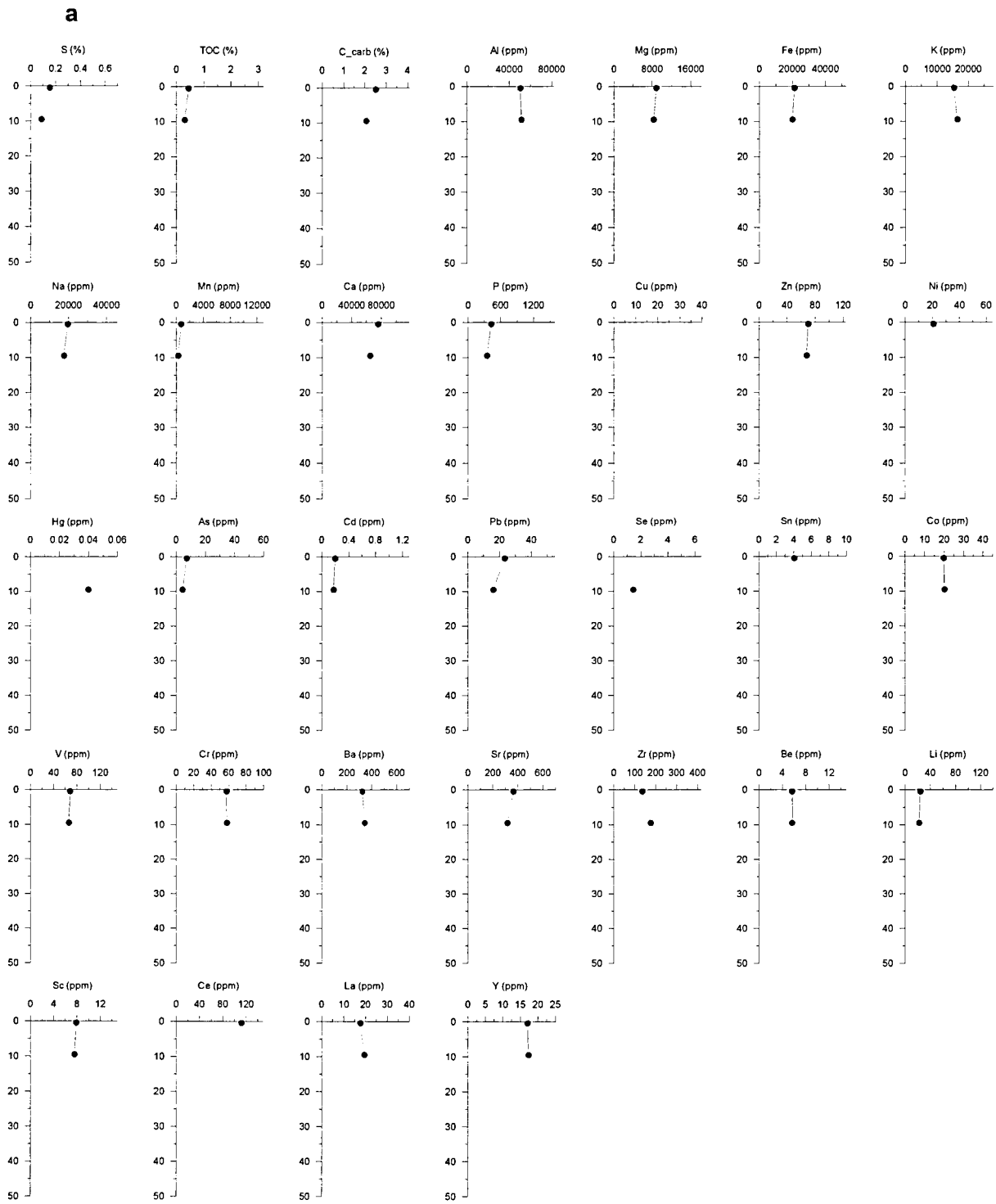


*Fig. 47. Concentration versus depth profiles of elements in the sediments of station 518: (a) constant x-axes of individual parameters at all stations; (b) variable x-axes, defined according to concentration ranges of individual parameters at each station.*

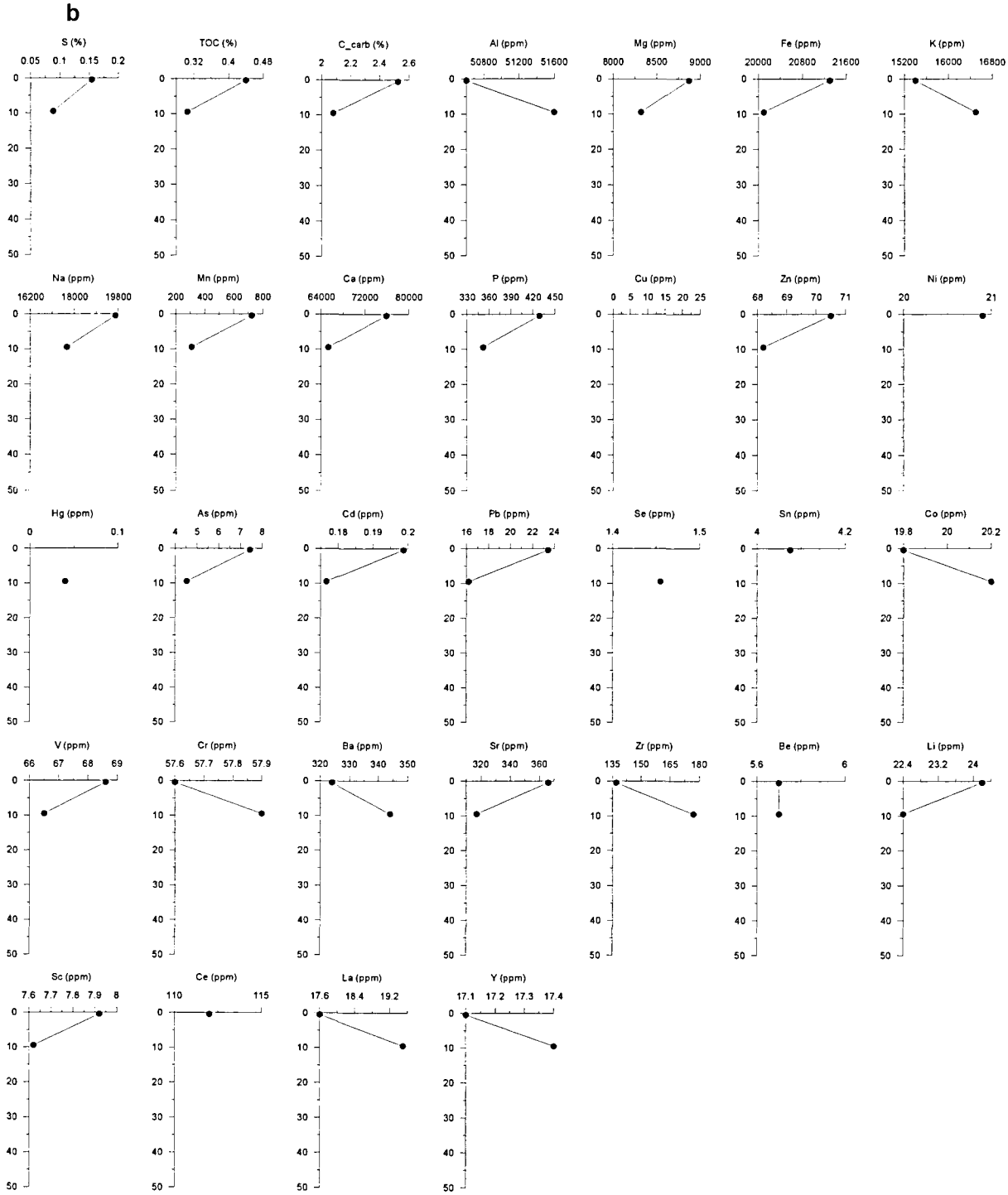


*Fig. 47. (continued).*

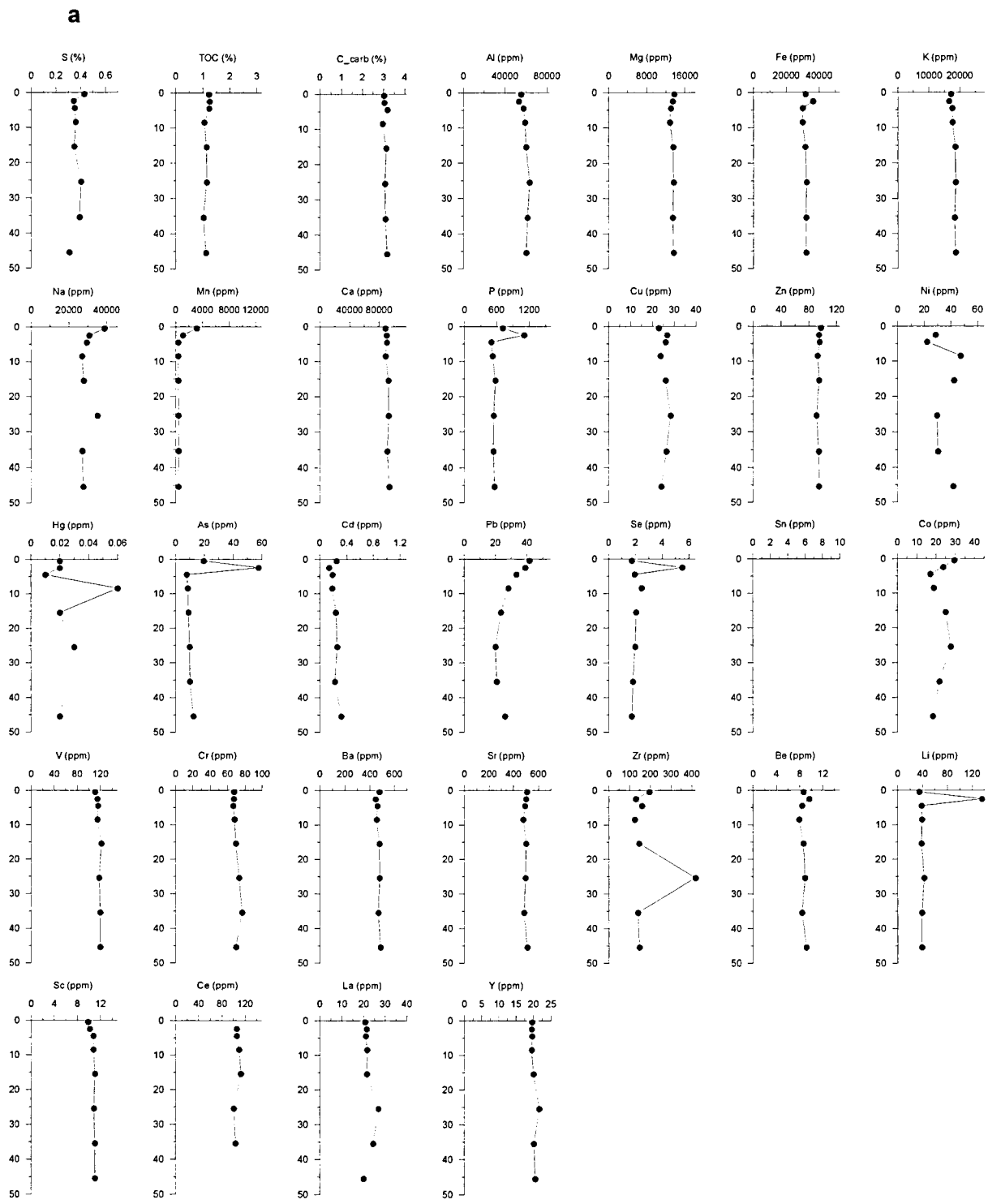


*Fig. 48. Concentration versus depth profiles of elements in the sediments of station 519: (a) constant x-axes of individual parameters at all stations; (b) variable x-axes, defined according to concentration ranges of individual parameters at each station.*

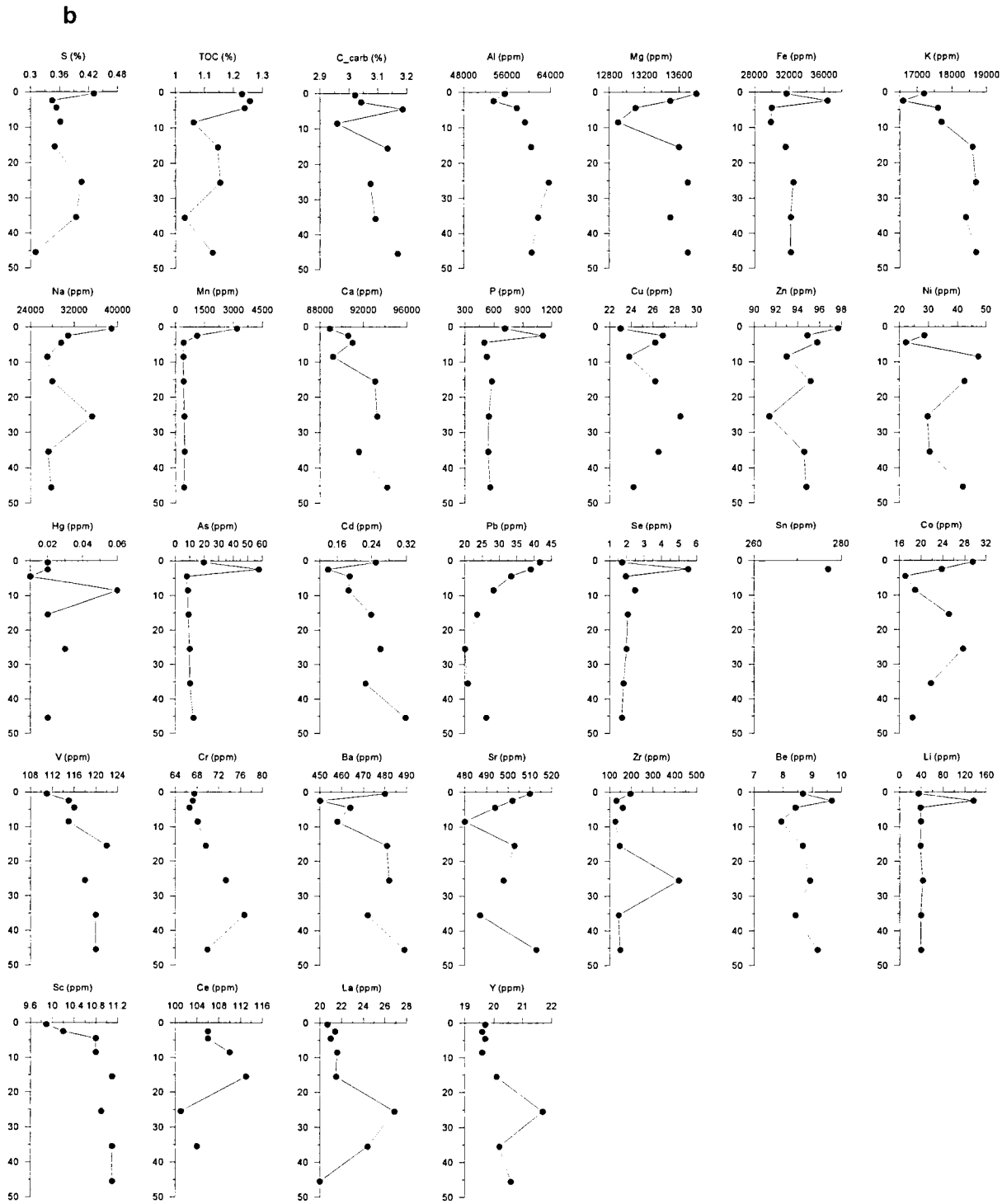


*Fig. 48. (continued).*

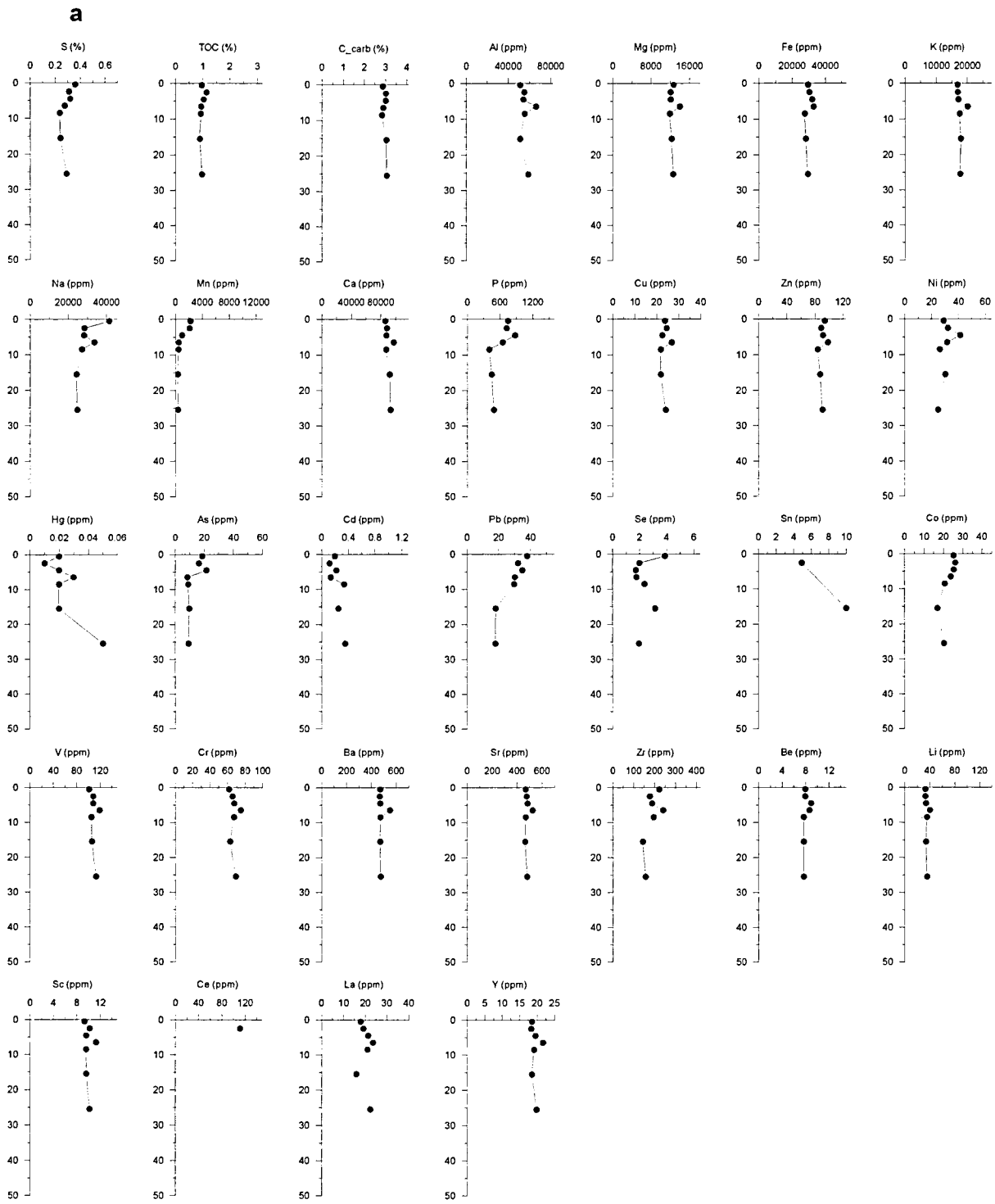


*Fig. 49. Concentration versus depth profiles of elements in the sediments of station 521: (a) constant x-axes of individual parameters at all stations; (b) variable x-axes, defined according to concentration ranges of individual parameters at each station.*

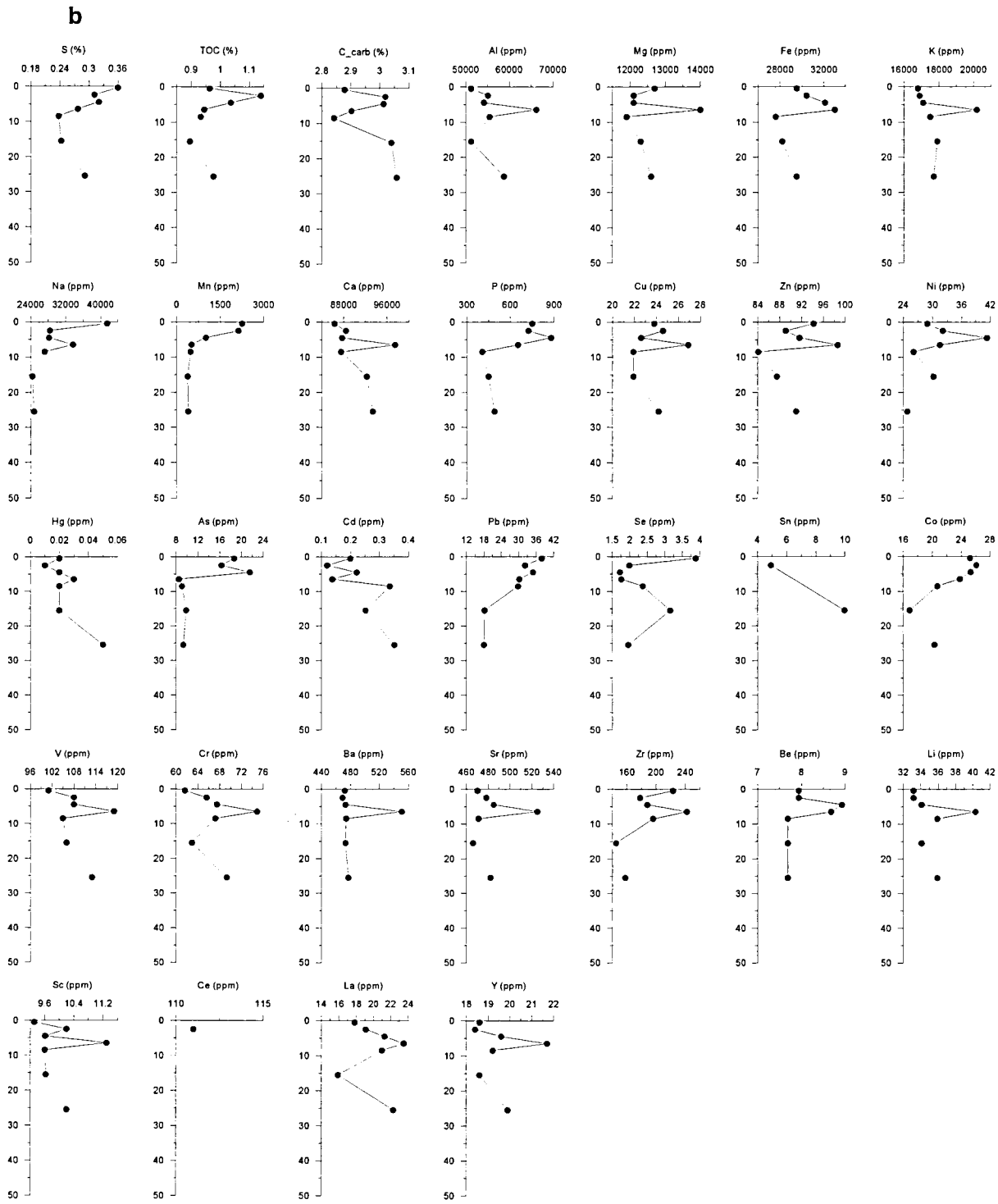


*Fig. 49. (continued).*

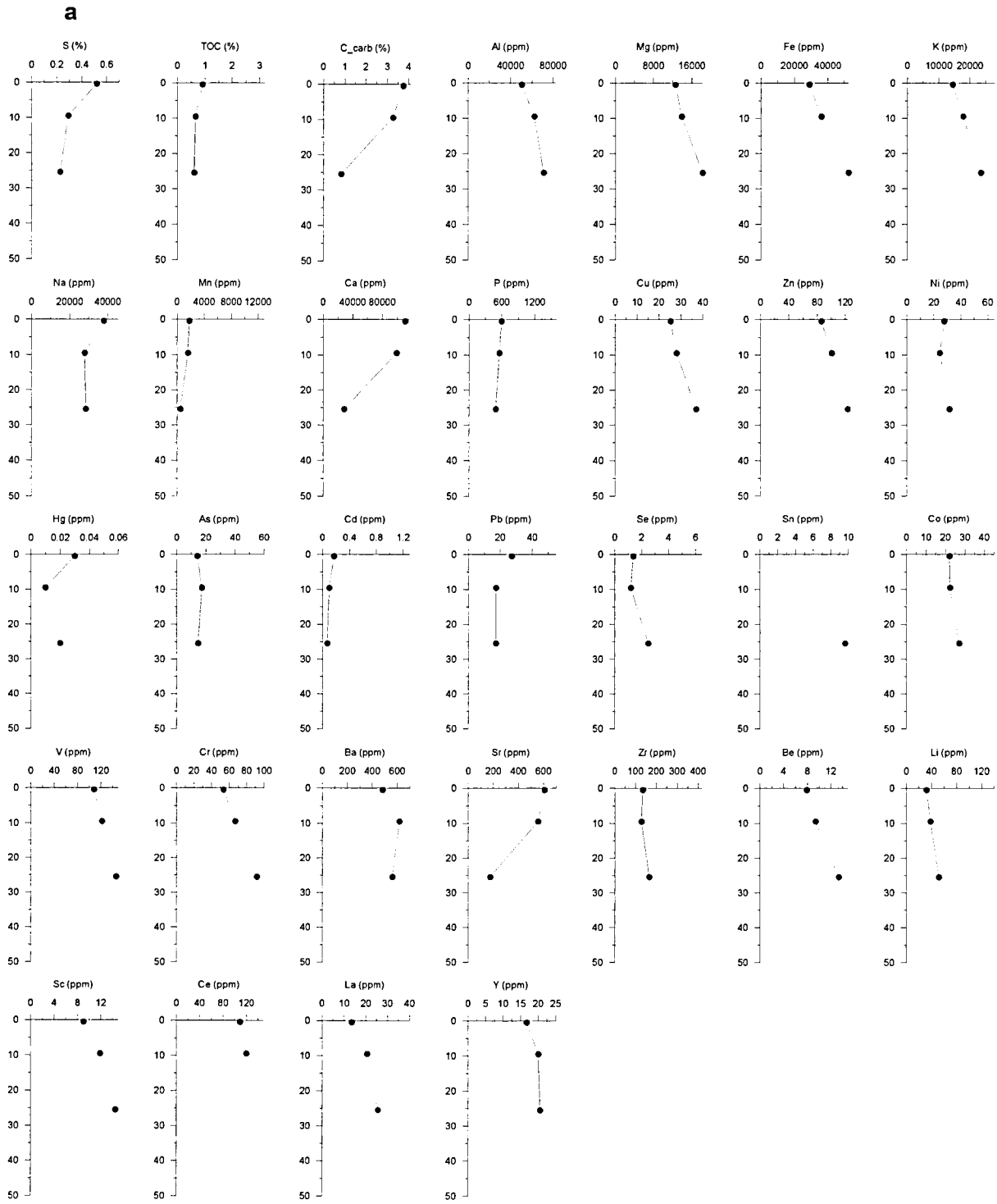


*Fig. 50. Concentration versus depth profiles of elements in the sediments of station 523: (a) constant x-axes of individual parameters at all stations; (b) variable x-axes, defined according to concentration ranges of individual parameters at each station.*

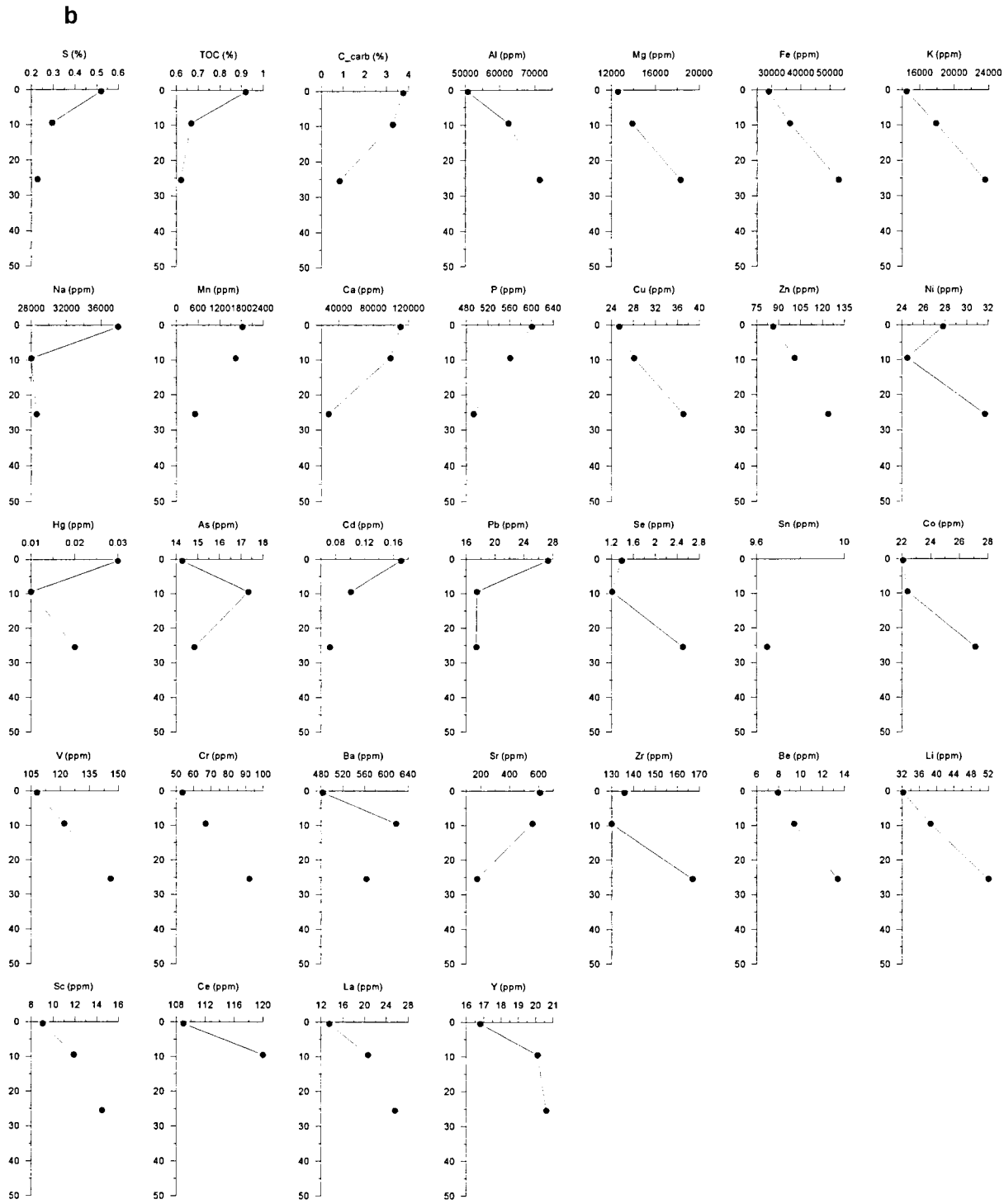


*Fig. 50. (continued).*

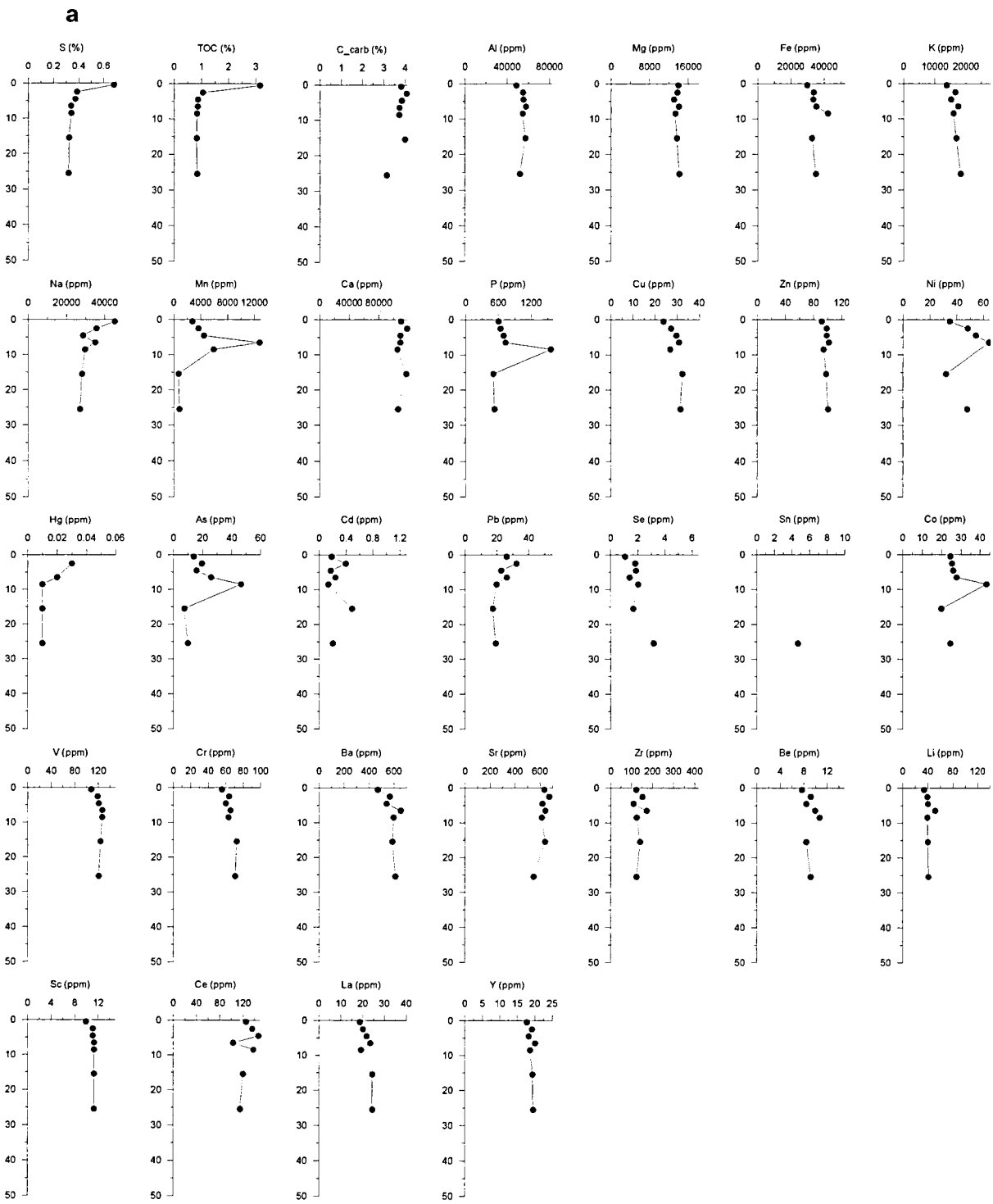


*Fig. 51. Concentration versus depth profiles of elements in the sediments of station 526: (a) constant x-axes of individual parameters at all stations; (b) variable x-axes, defined according to concentration ranges of individual parameters at each station.*

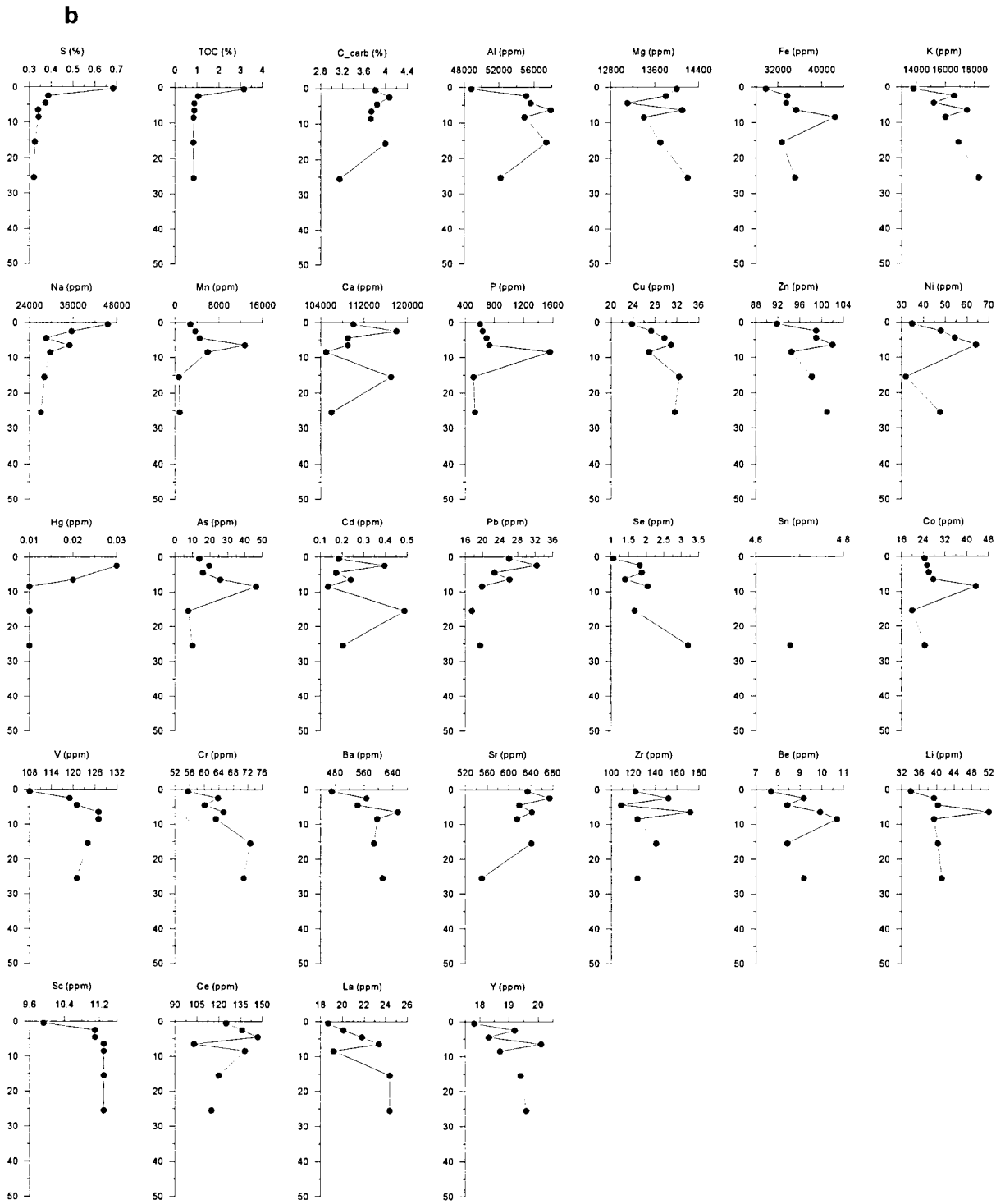


*Fig. 51. (continued).*

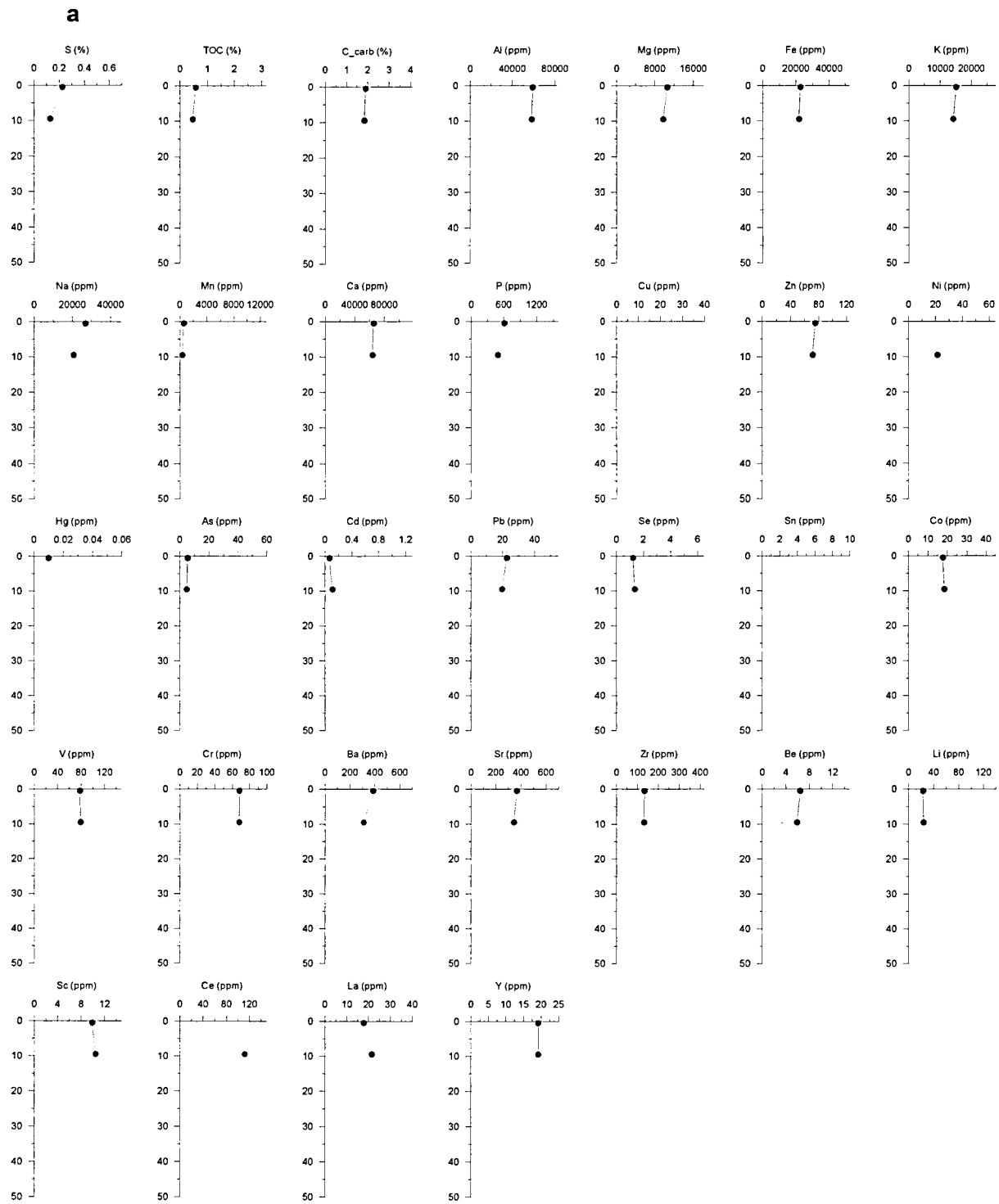


*Fig. 52. Concentration versus depth profiles of elements in the sediments of station 528: (a) constant x-axes of individual parameters at all stations; (b) variable x-axes, defined according to concentration ranges of individual parameters at each station.*

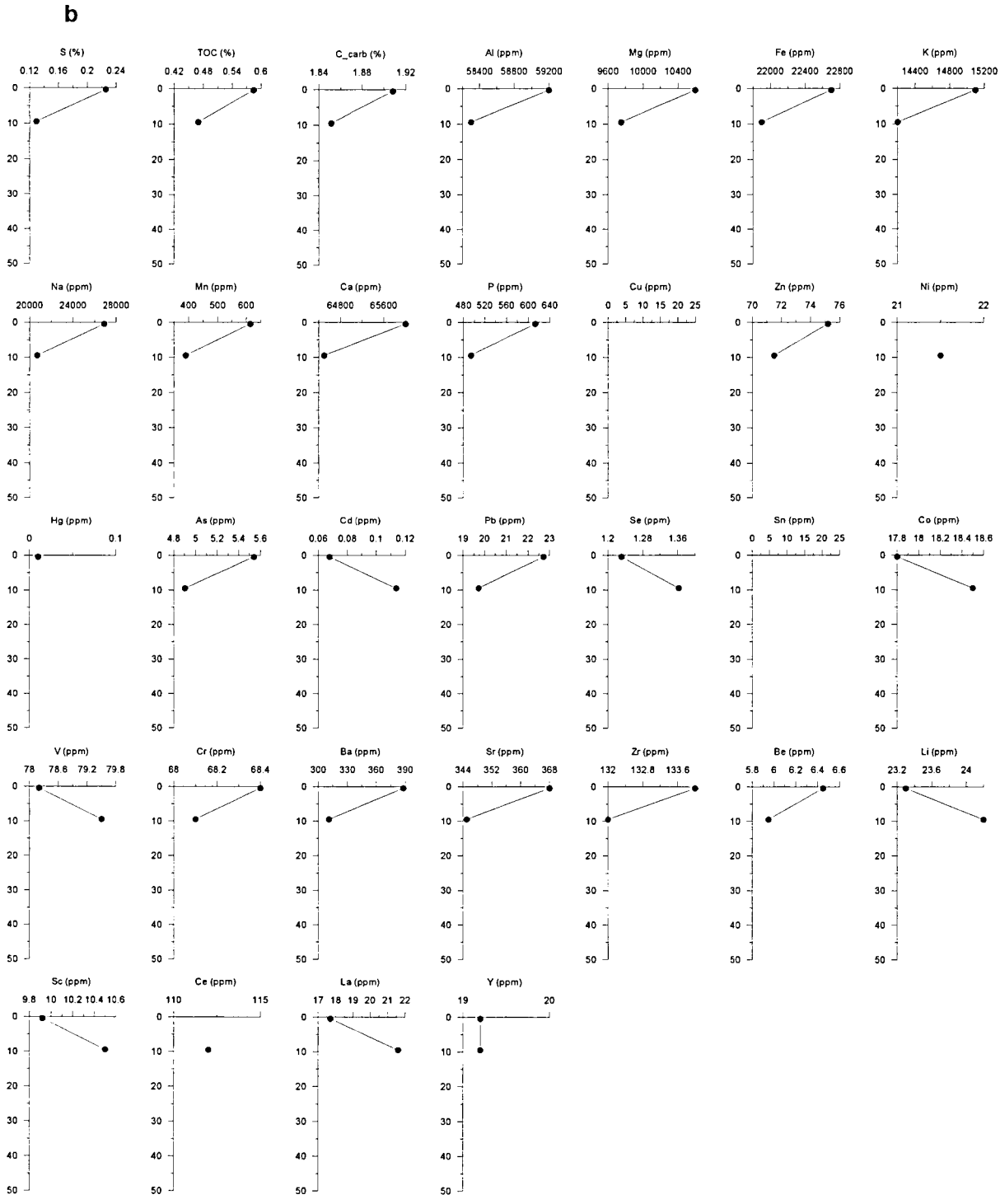


*Fig. 52. (continued).*

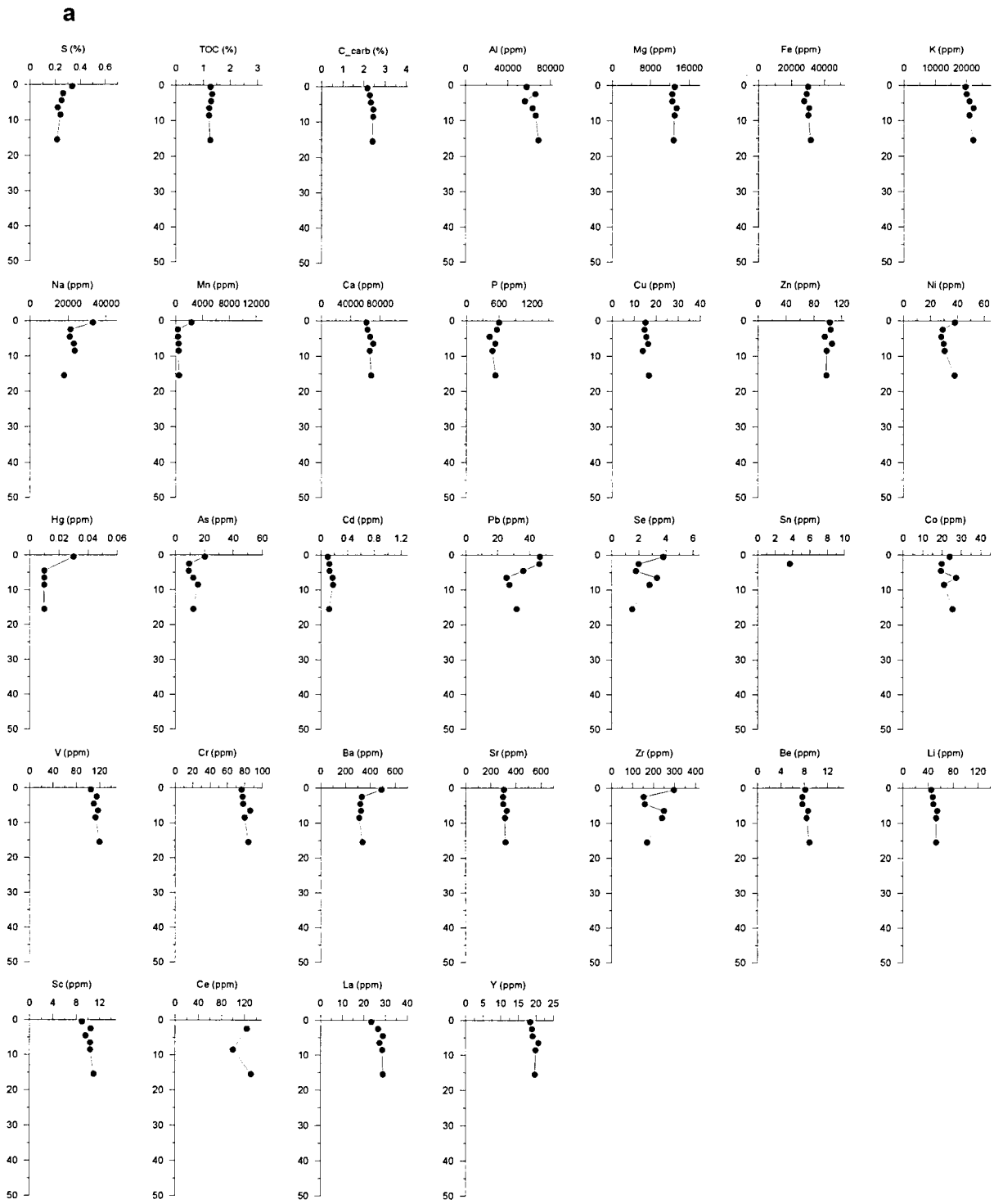


*Fig. 53. Concentration versus depth profiles of elements in the sediments of station 529: (a) constant x-axes of individual parameters at all stations; (b) variable x-axes, defined according to concentration ranges of individual parameters at each station.*

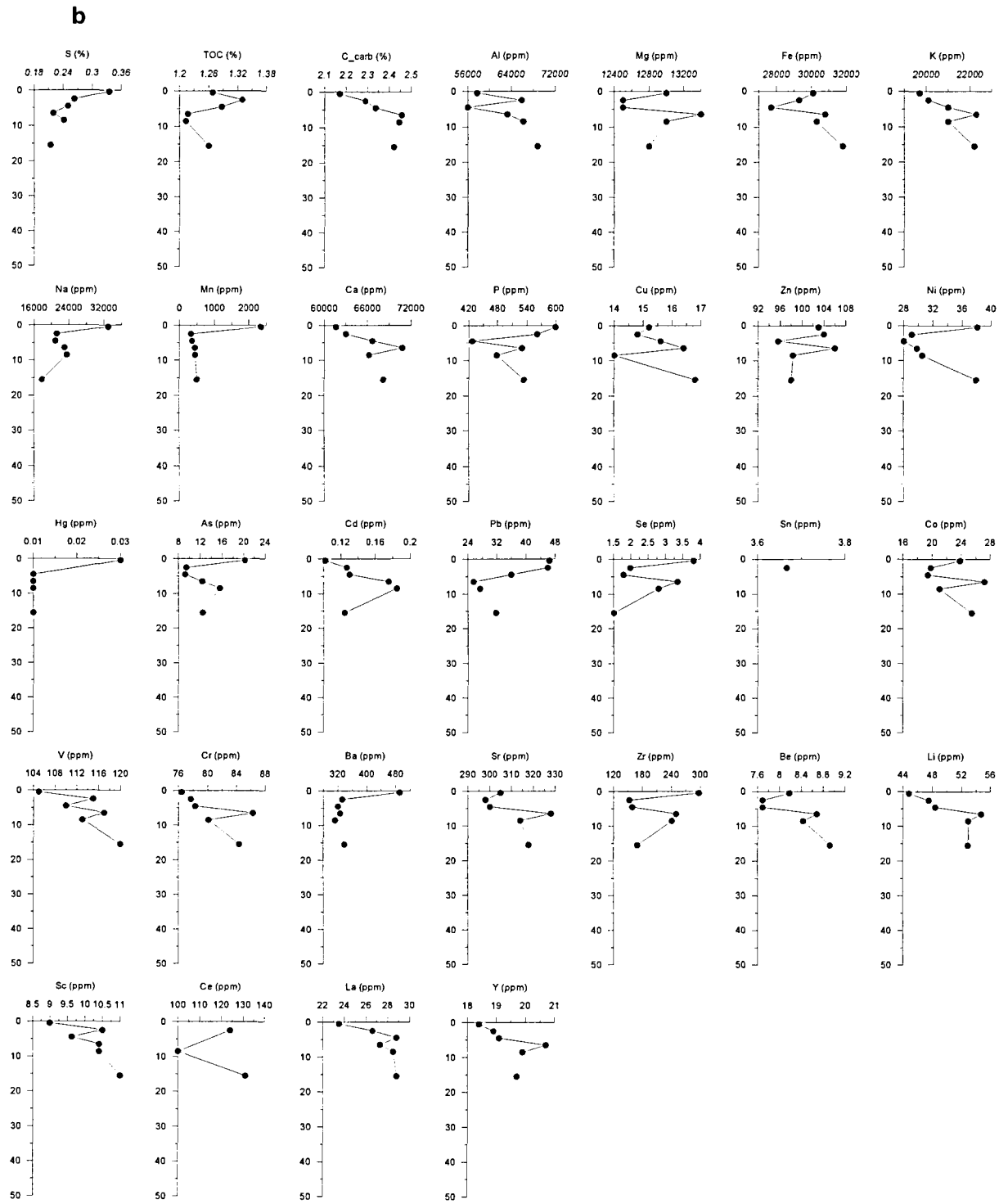


*Fig. 53. (continued).*

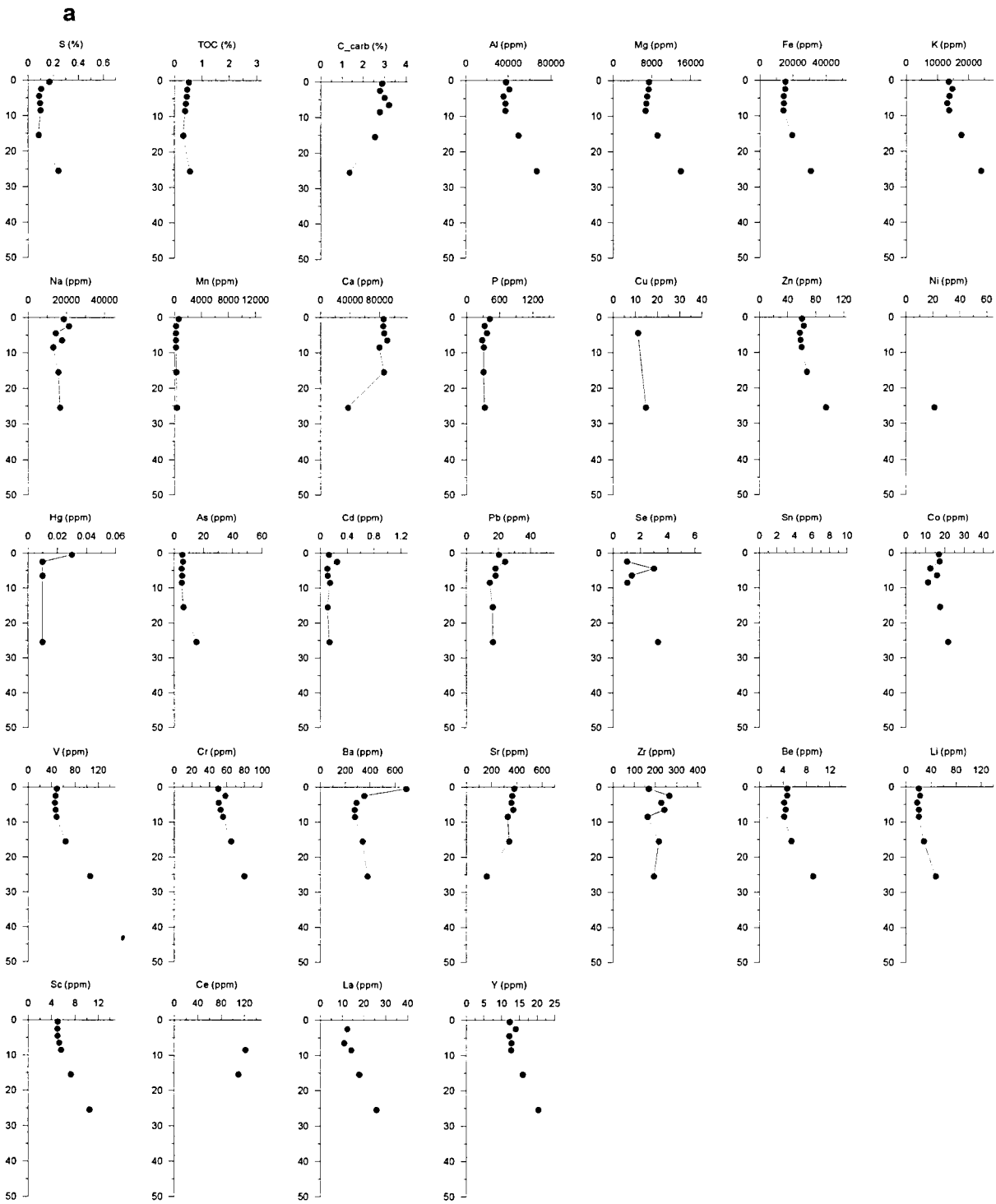


*Fig. 54. Concentration versus depth profiles of elements in the sediments of station 530: (a) constant x-axes of individual parameters at all stations; (b) variable x-axes, defined according to concentration ranges of individual parameters at each station.*

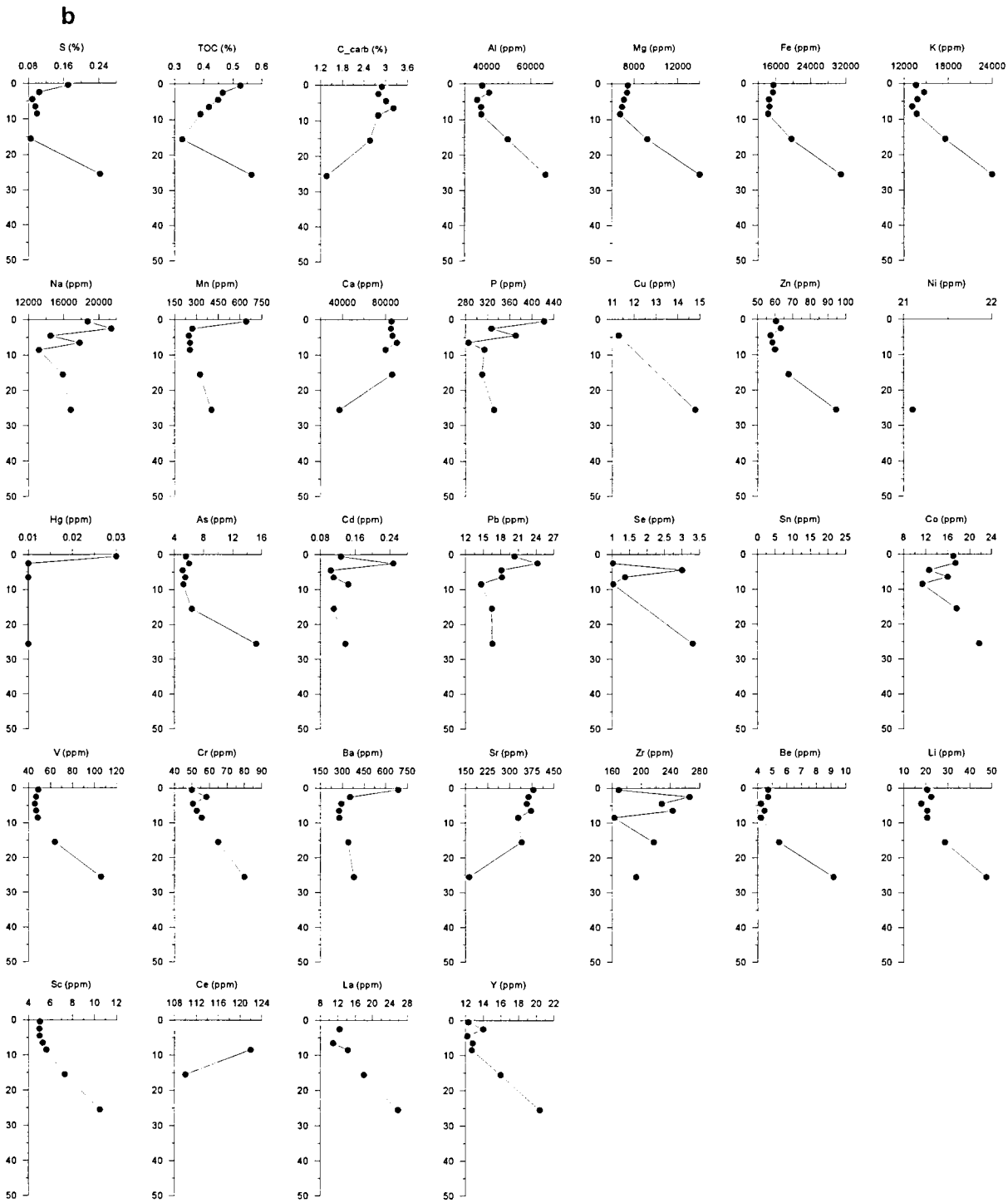


*Fig. 54. (continued).*

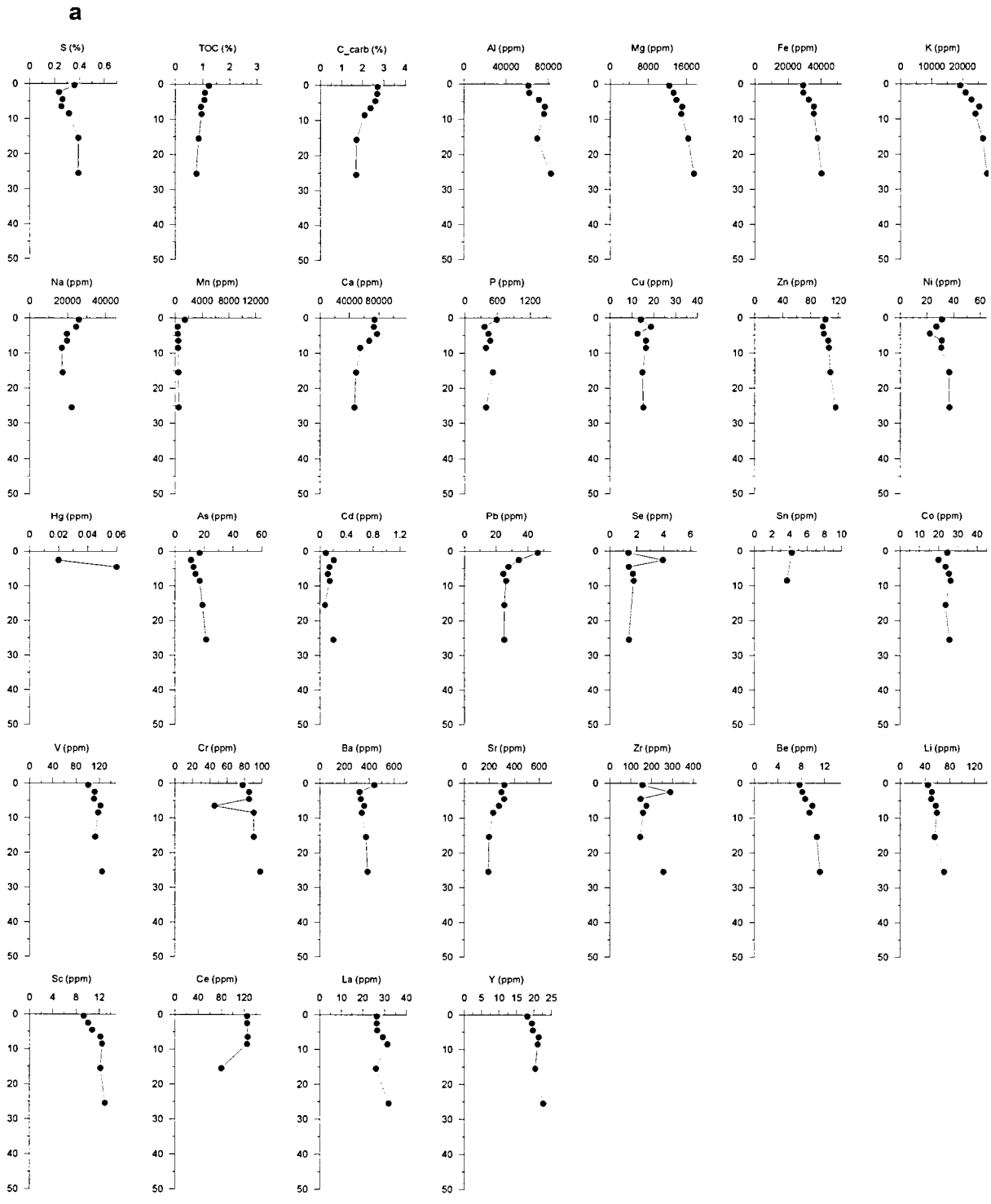


*Fig. 55. Concentration versus depth profiles of elements in the sediments of station 531: (a) constant x-axes of individual parameters at all stations; (b) variable x-axes, defined according to concentration ranges of individual parameters at each station.*

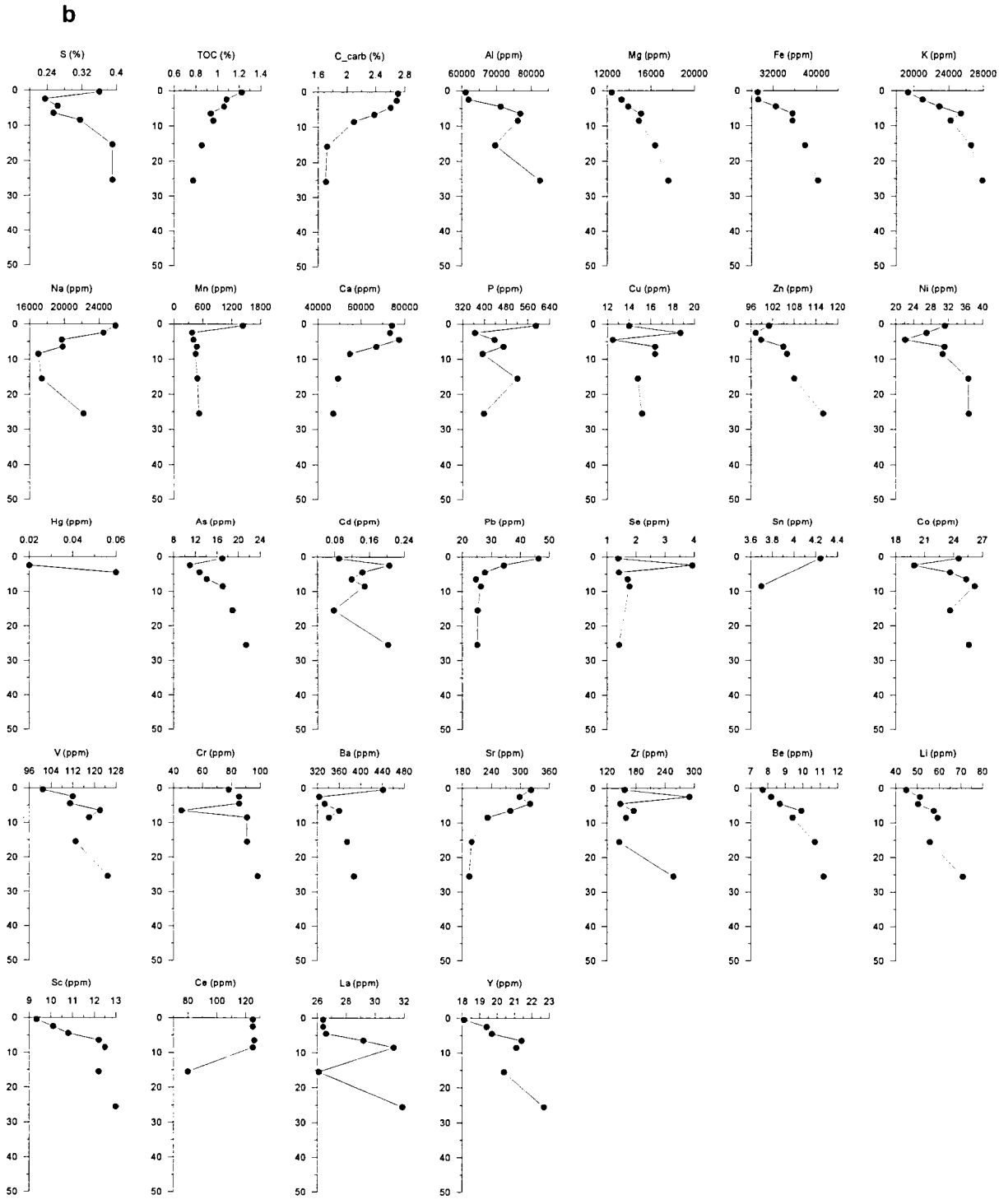


*Fig. 55. (continued).*

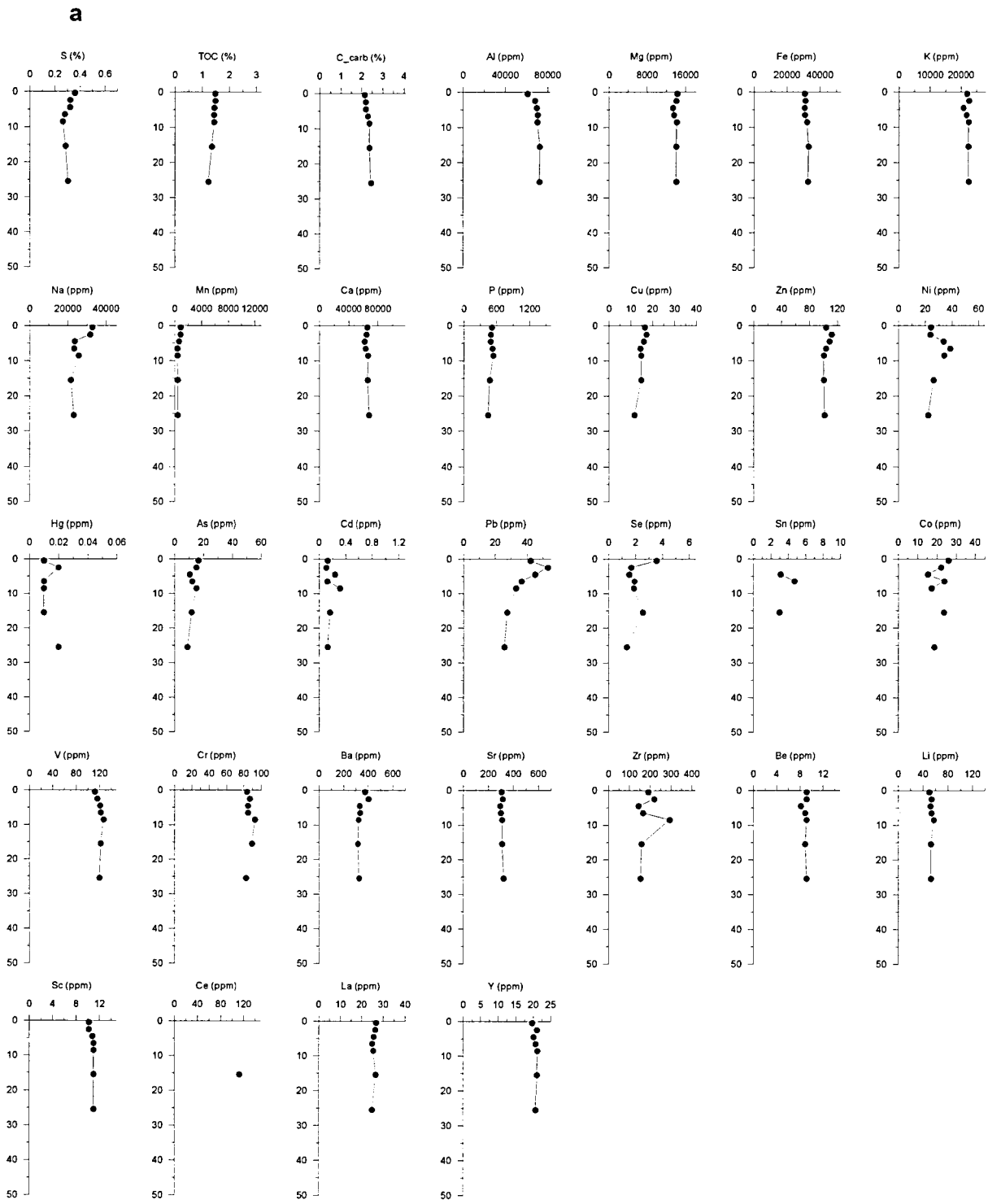


*Fig. 56. Concentration versus depth profiles of elements in the sediments of station 532: (a) constant x-axes of individual parameters at all stations; (b) variable x-axes, defined according to concentration ranges of individual parameters at each station.*

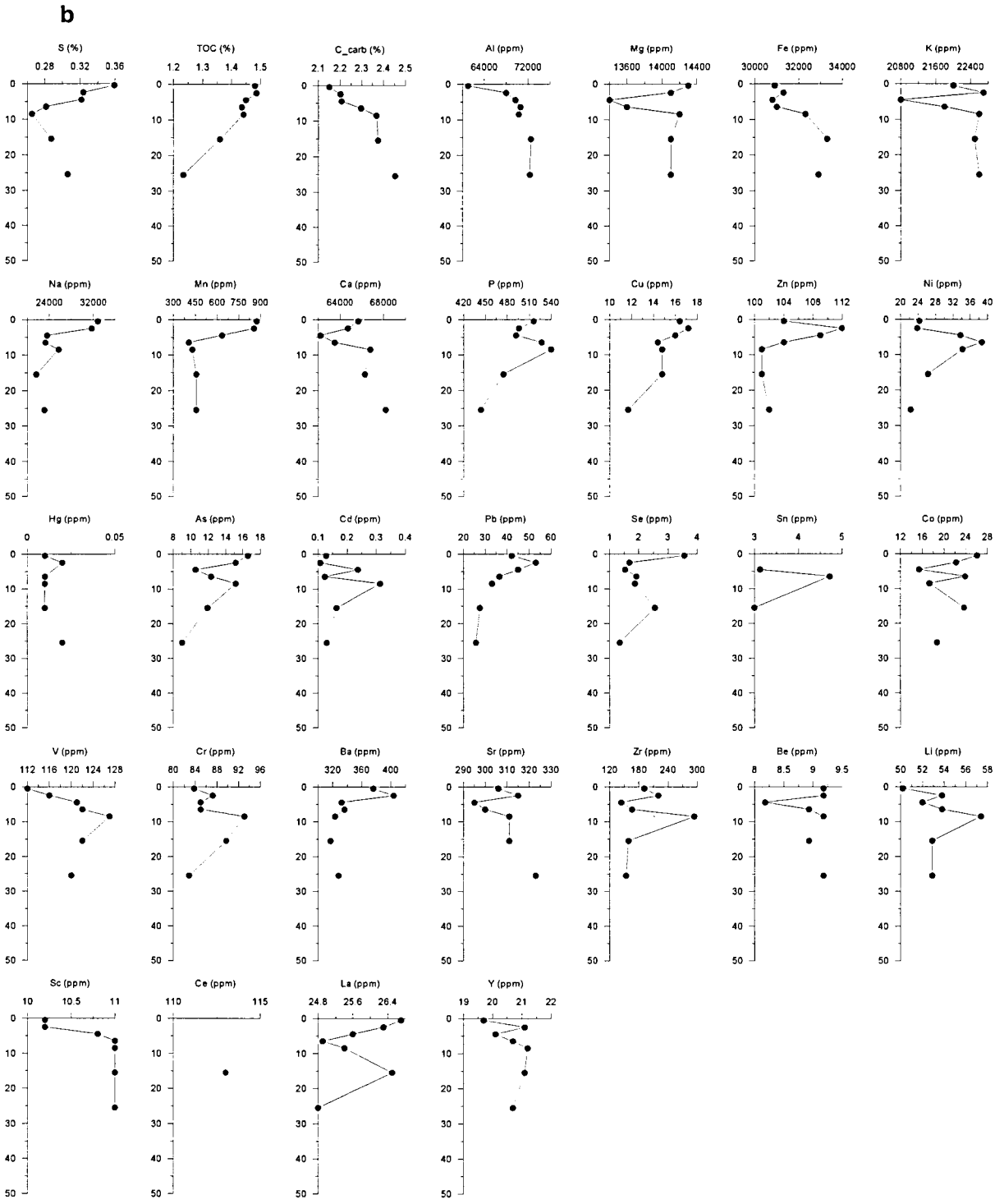


*Fig. 56. (continued).*

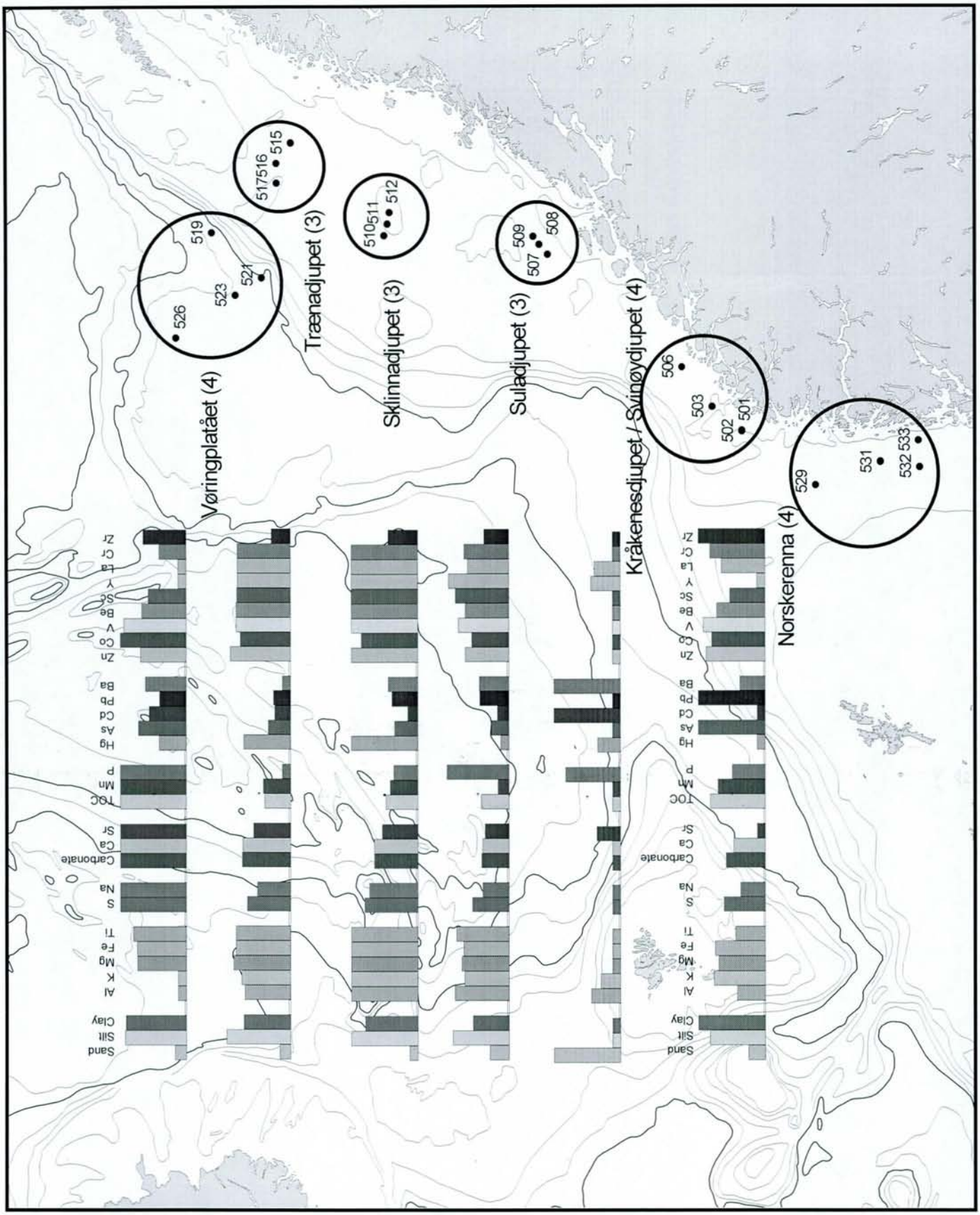


*Fig. 57. Comparison of average elemental abundances and textural characteristics in six geographically confined areas (see also Table 3). The number in parentheses behind the geographical name corresponds to the number of stations used for calculating averages for that area; the locations and identifications of those selected stations are also indicated. The y-axes of the bar diagrams are relative, scaled after highest and lowest average values for each parameter. The bar heights of parameters shown vary between 100% (highest value) and 10% (lowest value).*

## 7. REFERENCES


Barnett, P.R.O., Watson, J. & Connely, D., 1984. A multiple corer for taking virtually undisturbed samples from shelf, bathyal and abyssal sediments. Oceanologica Acta 53: 399-408.

Berner, R.A., 1980. Early Diagenesis, A Theoretical Approach. Princeton University Press, 241 pp.

Bjerkli, K., Klungsøyr, J., Moen, P.T. & Rise, L., 1999. Prøvetakning (NGU:9901, HI:999104) på midt-norsk sokkel, Vøringplatået og nordlige del av Norskerenna. Toktrapport. NGU rapport 99.050, 23 p.

De Haas, H., Okkels, E. & Van Weering, T.C.E., 1996. Recent sediment accumulation in the Norwegian Channel, North Sea. Nor. Geol. Unders. Bull., 430: 57-65.

Eisma, D. and Kalf, J., 1987. Dispersal, concentration and deposition of suspended matter in the North Sea. J. Geol. Soc. London, 144: 161-178.

Froelich, P.N., Klinkhammer, G.P., Bender, M.L., Luedtke, N.A., Heath., G.R., Cullen D., Dauphin, P., Hammond, D., Hartman, B. and Maynard V., 1979. Early oxidation of organic matter in pelagic sediments of the eastern equatorial Atlantic: suboxic diagenesis. Geochim. Cosmochim. Acta, 43: 1075-1090.

Gibbs, R.J., 1977. Transport phase of transition metals in the Amazon and Yukon rivers. Geological Society of America , 88: 829-843.

Glasby, G. P., 2000. Manganese: Predominant role of nodules and crusts. In: Marine Geochemistry, H.D. Schulz & M. Zabel (eds.), 335-372. Springer-Verlag Berlin Heidelberg New York.

Hong, S., Candelone, J.P., Patterson, C.C. & Boutron, C.F., 1994. Greenland ice evidence of hemispheric lead pollution two milleniaago by Greek and Roman civilizations. Science, 265: 1841-1843.

Hunt, C.D. & Kelly, J.R., 1988. Manganese cycling in coastal regions: response to eutrophication. Estuarine Coastal Shelf Sci., 26: 527-558.

Lepland, A., Thorsnes, T. & Sæther, O., 2000, Barium in the recent Skagerrak sediments: controls upon the geographic and stratiraphic trends. Marine Geology,163: 13-26.

Nriagu, J.O. & Pacyna, J.M., 1988. Quantitative assessmant og worldwide contamination of air, water and soils by trace metals. Nature, 323: 134-139.

Rise, L., 2000. Sedimentoligi og geotekniske undersøkelser på korte sedimentkjerner tatt i Norskerenna, forsenkninger / basseng på kontinentalsokkelen utenfor Midt-Norge, og

kontinentalskråningen utenfor Trænabanken samt Vøringplatået (tokt 9901). NGU rapport. 2000.026, 79 p.

Roy, S., 1992. Environments and Processes of Manganese Deposition. Econ. Geol., 87: 1218-1236.

Smith, D. & Flegal, A.R., 1995. Lead in the biosphere – recent trends. Ambio, 24: 21-23.

Sæther, M.O., Faye, G., Thorsnes, T., Rise, L., Longva, O. and Bøe, R., 1996. Regional distribution of manganese, phosphorus, heavy metals, barium, and carbon in sea bed sediments (0-2 cm) from the northern part of the Norwegian Skagerrak. Norw. Geol. Surv. Bull., 430: 103-112.

Thomson, J., Nixon, S., Croudace, I.W., Pedersen, T.F., Brown, L., Cook, G.T. & MacKenzie, A.P., 2001. Redox-sensitive element uptake in north-east Atlantic Ocean (Benthic Boundary Layer Experiment sites). EPSL,184: 535-547.

Wilson, T.R.S., 1975. Salinity and the major elements of sea water. In: Chemical Oceanography, J.P. Riley & G. Skirrow (eds.), Vol.1, 365-413. London: Academic Press.